12-2011

PROBABILISTIC APPROACHES TO STABILITY AND DEFORMATION PROBLEMS IN BRACED EXCAVATION

Zhe Luo
Clemson University, jerry8256@gmail.com

PROBABILISTIC APPROACHES TO STABILITY AND DEFORMATION PROBLEMS IN BRACED EXCAVATION

A Dissertation
Presented to
the Graduate School of
Clemson University

In Partial Fulfillment
of the Requirements for the Degree
Doctor of Philosophy
Civil Engineering

---

by
Zhe Luo
December 2011

Accepted by:
Dr. C. Hsein Juang, Committee Chair
Dr. Sez Atamturktur, Co-Chair
Dr. Ronald D. Andrus
Dr. William C. Bridges Jr.

ABSTRACT

This dissertation is aimed at applying probabilistic approaches to evaluating the basal-heave stability and the excavation-induced wall and ground movements for serviceability assessment of excavation in clays. The focuses herein are the influence of spatial variability of soil parameters and small sample size on the results of the probabilistic analysis, and Bayesian updating of soil parameters using field observations in braced excavations.

Simplified approaches for reliability analysis of basal-heave in a braced excavation in clay considering the effect of spatial variability in random fields are presented. The proposed approaches employ the variance reduction technique (or more precisely, equivalent variance method) to consider the effect of spatial variability so that the analysis for the probability of basal-heave failure can be performed using well-established first-order reliability method (FORM). Case studies show that simplified approaches yield results that are nearly identical to those obtained from the conventional random field modeling (RFM). The proposed approaches are shown to be effective and efficient for the probabilistic analysis of basal-heave in a braced excavation considering spatial variability. The variance reduction technique is then used in the probabilistic serviceability assessment in a case study.

To characterize the effect of uncertainty in sample statistics and its influence on the results of probabilistic analysis, a simple procedure involving bootstrapping is presented. The procedure is applied to assessing the probability of serviceability failure in a braced excavation. The analysis for the probability of failure, referred to herein as

probability of exceeding a specified limiting deformation, necessitates an evaluation of the means and standard deviations of critical soil parameters. In geotechnical practice, these means and standard deviations are often estimated from a very limited data set, which can lead to uncertainty in the derived sample statistics. In this study, bootstrapping is used to characterize the uncertainty or variation of sample statistics and its effect on the failure probability. Through the bootstrapping analysis, the probability of exceedance can be presented as a confidence interval instead of a single, fixed probability. The information gained should enable the engineers to make a more rational assessment of the risk of serviceability failure in a braced excavation. The case study demonstrates the potential of bootstrap method in coping with the problem of having to evaluate failure probability with uncertain sample statistics.

Finally, a Bayesian framework using field observations for back analysis and updating of soil parameters in a multi-stage braced excavation is developed. Because of the uncertainties in the initial estimates of soil parameters and in the analysis model and other factors such as construction quality, the updated soil parameters are presented in the form of posterior distributions. In this dissertation, these posterior distributions are derived using Markov chain Monte Carlo (MCMC) sampling method implemented with Metropolis-Hastings algorithm. In the proposed framework, Bayesian updating is first realized with one type of response observation (maximum wall deflection or maximum ground surface settlement), and then this Bayesian framework is extended to allow for *simultaneous* use of two types of response observations in the updating. The proposed

framework is illustrated with a quality excavation case and shown effective regardless of the prior knowledge of soil parameters and type of response observations adopted.

The probabilistic approaches presented in this dissertation, ranging from probability-based design of basal heave, to probabilistic analysis of serviceability failure in a braced excavation considering spatial variability of soil parameters, to bootstrapping for characterizing the uncertainty of sample statistics and its effect, and to MCMC-based Bayesian updating of soil parameters during the construction, illustrate the potential of probability/statistics as a tool for enabling more rational solutions in geotechnical fields. The case studies presented in this dissertation demonstrate the usefulness of these tools.

DEDICATION

I dedicate this dissertation to my parents. This dissertation exists because of their love and support.

ACKNOWLEDGMENTS

I would like to thank my advisors, Drs. Hsein Juang and Sez Atamturktur, for all of their untiring guidance and support during my doctoral research at Clemson University. Without their guidance and support, I would not have been able to complete my dissertation studies. I am also very grateful to my other committee members: Drs. Ronald Andrus, and William Bridges, for their assistance and review of my dissertation. They are all supportive and actively helped with my course study and the completion of this dissertation. Through their contribution my doctoral study and research have been an enjoyable and rewarding experience. Finally, I would like to thank the Glenn Department of Civil Engineering of Clemson University for the teaching assistantship during my doctoral study and research. I also wish to thank the Shrikhande family and the Glenn Department of Civil Engineering for awarding me the Aniket Shrikhande Memorial Annual Graduate Fellowship.

TABLE OF CONTENTS

Page

TITLE PAGE i

ABSTRACT ii

DEDICATION v

ACKNOWLEDGMENTS vi

LIST OF TABLES x

LIST OF FIGURES xi

CHAPTER

I. INTRODUCTION 1

Background – Purpose of the Research 1
Objectives and Scope of Dissertation 6
Significance of the Research 7
Structure of the Dissertation 8

II. RELIABILITY ANALYSIS OF BASAL-HEAVE IN A BRACED EXCAVATION IN A ONE-DIMENSIONAL RANDOM FIELD 10

Introduction 10
Factor of Safety against Basal-Heave Failure 13
Stationary Random Field Modeling of s_u/σ'_v 19
Spatial Averaging Effect 22
Reliability Analysis of Basal-Heave Stability Considering Spatial Variability 24
Reliability-Based Design Considering Spatial Variability 38
Summary 45

III. RELIABILITY ANALYSIS OF BASAL-HEAVE IN A BRACED EXCAVATION IN A TWO-DIMENSIONAL RANDOM FIELD 46

Introduction 46

Table of Contents (Continued)

Page

Two-Dimensional Random Field Modeling of s_u/σ'_v 47
Simplified Reliability Method for Assessing Probability of Basal-Heave Failure in Braced Excavation in 2-D Random Field 55
Summary 73

IV. PROBABILISTIC SERVICEABILITY ASSESSMENT IN A BRACED EXCAVATION CONSIDERING SPATIAL VARIABILITY 75

Introduction 75
Finite Element Modeling with a Small-Strain Nonlinearity Soil Model 77
Modeling Spatial Variability in Braced excavations in Clays 81
Fuzzy Sets Methodology - Modeling and Processing of Uncertain Parameters 84
Case Study – TNEC Excavation Case 93
Summary 108

V. EFFECT OF SMALL SAMPLE SIZE ON THE PROBABILISTIC SERVICEABILITY ASSESSMENT 110

Introduction 110
Performance Function for Probability of Exceedance 112
Point Estimate Method for Uncertainty Propagation and Probability of Exceedance 115
Variation of Sample Statistics Determined by Bootstrapping 117
Case Study – TNEC Excavation Case 120
Further Discussions 135
Summary 144

VI. BAYESIAN UPDATING OF SOIL PARAMETERS IN BRACED EXCAVATIONS 145

Introduction 145
Framework of Bayesian Updating with Markov Chain Monte Carlo Simulation 148
Example Application: TNEC Excavation Case 153
Summary 179

Table of Contents (Continued)

Page

VII. CONCLUSIONS AND RECOMMENDATIONS 180

Conclusions 180
Recommendations 189

REFERENCES 191

LIST OF TABLES

Table		Page
1.1	Criteria for excavation protection levels in Shanghai, China (PSCG 2000).	3
2.1	Parameters for a basal-heave stability problem shown in Figure 2.1	17
3.1	Input parameters for a basal-heave stability problem shown in Figure 3.1	55
4.1	Propping arrangement for the excavation and the stiffness of struts and floor slabs in the FEM analysis in TNEC case (after Kung et al. 2007a)	94
4.2	Soil profile and soil model parameters used in FEM analysis (from Kung et al. 2007a)	94
5.1	Coefficients for transformation of input variables (Kung et al. 2007b)	113
5.2	Small-stain triaxial test results for Taipei clay (adapted from Kung 2003).	123
5.3	Probability of exceedance in the TNEC excavation using PEM and bootstrapping method with 17 data points.	124
5.4	Probability of exceedance in the TNEC excavation using PEM and bootstrapping method with only 8 data points.	137
5.5	Probability of exceedance in the TNEC excavation under three excavation protection scenarios.	139
6.1	Statistics of four prior distributions used in the Bayesian updating scheme.	154

LIST OF FIGURES

Figure		Page
1.1	Schematic diagram of basal-heave failure	2
1.2	Schematic diagram of excavation effects (Hsiao 2007)	2
2.1	Geometry of slip circle method for basal-heave stability analysis (Adapted from Wu et al. 2010a)	15
2.2	Gamma sensitivity index at various COVs of s_u/σ'_v based on reliability analysis	18
2.3	Example of simulated spatial variability of normalized undrained shear strength s_u/σ'_v by means of random field modeling	26
2.4	Relative frequency of the computed factor of safety using random field modeling (under the scenario that mean $s_u/\sigma'_v = 0.3$, COV of $s_u/\sigma'_v = 0.3$ and $\theta = 2.5$m)	27
2.5	Relationship between probability of failure and factor of safety at various scales of fluctuation generated with MCS-based random field modeling	28
2.6	Mean of normalized resisting moment as a function of the scale of fluctuation and COV of s_u/σ'_v	30
2.7	COV of resisting moment (M_R) as a function of the scale of fluctuation and COV of s_u/σ'_v	32
2.8	Influence of COV and scale of fluctuation of s_u/σ'_v on the probability of failure	32
2.9	Flow chart for searching for the reduction factor for a given pair of standard deviation σ and scale of fluctuation θ	33
2.10	Back-calculated reduction factor Γ for various scales of fluctuation	36
2.11	Comparison between the reduction factors back-calculated using the MCS-based RFM and those derived based on Eq. (2.13) with different assumed characteristic lengths.	37

List of Figures (Continued)

Figure Page

2.12 Reliability-based procedure for evaluating failure probability of basal-heave 39

2.13 Comparison between the MCS-based random field modeling and the simplified approach 40

2.14 Effect of uncertainty in the scale of fluctuation on the probability of failure against basal-heave in a braced excavation in clay (scale of fluctuation = 2.5m, COV of s_u/σ'_v = 0.3) 42

2.15 Relationship between required factor of safety and scale of fluctuation at failure probability of 10^{-3} 43

3.1 Geometry of slip circle method and 2-dimensional random field modeling region for basal-heave stability analysis 48

3.2 Influence of scale of fluctuation on the 2-D random field modeling of s_u/σ'_v at given mean of 0.3 and COV of 0.3 52

3.3 Effect of 1-dimensional spatial variability on the relationship between failure probability and factor of safety in the reliability-based design 58

3.4 Effect of 2-dimensional spatial variability on the relationship between failure probability and factor of safety in the reliability-based design 59

3.5 Comparison between the reduction factors back-calculated using the MCS-based RFM and those computed using Eq. (3.8) with assumed characteristic lengths (L_v = 18m or L_h = 36m) 65

3.6 Reliability-based procedure for evaluating failure probability of basal-heave 68

3.7 Comparison between the MCS-based RFM solutions and those by the simplified approach 69

3.8 Effect of model bias of the slip circle method on the relationship between failure probability and factor of safety derived through reliability analysis 72

List of Figures (Continued)

Figure Page

4.1 Maximum wall deflections and maximum ground settlements at various stages of excavation of the TNEC case –A comparison of the observed values with those obtained by Kung et al. (2007a) using AFENA and in this study using PlaxisTM; both FEM codes implemented with the MPP soil model. 80

4.2 An example of failure surface in braced excavation 83

4.3 Example of triangular fuzzy number and α-cut interval 86

4.4 Vertex method for fuzzy FEM analysis of braced excavation 90

4.5 Fuzzy number that represents the model output. The shaded area normalized to the full area under the shape is the probability of exceeding the limiting response ($x_{\lim}$) 92

4.6 Schematic of checkerboard study on the variation of soil parameters in an FEM model of TNEC case 96

4.7 Influence of scale of fluctuation on wall deflection and ground settlement 97

4.8 Fuzzy input parameters at different scales of fluctuation 100

4.9 Resulting fuzzy numbers for maximum wall deflection and ground-surface settlement 102

4.10 Probability of exceedance computed at various levels of limiting wall deflection and ground surface settlement 106

5.1 Generation of one bootstrap sample from the original observations through random choice with replacement (adapted from Most and Knabe 2010) 119

5.2 Soil profile and excavation depth of TNEC case: LL,liquid limit; N, blow count; PI, plasticity index; w, moisture content (adapted from Kung et al. 2007a) 121

5.3 Probability distribution of the small-strain triaxial test results listed in Table 5.2 125

List of Figures (Continued)

Figure Page

5.4 Bootstrap samples generated from the original test data listed in Table 5.2 126

5.5 Probability distribution of the correlation coefficients for the generated bootstrap samples in Figure 5.4 127

5.6 Bootstrap mean and standard deviation of s_u/σ'_v and E_i/σ'_v with respect to number of bootstrap simulations. 128

5.7 Probability distribution of the mean value and standard deviation of s_u/σ'_v 129

5.8 Probability distribution of the mean value and standard deviation of E_i/σ'_v 130

5.9 Distribution of the reliability indices computed with the specified limiting (a) wall deflection and (b) ground settlement (at final excavation stage) 134

5.10 Confidence intervals for probability of exceedance in the TNEC excavation computed with various levels of limiting wall deflection and ground surface settlement 143

6.1 Effect of scaling factor on the efficiency of Markov chain sampling: (a) s = 0.01, (b) s = 3, (c) s = 20 156

6.2 Relationship between acceptance rate and scaling factor updated with both observed δ_{hm} and δ_{vm} 157

6.3 Influence of Markov chain length on the mean values and standard deviations of the posterior distributions estimated from 30 different Markov chains with s = 3 157

6.4 Sampling process of MCMC simulations with the observations from the 6th excavation stage (s = 3) 159

6.5 Histograms of posterior distribution for s_u/σ'_v and E_i/σ'_v with data from Figure 6.4 160

List of Figures (Continued)

Figure Page

6.6 Maximum settlement and wall deflection predictions prior to excavation stages 3, 4, 5, 6, 7 (using Prior distribution 1) 164

6.7 Updated mean value and one standard deviation bounds of the settlement predictions at target depth of 19.7 m prior to Stages 3, 4, 5, 6, and 7 of excavations (using Prior distribution 1 and the maximum settlement observations) 165

6.8 Updated mean value and one standard deviation bounds of wall deflection predictions at target depth of 19.7 m prior to Stages 3, 4, 5, 6, and 7 of excavations (using Prior distribution 1 and the maximum wall deflection observations) 166

6.9 Comparisons of updated predictions with three updating schemes (using Prior distribution 1) 169

6.10 Distributions of predictions prior to final stage of excavation (using Prior distribution 1) 170

6.11 Updated mean of soil parameters prior to Stages 3, 4, 5, 6, and 7 of excavations using various prior distributions 173

6.12 Updated COV of soil parameters prior to Stages 3, 4, 5, 6, and 7 of excavations using various prior distributions 174

6.13 Updated COV of soil parameters prior to Stages 3, 4, 5, 6, and 7 of excavations using mean value of Prior distribution 2 and various COVs 175

6.14 Updated distribution of soil parameters prior to final stage of excavation using mean value of Prior distribution 2 and COV = 0.30 176

6.15 Influence of correlation coefficient ρ between model biases on predictions updated with observed maximum settlement and wall deflection (using Prior distribution 1) 178

CHAPTER I

INTRODUCTION

Background – Purpose of the Research

In the urban environment, deep braced excavation is a commonly-used construction method for high-rise building basements, underground transportation stations, and underground parking and commercial spaces, etc. In the design of a braced excavation in clays, two important issues are inevitable, namely, (1) basal-heave stability during the construction, and (2) the serviceability issues such as the excavation-induced wall and ground responses. Basal-heave failure in a braced excavation in clays may be induced by insufficient shear strength, which supports the weight of soil within the critical zone around the excavation. During an excavation, soil outside the excavation zone moves downward and inward because of its own weight and surcharge; this tends to cause soil inside the excavation zone to heave up, as shown in Figure 1.1. Collapse of the bracing system may occur if the amount of basal-heave movement is excessive. On the other hand, even if the basal-heave stability can be achieved in the design, the adjacent structures may still be damaged because of the excessive wall deflection and ground surface settlement, as shown in Figure 1.2.

Failures of excavation projects have been reported worldwide: e.g., Infopedia (2004) and Chen et al. (2007). Considering that most braced excavation projects are conducted in the unban environment, the social, economic, and environmental impacts caused by the failure of an excavation project can be significant. In the design of a braced excavation, both stability and serviceability requirements should be guaranteed.

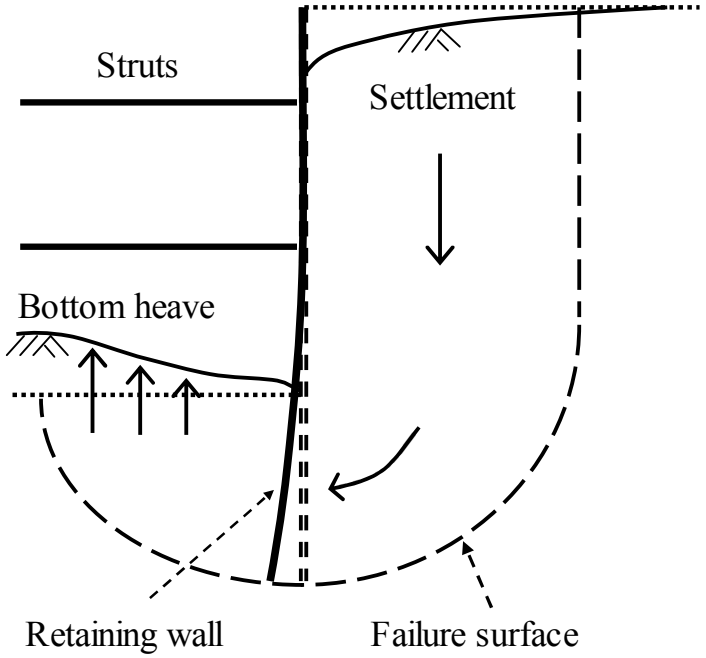

Figure 1.1: Schematic diagram of basal-heave failure.

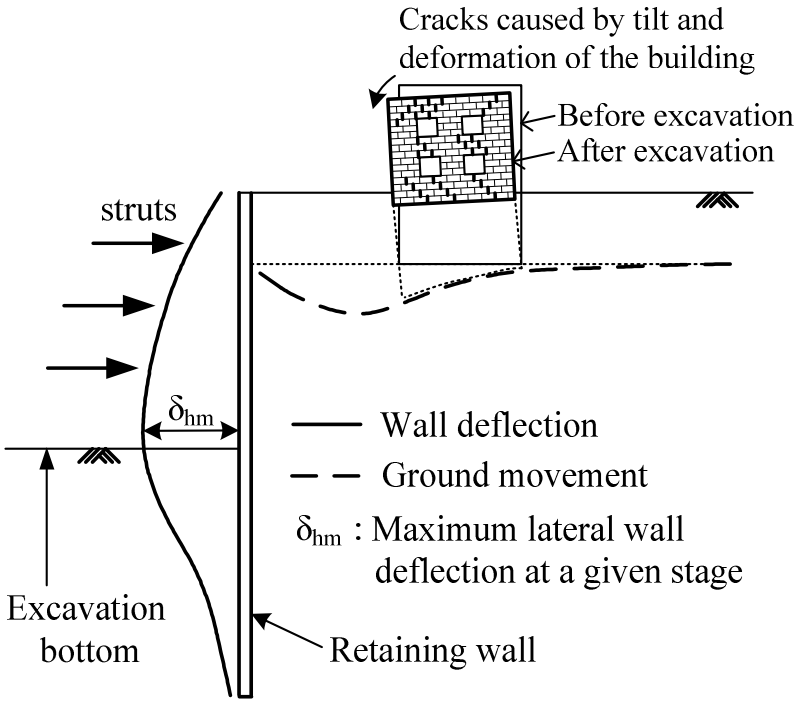

Figure 1.2: Schematic diagram of excavation effects (Hsiao 2007).

Table 1.1: Criteria for excavation protection levels in Shanghai, China (PSCG 2000).

Protection level	Limiting wall deflection and ground surface settlement	Requirements of the environmental protection
I	1. Maximum wall deflection $\leq 0.14\%H$ 2. Maximum ground surface settlement $\leq 0.1\%H$ 3. FS (basal stability) ≥ 2.2	Metro lines and important facilities such as gas mains and water drains exist within a distance of $0.7H$ from the excavation; safety has to be ensured.
II	1. Maximum wall deflection $\leq 0.3\%H$ 2. Maximum ground surface settlement $\leq 0.2\%H$ 3. FS (basal stability) ≥ 2.0	Important infrastructures or facilities such as gas mains and water drains exist within a distance of (1-2) H from the excavation.
III	1. Maximum wall deflection $\leq 0.7\%H$ 2. Maximum ground surface settlement $\leq 0.5\%H$ 3. FS (basal stability) ≥ 1.5	No important infrastructures or facilities exist within a distance of 2 H from the excavation

Note: H = final excavation depth; FS = factor of safety against basal heave, calculated using the slip circle method.

Conventionally, a safe design may be realized by satisfying the factor of safety (*FS*) requirements, as well as the wall and ground requirements as a means of preventing the excavation failure and damage to the adjacent infrastructures. An example of the design codes for braced excavations used in China (PSCG 2000) is illustrated in Table 1.1. The limiting *FS*, wall and ground deformations to prevent failure in the designs of excavations are suggested for various protection levels, depending on the requirements of the environmental protection. It should be noted that a design based on those limiting criteria in a deterministic approach may not guarantee safety, since it is always difficult to estimate the *FS*, wall and ground responses with *certainty* mainly due to the uncertainty of design soil parameters. The sources of parameter uncertainty include inadequate site investigation, measurement errors, as well as inherent and spatial variability of soil.

Inherent variability of soil parameters is interpreted by their probability distributions or sample statistics (e.g., mean value and standard deviation). Spatial variability is generally described by the scale of fluctuation, which is the maximum distance within which the spatially random parameters are correlated (Akbas and Kulhawy 2009). Spatial variability may be modeled with the random field theory (Vanmarcke 1977). Recent studies of random field modeling (RFM) based on Monte Carlo simulation (MCS) demonstrate that spatial variability plays an important role in reliability-based design in geotechnical engineering (Griffiths and Fenton 2009; Huang et al. 2010). Neglecting spatial soil variability in reliability analysis of geotechnical problems can lead to either overestimation or underestimation of the failure probability in a given design, depending on the specified limiting *FS*, wall deflection or ground

settlement levels (Wang et al. 2011b). In this regard, Chapters II and III of this dissertation are devoted to developing simplified approaches for the basal-heave stability analysis of braced excavations with the consideration of the effect of one-dimensional (1-D) and two-dimensional (2-D) spatial variability, respectively. Further, the influence of spatial variability on the probabilistic serviceability assessment in braced excavation is presented in Chapter IV.

Small sample size can lead to large uncertainty in soil parameters. Because of budget constraints, the geotechnical engineers often have to derive sample statistics from a small sample (i.e., a small data set), which can lead to uncertainty in the sample statistics: the accuracy of the estimated mean and standard deviation of the uncertain soil parameters is questionable. This issue is important because it can significantly influence the results of the reliability/probability analysis (Schweiger and Peschl 2005). Considering that the problem of small sample size of soil parameters in geotechnical projects is not uncommon, the effect of this uncertainty on the failure probability in braced excavation in clays should be examined. Thus, Chapter V of this dissertation is devoted to developing a simple procedure involving bootstrapping approach (Efron 1979) for assessing the uncertainty of sample statistics caused by small sample size. The procedure is then applied to the analysis of the probability of serviceability failure in a braced excavation. The failure probability (or the corresponding reliability index) is interpreted using confidence intervals in order to take into account of those uncertainties caused by small sample size.

Deep braced or supported excavations are generally performed with staged

construction. The predictions of wall and ground responses may not be accurate due to the uncertainty of design soil parameters. However, the soil parameters may be updated with the observed wall and ground responses to "refine" the knowledge of them. The predictions for the subsequent stages will be then improved with the updated soil parameters. It should be noted that in the traditional back analysis, the focus is on finding a set of fixed values for the parameters of concern, without considering the uncertainty in the observations and model bias. Because of the high degree of uncertainty involved in the soil-structure interaction, the fixed parameter values may not be feasible or physically meaningful. Therefore, parameters of concern are preferably treated as a random variable and the updated parameters are expressed in terms of posterior distributions. Through comparison of model predictions against observations in field, soil parameters are updated using Bayes' theory, which results in posterior distributions of soil parameters. To this end, Chapter VI is devoted to developing such a Bayesian framework using field observations for updating soil parameters in braced excavation in clays.

Objectives and Scope of the Research

The scope of this dissertation focuses on the applications of probabilistic approaches to evaluate the basal-heave stability and the excavation-induced wall and ground movement in clays for serviceability assessment. The specific objectives of this dissertation are:

1. Study the influence of spatial variability on the reliability-based design against

basal-heave stability in braced excavation in clays using random field modeling.

2. Develop simplified procedures for reliability-based design against basal-heave stability using equivalent variance technique.
3. Perform a probabilistic evaluation of the excavation-induced wall and ground responses considering spatial variability.
4. Study the influence of small sample size of soil parameters on the probabilistic serviceability assessment in braced excavation in clays.
5. Develop a Bayesian framework for updating key soil parameters in braced excavation using observed excavation-induced wall and ground responses.

Significance of the Research

The spatial variability of soil has significant influence on the reliability-based design in geotechnical engineering. It is difficult to apply random field modeling (RFM), which necessitates the use of Monte Carlo simulation, in a complicated soil-structure problem such as braced excavation. Therefore, the main contribution of this dissertation is the development of simplified approaches, which employ equivalent variance technique and first-order reliability method (FORM), for the reliability-based design against basal-heave stability considering spatial variability. Through properly selecting the characteristic lengths, those simplified approaches are shown to be equivalent to RFM. The simplified approaches are implemented in a spreadsheet and require much less computation effort. The simplified approaches are easy to use, and have potential as a practical tool for reliability-based design that has to deal with spatial

variability of soils.

Another contribution of this dissertation is the development of Bayesian framework for the updating key soil parameters. In this framework, the updating procedure starts with an assumption for the prior distributions for soil parameters, based on published opinions and engineering judgment. After the initial excavation stage is conducted, the maximum wall deflection and maximum settlement are observed. Those observations are used to update the distributions of soil parameters, and the updated soil parameters are then used to predict the responses in the subsequent stages. This straightforward procedure is repeated as the staged excavation proceeds, and the soil parameters are updated accordingly. The predictions using updated soil parameters can reproduce the reality with improved fidelity, comparing to those obtained with the prior distributions. Furthermore, the two types of observations in the serviceability assessment, maximum wall deflection and maximum ground surface settlement, may be simultaneously employed to refine the knowledge of uncertain soil parameters and the predictions of the wall and ground responses.

The Structure of the Dissertation

This dissertation consists of seven chapters. In Chapter I, the current chapter, an introduction is presented to organize the entire dissertation. The purpose and the scope of the research and the outline of the dissertation are also presented. Chapter II through Chapter VI present the major contents of this dissertation and Chapter VII presents the conclusions of this dissertation. In Chapter II, a simplified approach for

reliability analysis of basal-heave in a braced excavation considering the 1-D spatial variability of soil parameters is presented. In Chapter III, the aforementioned simplified approach is extended to consider the 2-D spatial variability. In Chapter IV, the simplified approach using equivalent variance technique is applied in the probabilistic serviceability assessment in braced excavation. In Chapter V, the effect of small sample size of soil parameters on the probabilistic serviceability assessment is examined through bootstrapping approach. Chapter VI demonstrates the development of the Bayesian framework for updating soil parameters in braced excavation. Finally, in Chapter VII, the main conclusions of this dissertation are presented.

CHAPTER II

RELIABILITY ANALYSIS OF BASAL-HEAVE IN A BRACED EXCAVATION IN A ONE-DIMENSIONAL RANDOM FIELD*

Introduction

Conventionally, basal-heave stability in a braced excavation in clay is evaluated with a factor of safety (*FS*), defined as the ratio of the resistance over the load (e.g., Terzaghi 1943; Bjerrum and Eide 1956). In designs based on *FS*, soil parameters are generally considered as constant inputs for simplicity. However, it is well known that *FS* greater than unity does not guarantee basal-heave stability in clay due to the inherent variability of soil parameters such as undrained shear strength and unit weight. Although uncertainty in the soil parameters is often dealt with by use of conservative parameter values, the probabilistic approach using reliability analysis offers a more direct and consistent way to consider soil variability *explicitly*. Examples of the reliability-based design for basal-heave stability of a braced excavation can be found in Goh et al. (2008) and Wu et al. (2010a), in which a design chart that relates the probability of basal-heave failure (p_f) to the factor of safety *FS* is provided.

In traditional reliability analysis, uncertain soil parameters are interpreted as continuous random variables defined by their probability distributions or sample statistics (e.g., mean value and standard deviation). The soil parameters are often considered as homogeneous or "spatially constant" fields in such analysis. However, the uncertainty

* A similar form of this chapter has been published at the time of writing: Luo Z, Atamturktur S, Cai Y, Juang CH. Simplified approach for reliability-based design against basal-heave failure in braced excavations considering spatial effect. Journal of Geotechnical and Geoenvironmental Engineering, doi:10.1061/(ASCE)GT.1943-5606.0000621.

stems not only from the inherent variability, but also from *spatial* variability. For the latter, the variation of soil parameters may be modeled with the random field theory (Vanmarcke 1977). Spatial variability is generally described by the scale of fluctuation, which is the maximum distance beyond which the spatially random parameters are uncorrelated (Akbas and Kulhawy 2009). As the scale of fluctuation decreases, the soil parameters in the random field tend to vary more rapidly; conversely, as the scale of fluctuation increases, the soil parameters in the random field tend to vary less and become more uniform.

The effect of spatial variations of soil properties can be significant in many geotechnical problems, as demonstrated by recent studies of random field modeling (RFM) by Griffiths and his colleagues (Fenton and Griffiths 2003; Fenton et al. 2005; Griffiths and Fenton 2009; Huang, et al. 2010). In their studies, Griffiths and his colleagues adopted local averaging subdivision techniques to model the random field. Of course, the random field can also be modeled using other approaches such as the *Cholesky decomposition* method (Fenton 1997; Haldar and Babu 2008; Srivastava et al. 2010; Suchomel and Mašín 2010). The conventional random field modeling (RFM), however, has to be realized with Monte Carlo simulations (MCS), and a large number of simulations are needed to obtain convergent results.

As an alternative to the conventional RFM, simplified methods that implement a proper spatial averaging strategy have been shown to be effective in considering the effect of spatial variability of soil properties (e.g., Phoon and Kulhawy 1999a,b; Goh et al. 2008; Klammler et al. 2010; Most and Knabe 2010). To consider spatial averaging in

the reliability analysis, variances of soil parameters are reduced by multiplying a reduction factor that is a function of *scale of fluctuation* and *characteristic length* (Vanmarcke 1983). Typical scales of fluctuation for commonly used soil properties have been reported by Phoon and Kulhawy (1999b). The characteristic length often depends on the problem under investigation, and is generally assumed to be equivalent to the length of the failure surface (Schweiger and Peschl 2005; Most and Knabe 2010) or taken as the distance in the random field over which the variance reduction is calculated (Cherubini 2000; Babu and Dasaka 2008). Recent studies (Peschl and Schweiger 2003; Suchomel and Mašín 2010) show that the variance reduction-based simplified approach can capture the overall trend derived from the conventional RFM approach.

Although RFM coupling with Monte Carlo simulation (MCS) is a rigorous approach to account for spatial variability, use of this approach is quite limited in geotechnical reliability-based design for at least two reasons: (1) a rigorous simulation of the random field is very time-consuming, which is not practical, especially for complicated problems such as braced excavations; (2) MCS is further complicated by the lack of knowledge on spatial variability (for example, the scale of fluctuation could be uncertain). Contrarily, with the variance reduction-based simplified approach, traditional reliability methods can be adopted in lieu of MCS to reduce the computational effort. However, the application of such simplified approach requires a proper assessment of the characteristic length, which is problem-specific and may be difficult to determine.

In this chapter, a simplified approach that considers the spatial variability of soil parameters for reliability analysis of basal-heave stability in a braced excavation in clay is

presented. This approach is developed and presented in 5 steps. Firstly, the conventional RFM using the exponential correlation function is conducted in a study of basal-heave stability to provide a reference for further development. Secondly, by trial-and-error, the variance reduction factor is determined, with which the simplified approach can yield results that are comparable to those obtained using the conventional RFM. Thirdly, the characteristic length for the stability analysis is back-calculated based on the derived variance reduction factors. Fourthly, the proposed approach, which is first-order reliability method (FORM) implemented with the variance reduction to account for the spatial variability, is adopted for reliability analysis of basal-heave stability. Lastly, the effect of uncertainty of the scale of fluctuation (because of the lack of knowledge) is further evaluated with the proposed approach. It concludes that the proposed simplified approach is easy to use and yields results that are comparable to those obtained with the computationally expensive RFM approach.

Factor of Safety against Basal-Heave Failure

Slip circle method

The basal-heave failure in a braced excavation in clay occurs when the shear strength of the soil cannot support the weight of the soil within the critical zone around the excavation. Soil outside the excavation zone moves downward and inward because of its own weight and the soil inside the excavation zone is forced to heave. The bracing system will collapse if the amount of basal-heave movement is excessive. Traditionally, the basal-heave stability is evaluated with *FS* using the deterministic

approach. Semi-empirical methods (Terzaghi 1943; Bjerrum and Eide 1956; Eide et al. 1972; Chang, 2000) to estimate *FS* are widely used in the traditional deterministic design.

In this chapter, the slip circle method adopted by Japanese, Chinese, and Taiwanese building codes (JSA 1988; PSCG 2000; TGS 2001) to calculate the *FS* against basal-heave is used for its simplicity to consider the increase of undrained shear strength with depth, and for its convenience to implement random field theory. With the slip circle method, the *FS* is defined below (see Figure 2.1):

$$FS = \frac{M_R}{M_D} \tag{2.1}$$

where M_R and M_D are resistance moment and driving moment respectively. The driving moment M_D is caused by the weight of soil and possible surcharge:

$$M_D = W \cdot \frac{r}{2} + q_s \cdot \frac{r^2}{2} \tag{2.2}$$

where W is the total weight of the soil in front of the vertical failure plane and above the excavation surface, q_s is the surcharge, r is the radius of the slip circle, and $r = H_w - H_s$ in which H_w is the length of diaphragm wall and H_s is the depth of the final strut. The resistance moment M_R comes from three arcs (***bc***, ***cd***, ***de***) along the slip surface, as show in Figure 2.1. Although uniform undrained shear strength may be used in the computation of *FS*, the undrained shear strength generally increases with depth for most normally consolidated clay. However, the ratio of undrained shear

strength over the effective overburden stress (s_u / σ'_v) remains roughly constant (Ladd and Foott 1974). For this reason, the slip circle method can be easily adapted to consider the increase of s_u with depth. The total resistance moment M_R is computed by summing the resistances contributed by all the small arcs:

$$M_R = r \cdot \int_0^{\pi/2+\alpha} s_u \cdot r \cdot d\beta \tag{2.3}$$

where β is the angle from $\overline{ob}$ to the current slice as shown in Figure 2.1.

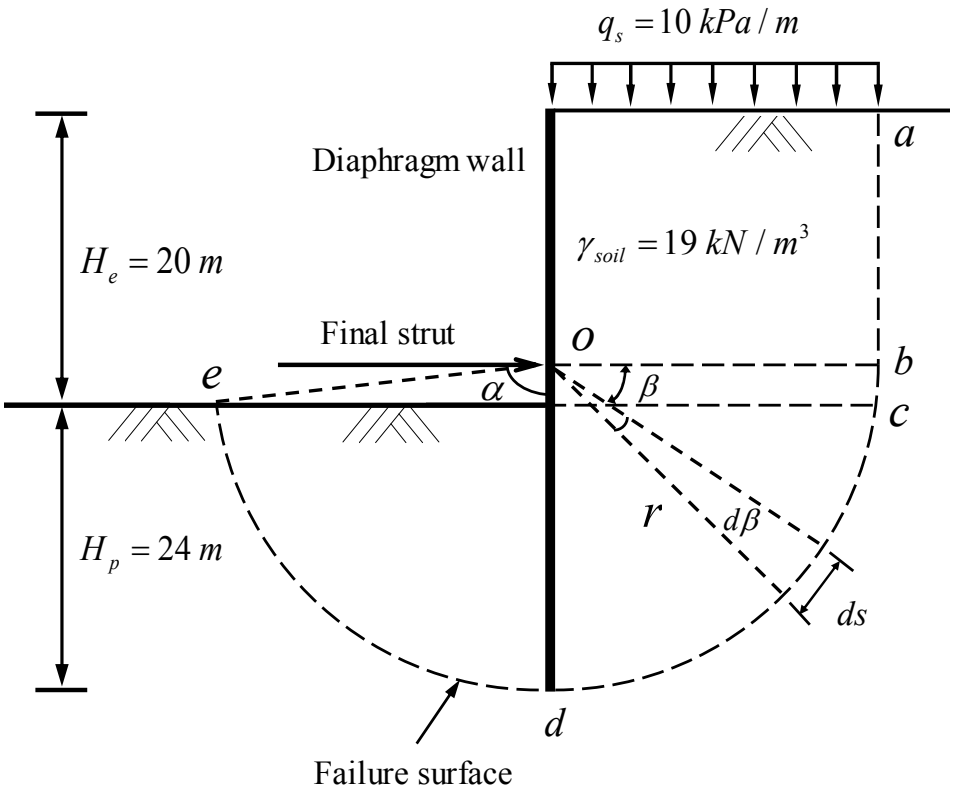

Figure 2.1: Geometry of slip circle method for basal-heave stability analysis (Adapted from Wu et al. 2010a).

In a deterministic analysis of basal-heave stability in a braced excavation in clay, the required *FS* generally depends on the method used. The recommended minimum required *FS* is 1.2 (JSA 1988; PSCG 2000; TGS 2001) when the slip circle method is employed. In the slip circle method, the resistance is computed using the summation of the resistance of numerous small arcs [Eq. (2.3)]. This formulation makes it easy to implement the random field model, which is the main reason behind the choice of the slip circle method in this study.

Gamma sensitivity index

Many factors influence the basal-heave stability in a braced excavation in clay as reflected in Eqs. (2.2) and (2.3). The relative importance of those input variables is first examined using the gamma sensitivity index (Der Kiureghian and Ke 1985), which is a by-product of reliability analysis. This index is expressed as:

$$\gamma_i = \frac{\left|\alpha J_{y,x} M\right|}{\left\|\alpha J_{y,x} M\right\|} \tag{2.4}$$

where γ_i = gamma sensitivity index for the i^{th} input variable, α = directional cosine at the design point in the original random variable space, $J_{y,x}$ = Jacobian matrix with element of $\partial y / \partial x$ with $y = T(x)$ where $T(\cdot)$ is an orthogonal transformation function, y_i = uncorrelated standard normal random variable, and M = diagonal matrix of the standard deviation of each parameter x_i. The uncertain variables

considered in this study include $x_1 = s_u / \sigma'_v$ (normalized undrained shear strength), $x_2 = H_e$ (excavation depth), $x_3 = H_w$ (length of diaphragm wall), $x_4 = H_s$ (depth of the final strut), $x_5 = D$ (depth of ground water table), $x_6 = \gamma$ (unit weight of soil), and $x_7 = q_s$ (surcharge). The gamma sensitivity index indicates the relative contribution of each of these input variables to the computed reliability index or failure probability. A higher gamma sensitivity index value indicates a greater influence of the variable of concern on the failure probability.

Table 2.1: Parameters for a basal-heave stability problem shown in Figure 2.1.

Parameters	Notations	Statistics of parameter	
		Mean	Coefficient of variation
Normalized undrained shear strength	s_u/σ_v'	0.30	0.1 – 0.6
Unit weight of soil	γ	19 kN/m^3	0.05[(1)]
Surcharge	q_s	10 kPa/m	0.2[(2)]
Depth of GWT	D	2 m	0.05[(3)]
Final excavation depth	H_e	20 m	0.05[(3)]
Final strut depth	H_s	17 m	0.05[(3)]
Penetration depth	H_p	24 m	0.05[(3)]

[(1)] Based on the COV values given by Harr (1987) and DiMaggio (2008)
[(2)] Wu et al. (2010a)
[(3)] Hsiao et al. (2008)

Based on the first order reliability method (FORM) analysis of basal-heave stability without considering spatial variability, the gamma sensitivity index for each of the seven input parameters is obtained with Eq. (2.4). The statistics of the uncertain parameters used in this FORM analysis are summarized in Table 2.1. For this gamma

sensitivity analysis, the mean of s_u/σ'_v (normalized undrained shear strength) is set at 0.3 and the coefficient of variation (COV) of s_u/σ'_v is varied between 0.1 and 0.6. As shown in Figure 2.2, the parameter s_u/σ'_v is found to have the greatest influence on the probability of basal-heave failure, and all other factors are *relatively* insignificant. The gamma sensitivity index of s_u/σ'_v is also found to increase drastically with the coefficient of variation (*COV*) of s_u/σ'_v. Thus, this study is focused on the effect of the spatial variability of the normalized undrained shear strength s_u/σ'_v on the probability of basal-heave failure in a braced excavation.

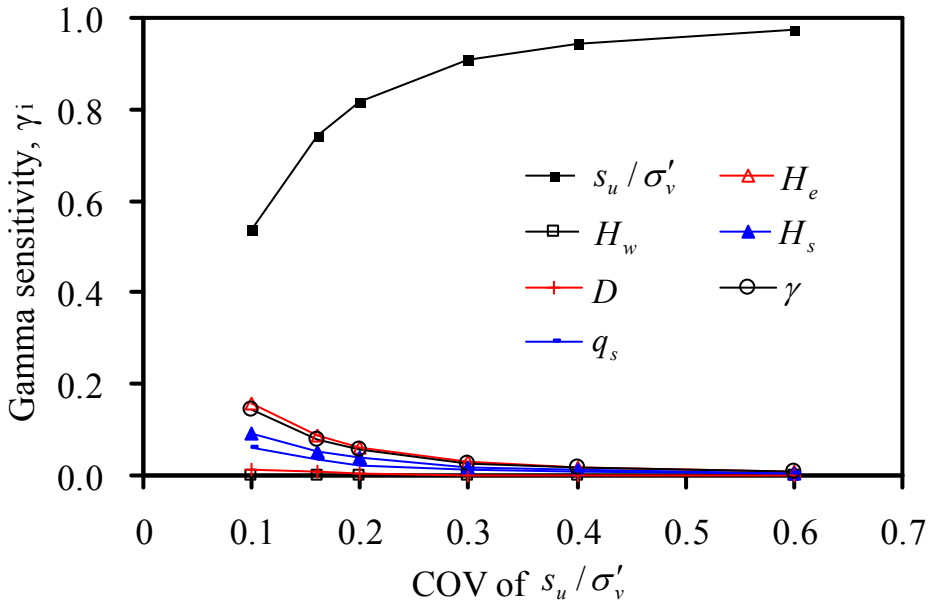

Figure 2.2: Gamma sensitivity index at various *COV*s of s_u/σ'_v based on reliability analysis.

Stationary Random Field Modeling of s_u/σ'_v

To provide a reference for the proposed simplified approach for reliability-based design against basal-heave failure in a braced excavation considering spatial random effect, the conventional random field modeling of the normalized undrained shear strength s_u/σ'_v is first conducted in this study. Here, the parameter s_u/σ'_v is modeled using a stationary lognormal random field. It should be noted that the *mean* of the undrained shear strength s_u of the clay often increases linearly with depth; however, this trend is removed herein by adopting the normalized parameter s_u/σ'_v. The stationary random field of s_u/σ'_v has the characteristics of a "second-order process" (Baecher and Christian 2003): (1) the mean and variance of $s_u/\sigma'_v(z)$ are the same regardless the "absolute" location of z, and (2) the correlation coefficient between $s_u/\sigma'_v(z_1)$ and $s_u/\sigma'_v(z_2)$ is the same regardless of the "absolute" locations of z_1 and z_2; rather, it depends only on the distance between z_1 and z_2. All other input parameters are modeled as *spatially-constant* lognormal variables or constants. The assumption of lognormal distribution for inherent variability for soil properties is not uncommon in the RFM (e.g., Akbas and Kulhawy 2009; Griffiths et al. 2009). The assumption of lognormal distribution prevents negative values for soil parameters, and is supported by past studies (e.g., Phoon and Kulhawy 1999b).

Variations of s_u/σ'_v in the field are represented by its scale of fluctuation θ, mean value $\mu_{\ln}$, and coefficient of variation $COV_{\ln}$ (note: the subscript in the last two terms, "ln", denotes the statistic for lognormal distribution). The standard deviation and

mean of the equivalent normal distribution of s_u/σ'_v, denoted as $\ln(s_u/\sigma'_v)$, are expressed as:

$$\sigma_n = \sqrt{\ln\left(1 + COV_{\ln}^2\right)} \tag{2.5}$$

$$\mu_n = \ln \mu_{\ln} - \frac{1}{2}\sigma_n^2 \tag{2.6}$$

where the subscript "*n*" denotes normal distribution. The lognormally distributed random field of s_u/σ'_v can be obtained by the transformation (Fenton et al. 2005):

$$s_u/\sigma'_v(x_i) = \exp\{\mu_n + \sigma_n \cdot G_n(x_i)\} \tag{2.7}$$

where μ_n and σ_n are determined from Eqs. (2.5) and (2.6); x_i is the spatial position at which s_u/σ'_v is modeled; $G_n(x_i)$ is a normally distributed random field with zero mean, unit variance and correlation function $\rho(\tau)$, where $\rho(\tau)$ is defined as an exponentially decaying correlation function (Jaksa et al. 1999; Haldar and Babu 2008):

$$\rho(\tau) = \exp\left(-\frac{2\tau}{\theta}\right) \tag{2.8}$$

where $\tau = |x_i - x_j|$ is the absolute distance between any two points in the random field and θ is the scale of fluctuation. The correlation matrix is built with the correlation function and can be decomposed by *Cholesky decomposition* (Fenton 1997; Haldar and Babu 2008; Suchomel and Mašín 2010; Srivastava et al. 2010):

$$L \cdot L^T = \rho \tag{2.9}$$

With the matrix L, the correlated standard normal random field can be obtained by linearly combining the independent variables as follows (Fenton 1997):

$$G_n(x_i) = \sum_{j=1}^{i} L_{ij} Z_j \qquad i = 1, 2, \cdots, M \tag{2.10}$$

where M is the number of points in the random field; Z_j is the sequence of independent standard normally distributed random variables.

To begin with, two random variables uniformly distributed between 0 and 1, U_j and U_{j+1}, are generated first. Then two independent standard normally distributed variables are given by:

$$Z_j = \sqrt{-2\ln(1-U_j)}\cos(2\pi \cdot U_{j+1}) \tag{2.11}$$

$$Z_{j+1} = \sqrt{-2\ln(1-U_j)}\sin(2\pi \cdot U_{j+1}) \tag{2.12}$$

The stationary random field of the normalized undrained shear strength s_u / σ'_v at each spatial position is obtained by Eq. (2.7) for a specified mean, standard deviation, and scale of fluctuation. The Monte Carlo simulation (MCS) is then used to generate samples in the lognormal random field. Each simulation of the Monte Carlo process involves the same mean, standard deviation and scale of fluctuation of s_u / σ'_v. However, the spatial distribution varies among these simulations. Given a sufficient number of simulations, the

output such as M_R [Eq. (2.3)] or FS [Eq. (2.1)] can be obtained and statistically analyzed to produce estimates of the probability density function of M_R or FS and the failure probability p_f. The failure probability p_f is computed as the ratio of the number of simulations that yield failure ($FS < 1$) over the total number of simulations N. The number of MCS samples should be at least 10 times of the reciprocal of the target failure probability (Ang and Tang 2007; Wang et al. 2011a). In this study, the level of failure probability of interest is greater than 10^{-4}, therefore N is set at 10^5.

Spatial Averaging Effect

Spatial averaging is a concept with which, the spatial variability of the soil property is averaged in order to approximate a random variable that represents a soil parameter (Vanmarcke 1977). The variability of the averaged soil property over a large domain is less than over a small domain. The reduced variability of the soil properties over a large domain can be quantified with the *variance reduction technique*. The reduction is computed using the variance reduction function, which is a function of the scale of fluctuation θ and characteristic length L. The form of the variance reduction function depends on the type of correlation function employed.

To consider spatial averaging in a reliability analysis, the variances of soil parameters may be reduced by multiplying a factor known as the *variance reduction factor* which is computed using the variance reduction function (Vanmarcke 1983). Many successful applications of the *variance reduction technique* have been reported in the literature, e.g., constant model (Cherubini 2000; Schweiger and Peschl 2005),

triangular model (Babu and Dasaka 2008), exponential model (Most and Knabe 2010). The exponential model, which is often employed in the RFM in geotechnical engineering, is adopted herein. The variance reduction function for the exponential model is given as follows (Vanmarcke 1983):

$$\Gamma^2 = \frac{1}{2}\left(\frac{\theta}{L}\right)^2\left[\frac{2L}{\theta} - 1 + \exp\left(-\frac{2L}{\theta}\right)\right] \tag{2.13}$$

where θ is the scale of fluctuation and L is the characteristic length. Given the variance reduction factor Γ^2, the reduced variance σ_Γ^2 can be obtained with the following equation:

$$\sigma_\Gamma^2 = \Gamma^2 \cdot \sigma^2 \tag{2.14}$$

where σ is the standard deviation of the soil parameter of concern (s_u/σ_v' in this study). It is noted that the positive square root of the variance reduction factor is referred to herein as the standard deviation reduction factor or simply the *reduction factor* (Γ) to differentiate it from the variance reduction factor Γ^2.

Unlike RFM, the FORM analysis using the variance reduction technique does not require MCS. Therefore, this approach of using the variance reduction technique requires much less computational effort and is more practical than with RFM in engineering practice. Past investigators (Peschl and Schweiger 2003; Suchomel and Mašín 2010) have shown that the reliability analysis with the variance reduction method can capture the overall trend derived with RFM.

However, the choice of characteristic length is critical to the reliability analysis with the variance reduction technique. For analysis of braced excavations in clay, it has been suggested that the characteristic length may be assumed to be the length of the sliding surface (Schweiger and Peschl 2005). In this study, an effort is made to investigate the appropriate characteristic length to use and to examine the effect of the variation of the characteristic length on the probability of basal-heave failure.

Reliability Analysis of Basal-Heave Stability Considering Spatial Variability

Random field modeling of clay for basal-heave stability analysis

Past studies (e.g., Goh et al. 2008; Wu et al. 2010a) on basal-heave stability have shown that high failure probability p_f can exist in a design that meets the minimum *FS* requirement specified in the codes. However, yielding high failure probabilities for those designs that are known to be "safe" raises questions, since the codes are generally conservative and thus exceeding the minimum *FS* requirement would indicate a safe design. One possible reason for having a higher *computed* failure probability than what the experience or the code would suggest is overestimation of the variation of soil parameters, which might be caused by the negligence of the effect of spatial variability in traditional reliability analysis.

In this study, the above issue is examined within the context of basal-heave stability. Here, basal-heave stability in a braced excavation is examined using the conventional random field model with the *Cholesky decomposition* method. The excavation case analyzed by Wu et al. (2010a), illustrated in Figure 2.1 and with

additional data shown in Table 2.1, is employed in this study. In reference to Figure 2.1 and Table 2.1, all soil and structural parameters, except the normalized undrained shear strength s_u / σ'_v, are treated as spatially-constant random variables or constants. The parameter s_u / σ'_v is modeled as a spatially random variable.

The *COV* of undrained shear strength s_u can be as high as 0.8 but typically is about 0.3 (Phoon and Kulhawy 1999a). In this study, the *COV* of s_u / σ'_v is first selected as 0.3. However, the effect of the variation of this *COV* will be examined later. According to Phoon and Kulhawy (1999a), the average horizontal and vertical scales of fluctuation for clay are 50.7m and 2.5m, respectively. Thus, only the vertical spatial randomness is modeled in this study, as the horizontal scale of fluctuation is much greater and its effect is far less significant. It should be noted that for basal-heave stability analysis in a braced excavation, only the random field from the depth of the final strut to the bottom of the diaphragm wall (see Figure 2.1) needs to be considered since the resistance moment comes only from this region.

It should be noted that the *Cholesky decomposition* method is not practical if the number of points in the random field exceeds 500 (Fenton 1997). In this study, Arc ***bcd*** on the slip circle, as shown in Figure 2.1, is subdivided by means of "equal vertical distance" into 100 small arcs (elements) which are considered sufficient in both stability analysis and random field modeling. Note that Arc ***de*** is subdivided in the same way as for Arc ***cd***. Further refinement with more than 100 elements (arcs) is not necessary as it yields practically the same results.

Figure 2.3 shows an example of the simulated spatial variability of normalized

undrained shear strength s_u / σ'_v with different scales of fluctuation (θ = 0.5m, 2.5m and 10m). As expected, the spatial variation in the case of smaller θ is much more significant than that for larger θ. As θ decreases toward zero, the random field s_u / σ'_v tends to vary drastically from point to point; conversely, as θ increases toward infinity, the random field s_u / σ'_v tends to become uniform (or spatially constant) in each simulation. Traditional reliability analysis often assumes the field to be spatially constant and the effect of spatial correlation is ignored.

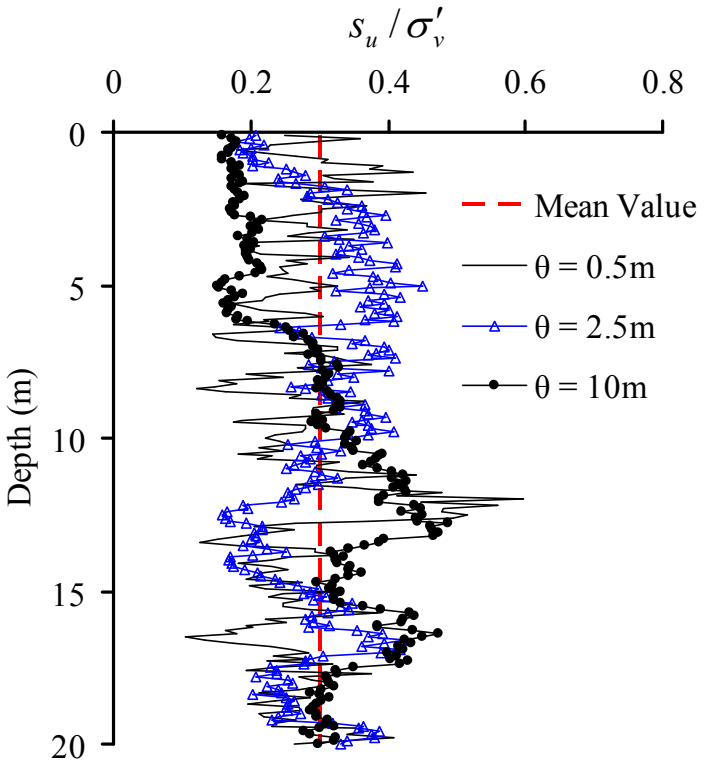

Figure 2.3: Example of simulated spatial variability of normalized undrained shear strength s_u/σ'_v by means of random field modeling.

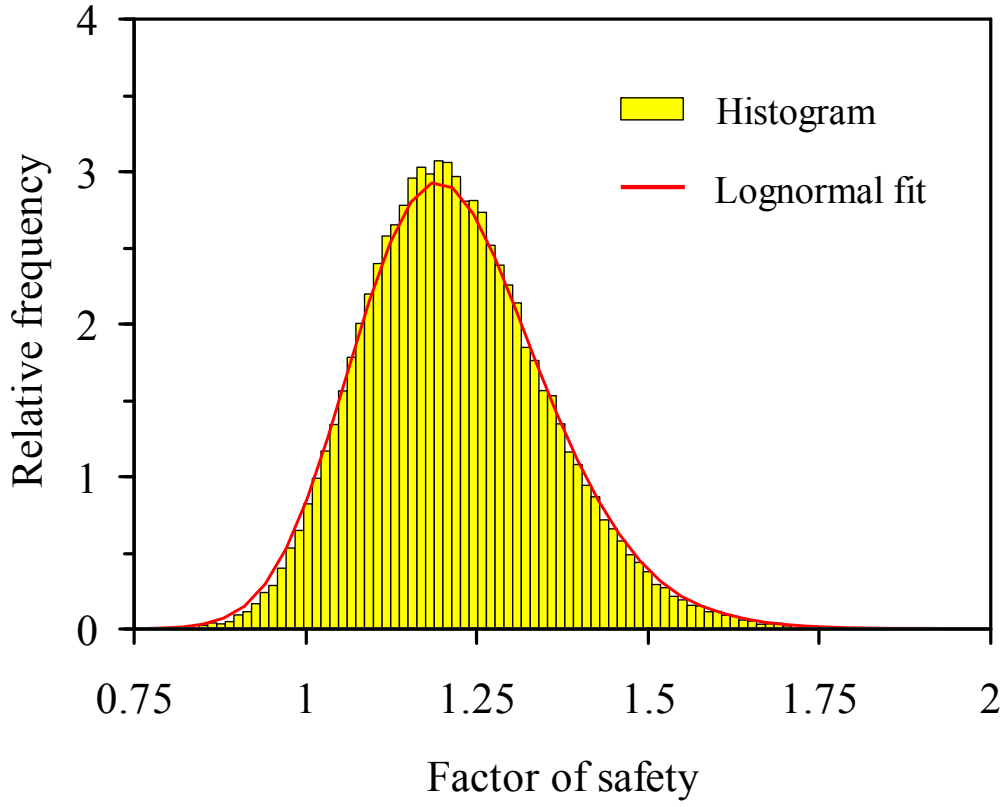

Figure 2.4: Relative frequency of the computed factor of safety using random field modeling (under the scenario that mean $s_u/\sigma'_v = 0.3$, COV of $s_u/\sigma'_v = 0.3$ and $\theta = 2.5$m).

For a given mean, *COV* and θ of s_u/σ'_v, Monte Carlo simulation (MCS) may be carried out and in each simulation, the same mean, *COV* and θ are used to generate the random field. After a sufficient number of simulations (10^5 in this study), the histogram or the probability density for the output variable (for example, *FS*) can be obtained. Figure 2.4 shows an example of histogram of the computed *FS* using the conventional RFM with 100,000 simulations under the following scenario: mean of s_u/σ'_v = 0.3, *COV* of s_u/σ'_v = 0.3 and θ = 2.5m. The shape of the histogram suggests a lognormal

distribution. The failure probability p_f is determined by the ratio of the number of simulations with $FS < 1.0$ over the total number of simulations, which is the area under the fitted curve for $FS < 1.0$.

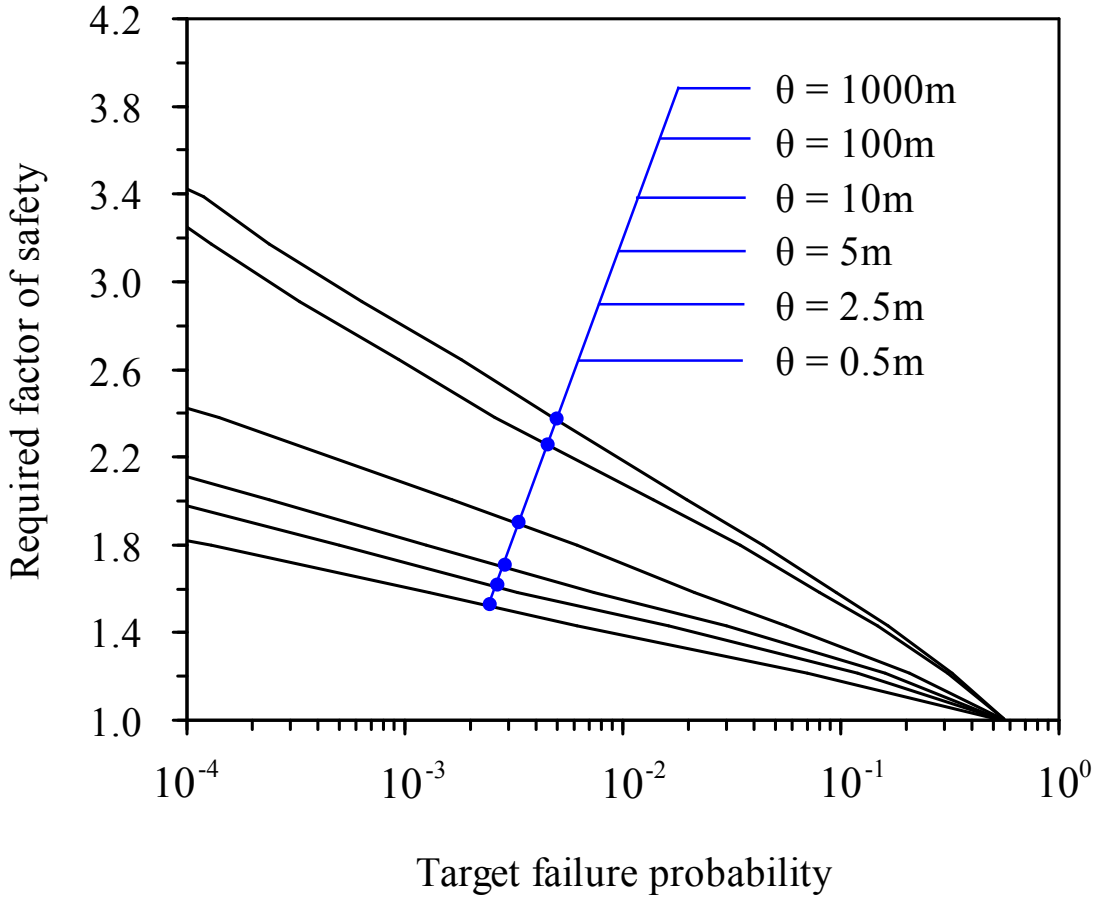

Figure 2.5: Relationship between probability of failure and factor of safety at various scales of fluctuation generated with MCS-based random field modeling.

To study the effect of spatial variability, a series of scales of fluctuation (θ = 0.5m, 2.5m , 5m, 10m, 100m and 1000m) is selected in the reliability analysis. For each scale of fluctuation, 10^5 simulations using MCS are conducted and the results are shown in

Figure 2.5. Note that for each data point in Figure 2.5, the execution time for 10^5 simulations is approximately 4 minutes on a laptop PC equipped with an Intel Pentium Dual CPU T2390 running at 1.86GHz. The effect of the scales of fluctuation is quite obvious: smaller scale of fluctuation results in smaller p_f at the same *FS*. As shown in Figure 2.5, if the target p_f is set at 10^{-3}, the required *FS* is about 1.7 at θ = 2.5m [note: this θ value is mean of the vertical scale of fluctuation for clay as per Phoon and Kulhawy 1999a], and is about 2.6 at θ = 1000m (note: this θ value is close to spatially-constant condition). On the other hand, for *FS* = 1.2, the minimum value that is adopted in many codes (JSA 1988; PSCG 2000; TGS 2001) for the design of excavations against basal-heave based on the slip circle method, the failure probability p_f is about 0.32 under the condition of θ = 1000m (≈ spatial constant). As basal-heave failure occurs infrequently, these codes are considered adequate in practice; therefore, the failure probability of 0.32 obtained from the reliability analysis that does not consider spatial variability (emulated by the case with θ = 1000m) is likely to be over-estimated.

Finally, it should be noted that the analysis of basal-heave stability presented in this section for RFM of clay is primarily used as a reference for the subsequent study of the effect of spatial variability using the variance reduction-based simplified approach.

Parametric study

A series of parametric analyses are conducted to study the influence of spatial variability on the reliability-based design of braced excavation (basal-heave stability) in clay. For these analyses, only the inherent variability and the spatial variability of

s_u / σ'_v are considered to assess the effect of the spatial correlation. All other input parameters are treated as constant parameters (only the mean values listed in Table 2.1 are used in the analysis). For s_u / σ'_v, the following ranges of parameters are analyzed:

COV = 0.1, 0.2, …, 1.0

θ = 0.5m, 1m, 2.5m , 5m, 10m, 25m, 50m, 100m, ∞

For each pair of COV and θ, 10^5 MCS runs are executed, and the mean and COV of the resulting 10^5 resistance moments M_R are obtained.

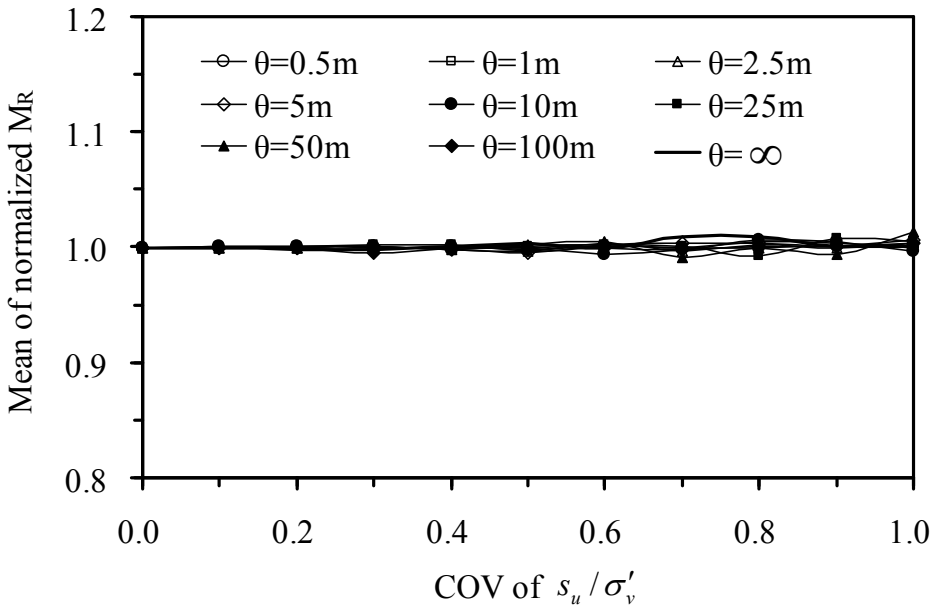

Figure 2.6: Mean of normalized resisting moment as a function of the scale of fluctuation and COV of s_u / σ'_v .

Figure 2.6 shows how the mean of the normalized M_R, defined as the ratio of the

M_R obtained from MCS for a given pair of *COV* and θ values over the M_R obtained from a deterministic analysis that uses the mean values of all input parameters, varies with the *COV* and θ of s_u/σ'_v. The mean of the normalized M_R is shown to be around 1.0, indicating that the mean of the M_R through 10^5 simulations is consistent with the deterministic solution regardless of the inherent variability and the spatial variability of s_u/σ'_v. This is expected as the resisting moment M_R in the slip circle method is a linear function of undrained shear strength s_u.

Figure 2.7 shows how the *COV* of M_R changes with the *COV* and θ of s_u/σ'_v. Two observations can be made: (1) at the same θ level, the *COV* of M_R increases almost linearly with the *COV* of s_u/σ'_v; (2) at the same *COV* of s_u/σ'_v, the *COV* of M_R increases with increasing θ and reaches the maximum value at $\theta = \infty$. The *COV* of M_R at $\theta = \infty$ approaches to the 1:1 line. As shown in Figure 2.7, smaller θ results in smaller variability of M_R, which corresponds to smaller variability of s_u/σ'_v. This observation is consistent with the concept of spatial averaging effect that a smaller scale of fluctuation results in a larger variance reduction in the soil parameters, which would yield a smaller variation of output responses.

Furthermore, the failure probability p_f for each combination of *COV* and θ is shown in Figure 2.8. The p_f increases with both *COV* and θ of s_u/σ'_v. For a given *COV*, the maximum p_f is reached at $\theta = \infty$; the implication is that the design can be too conservative without considering the effect of spatial variability of soil parameters.

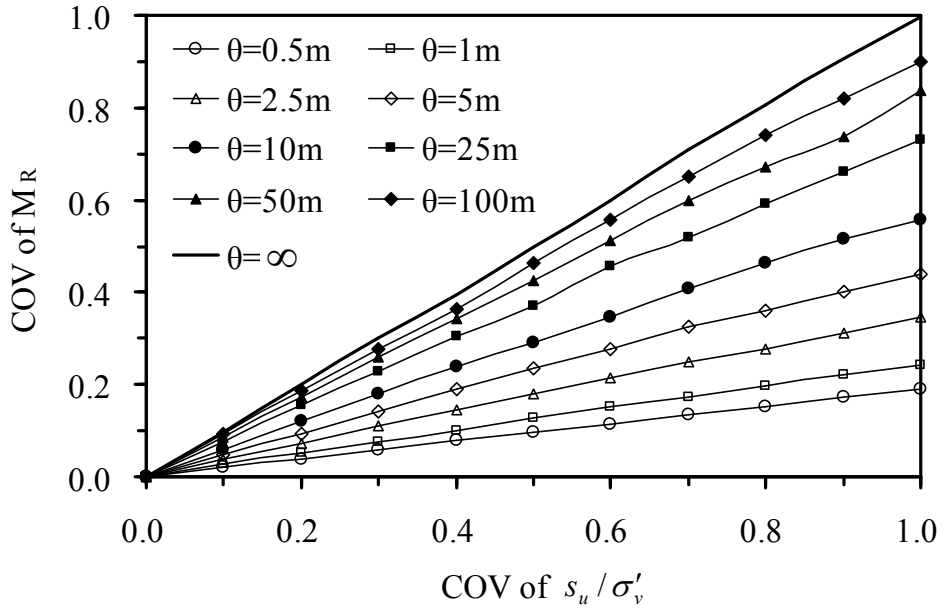

Figure 2.7: *COV* of resisting moment (M_R) as a function of the scale of fluctuation and COV of s_u/σ'_v.

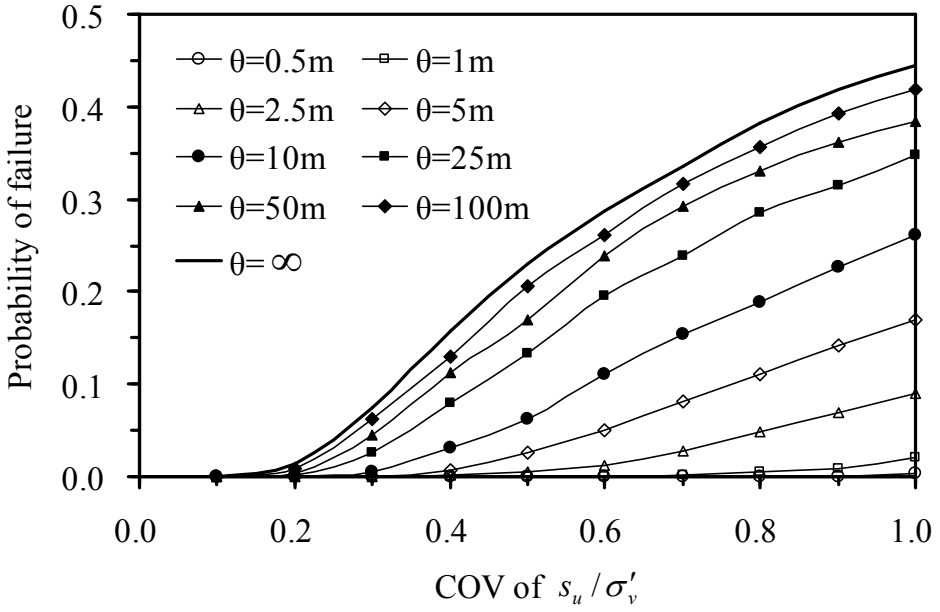

Figure 2.8: Influence of *COV* and scale of fluctuation of s_u/σ'_v on the probability of failure.

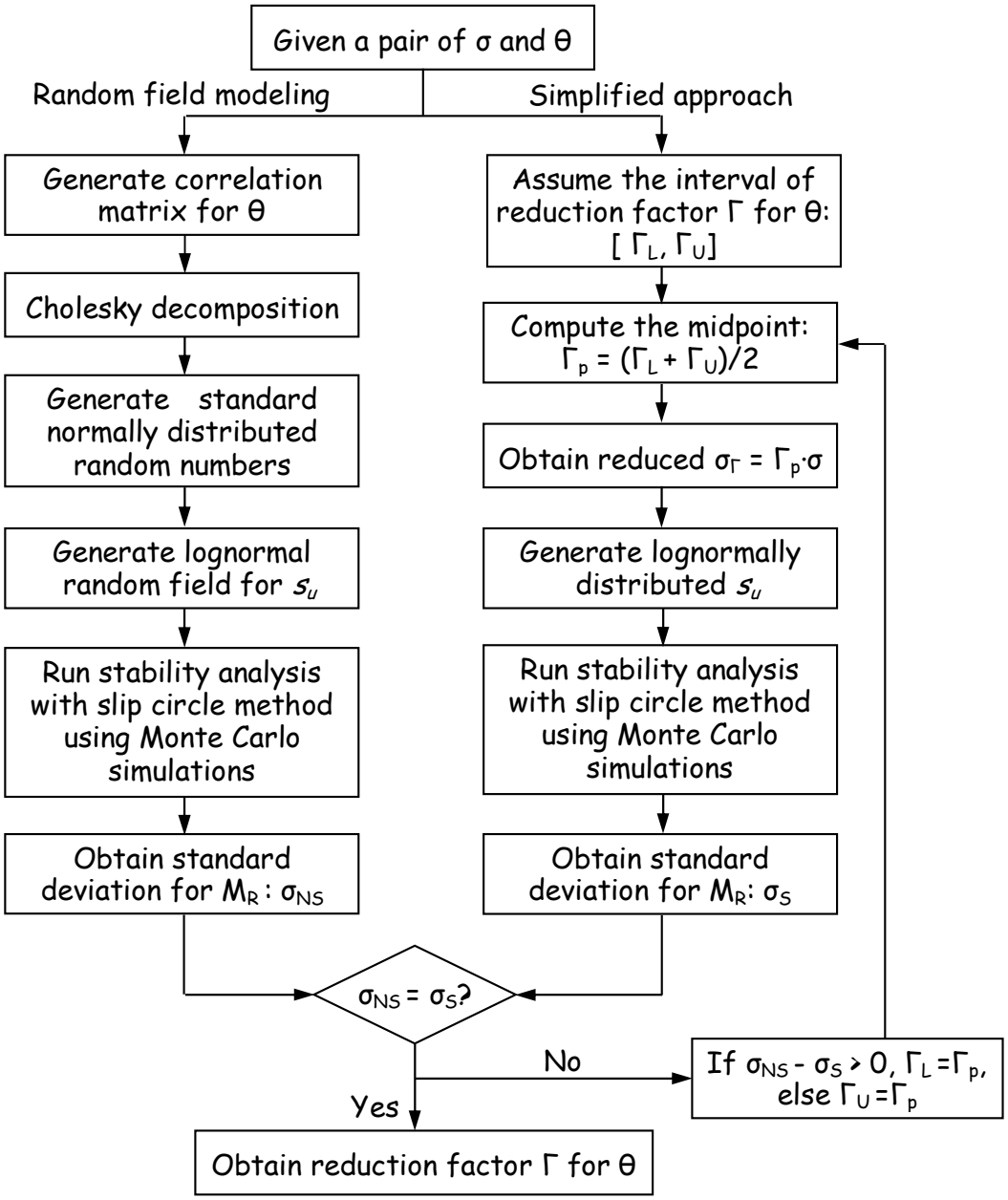

Figure 2.9: Flow chart for searching for the reduction factor for a given pair of standard deviation σ and scale of fluctuation θ.

Simplified approach using variance reduction technique

As mentioned previously, the focus of this study is on the simplified approach

using the variance reduction technique. To apply this technique, it is necessary to determine an appropriate characteristic length L. In this regard, the variance reduction factor Γ^2 for the simplified approach is first established by matching the solutions obtained from the variance reduction-based simplified approach with those by RFM. Again, only s_u / σ'_v is modeled as a spatially random variable herein in order to study the influence of the inherent variability and the spatial variability of s_u / σ'_v. All other parameters are treated as constants. The criterion for matching the two approaches (the simplified approach versus RFM) is to achieve the same level of variability of the response (M_R in this case), since the mean M_R is expected to be approximately the same (as shown in Figure 2.6). Through this calibration, the variance reduction factor Γ^2 to be used in the simplified approach for a given case is obtained. Figure 2.9 shows a flowchart for searching for the *reduction factor* Γ for a given pair of standard deviation (σ) and scale of fluctuation (θ) of s_u / σ'_v.

In Figure 2.9, the flow sequence on the left summarizes the procedure of the conventional RFM with the *Cholesky decomposition* method [Eqs. (2.7-2.12)]. After 10^5 simulations of the basal-heave stability analysis, the standard deviation of M_R (denoted as σ_{NS}) is obtained. In Figure 2.9, the flow sequence on the right summarizes the procedure of simplified approach using the equivalent variance technique. First, an interval of the reduction factor, [Γ_L Γ_U], is assumed for this case (with the same σ and θ of s_u / σ'_v). Γ_L and Γ_U are the assumed lower and upper bounds, which may be set at 0 and 1, respectively. Then the bisection method is used to search for the equivalent

variance: the interval is divided into two segments by the midpoint $\Gamma_p = (\Gamma_L + \Gamma_U)/2$, and the variance is reduced with Γ_p. With the reduced variance σ_Γ [obtained from Eq. (2.14)], MCS may be performed without the Cholesky decomposition. The standard deviation of M_R, denoted herein as σ_S, is then obtained from 10^5 MCS of the basal-heave analysis of the same case, as in the RFM analysis (left side of the flowchart shown in Figure 2.9). If the reduction factor Γ_p is correct, the two standard deviations, σ_{NS} and σ_S, will be equal to each other for the given pair of standard deviation σ and scale of fluctuation θ of s_u/σ'_v. In this study, the Γ value at which $\sigma_{NS} \approx \sigma_S$ (or $|\sigma_{NS} - \sigma_S|/\sigma_{NS} \le 10^{-3}$) is the target reduction factor for a given pair of σ and θ of s_u/σ'_v. As shown in Figure 2.9, if the above stopping criterion ($|\sigma_{NS} - \sigma_S|/\sigma_{NS} \le 10^{-3}$) is not satisfied, the interval of Γ is shortened by setting $\Gamma_L = \Gamma_p$ (for $\sigma_{NS} - \sigma_S > 0$) or $\Gamma_U = \Gamma_p$ (for $\sigma_{NS} - \sigma_S < 0$). The new midpoint Γ_p is then computed and the aforementioned procedure is repeated until the final reduction factor for a given pair of σ and θ of s_u/σ'_v is obtained. It should be noted that for this "equivalency" analysis, the simplified approach is implemented with the MCS. As will be shown later, the simplified approach can also be implemented with FORM to further reduce the computational effort.

Figure 2.10 shows the *back-calculated* Γ values for various pairs of σ (or *COV*) and θ of s_u/σ'_v using the MCS-based RFM approach. It is apparent that the inherent variability rarely influences the variance reduction at the same θ level. The reduction factor Γ depends only on θ at the same *COV* level, which is consistent with the variance reduction models presented in the literature (e.g., Vanmarcke 1983).

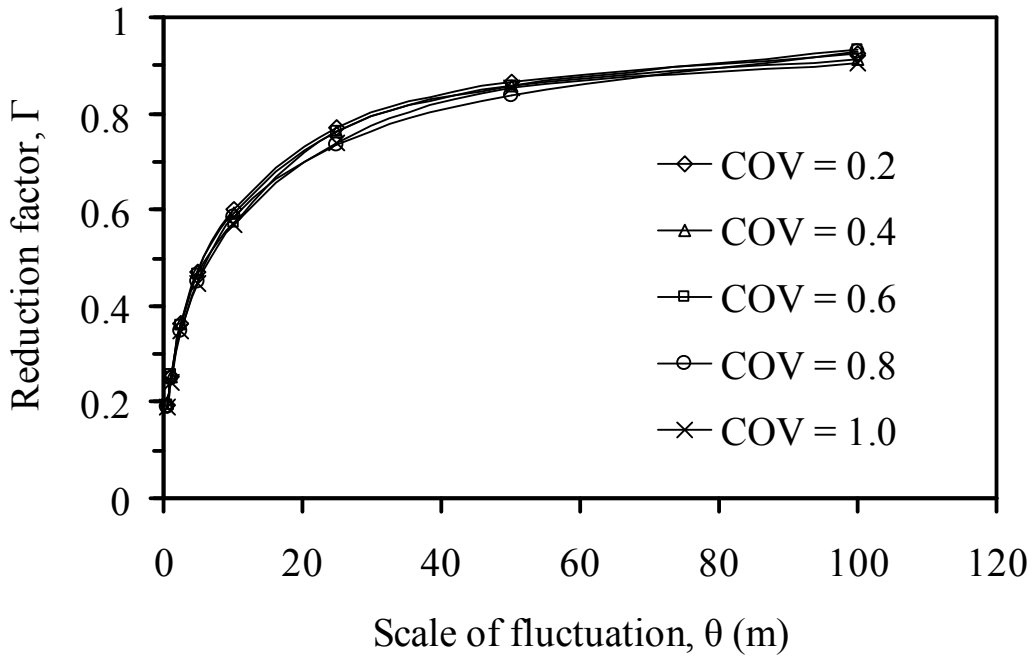

Figure 2.10: Back-calculated reduction factor Γ for various scales of fluctuation.

Alternatively, the reduction factor Γ can also be determined using the variance reduction function if the characteristic length is known. To find an appropriate characteristic length for the basal-heave problem, the reduction factors are evaluated using the exponential model [Eq. (2.13)] with three *assumed* characteristic lengths: (1) L = 27m, (2) L = 39m, and (3) L = 98m. The first characteristic length L = 27m is the distance $\overline{od}$ (from the depth of the final strut to the bottom of the diaphragm wall), as shown in Figure 2.1. This length is the vertical scale of the spatially random region. The second characteristic length L = 39m is the length of Arc ***cd***, and the third characteristic length L = 98m is the length of the sliding surface (Arc ***abcde***). The reduction factors computed with the assumed characteristic lengths are shown in Figure 2.11 and compared

with the back-calculated reduction factors obtained previously. As shown in Figure 2.11, the assumption of L = 27m yields reduction factors that are most consistent with those back-calculated using the MCS-based RFM approach. This is reasonable as L = 27m is actually the distance between the depth of the final strut to the bottom of the diaphragm wall, which is the only region that contributes to the resistance moment in the random field. Thus, the above analysis shows that the vertical "averaging" length in the random field modeling of the basal-heave stability can be taken as the distance between the depth of final strut and the bottom of the diaphragm wall.

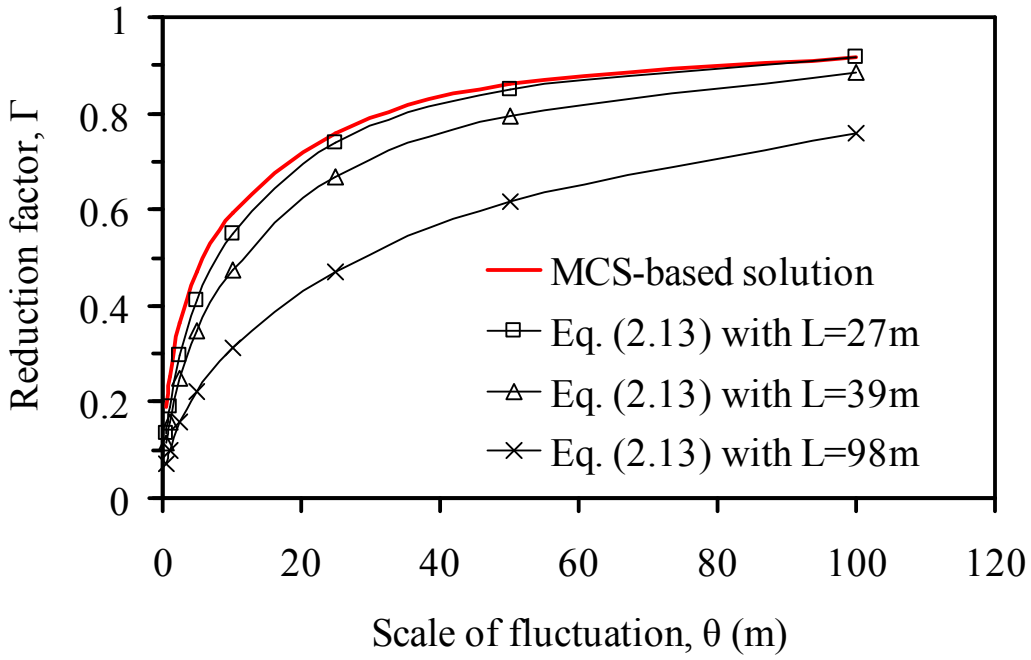

Figure 2.11: Comparison between the reduction factors back-calculated using the MCS-based RFM and those derived based on Eq. (2.13) with different assumed characteristic lengths.

In summary, the variance reduction-based simplified approach is suitable for basal-heave stability analysis if an appropriate characteristic length (and thus reduction factor) can be determined. The variance reduction-based simplified approach yields almost identical results with those obtained using the MCS-based RFM approach; however, the former is easy to apply, less demanding on resources, and offers significant advantages in engineering practice.

It should be noted that the approach described above (Figure 2.9) for back-calculating the variance reduction factor and characteristic length is demonstrated to be effective for the problem of basal heave that involves a linear limit state that has an explicit form. For other geotechnical problems that involve more complicated and nonlinear limit states, further study is needed to examine its general applicability.

Reliability-Based Design Considering Spatial Variability

With the validated variance reduction technique for basal-heave stability, the reliability analysis using FORM, in lieu of MCS, can be performed, which is an effective and efficient means to consider spatial variability. The principle and procedure of FORM is well documented (e.g., Ang and Tang 1984). A spreadsheet solution implementing FORM (Low and Tang 1997) has shown to be effective and can be a practical tool in engineering practice. Figure 2.12 shows the setup of a spreadsheet solution for reliability analysis of the braced excavation case presented previously (see Figure 2.1 and Table 2.1).

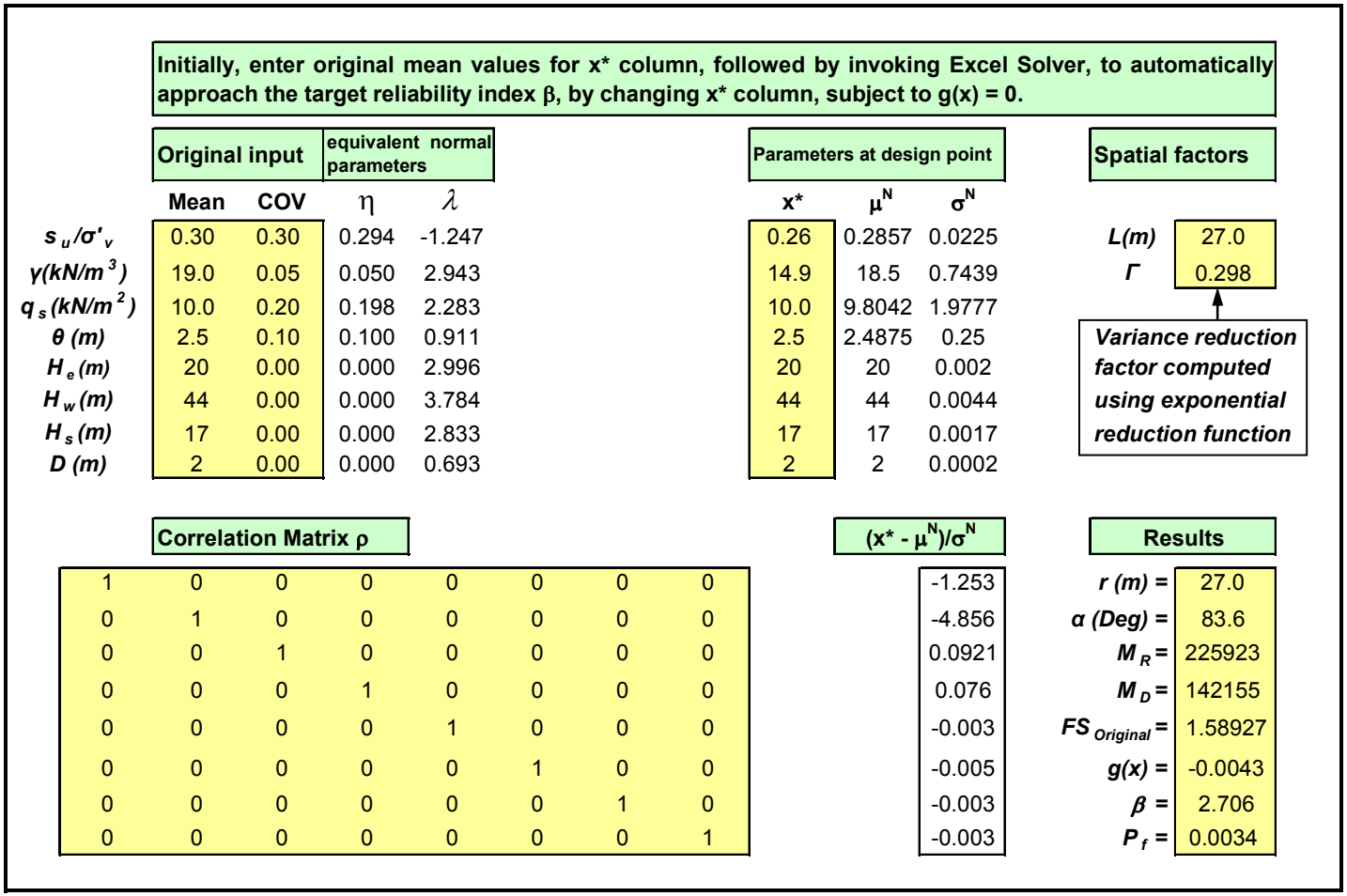

Figure 2.12: Reliability-based procedure for evaluating failure probability of basal-heave.

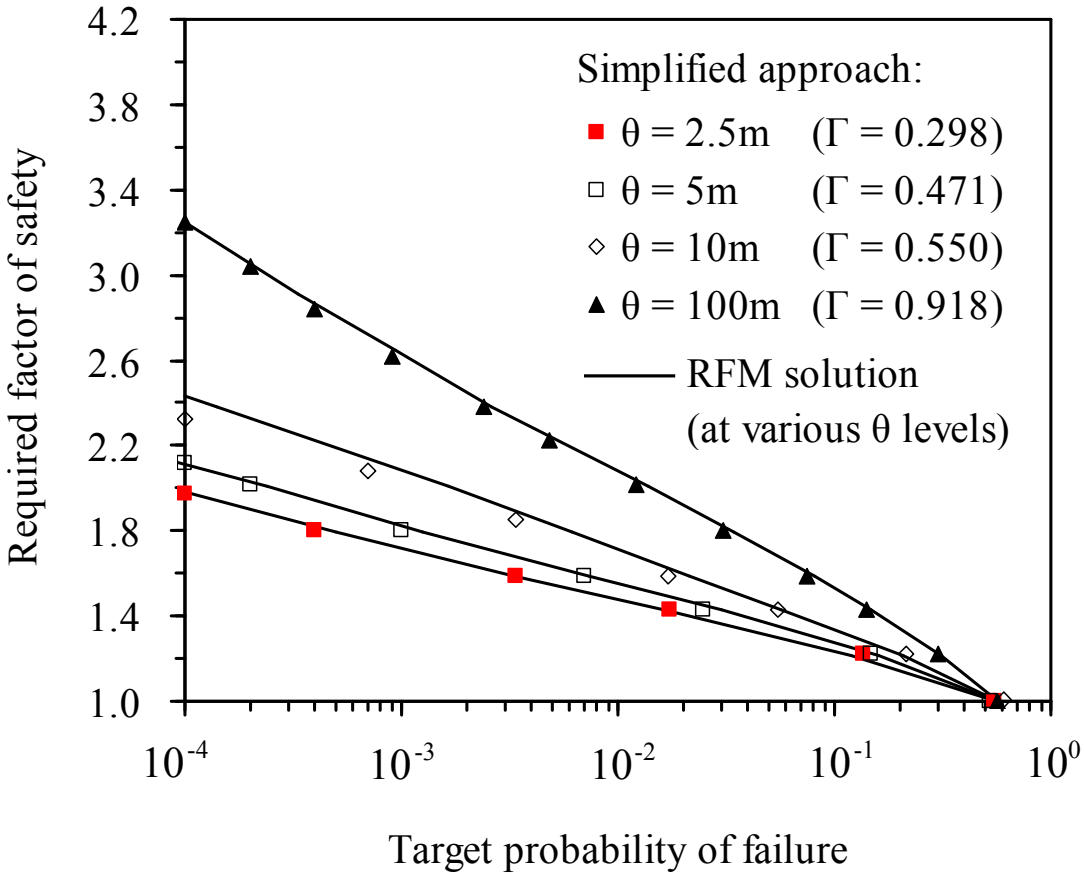

Figure 2.13: Comparison between the MCS-based random field modeling and the simplified approach.

Since the scale of fluctuation is found to be an important parameter, and knowledge about which is limited, it should be of interest to also examine the effect of the possible uncertainty of this parameter. Thus, the scale of fluctuation θ of s_u / σ'_v is treated as a lognormally distributed random variable in the spreadsheet solution as shown in Figure 2.12. The simplified approach to consider the spatial effect of s_u / σ'_v is realized using the exponential variance reduction function [Eq. (2.13)]. All other input parameters are treated as spatially-constant random variables or simply constants.

With the spreadsheet solution set up as shown in Figure 2.12, the influence of spatial variability can easily be assessed by considering several scales of fluctuation: θ = 2.5m, 5m, 10m and 100m. For this series of analysis, the scale of fluctuation is considered as a constant input, which is typical for these kinds of studies. The relationship between p_f and *FS* for each scale of fluctuation is numerically derived, as shown in Figure 2.13. The reduction factor derived from the spreadsheet solution is also shown in Figure 2.13. For comparison purposes, the results from the conventional RFM conducted in this study (presented previously in Figure 2.5) are re-drawn and also included in Figure 2.13. Again, both approaches (RFM versus the simplified approach using FORM with variance reduction) yield approximately the same results. Furthermore, the significant effect of spatial variability on the computed failure probability can be observed.

Finally, the effect of uncertainty in the scale of fluctuation in the reliability analysis of basal-heave stability is examined. As an example in this demonstration analysis, the *COV* of the scale of fluctuation is set to 0.1, 0.3, 0.6 and 0.9; the scale of fluctuation is set to the typical mean value of 2.5m and the COV of s_u/σ'_v is set to 0.3. The influence of uncertainty (in terms of *COV*) in the scale of fluctuation on the computed failure probability is shown in Figure 2.14. It is found that for *FS* smaller than 1.2, the variability of the scale of fluctuation has virtually no effect on the computed failure probability p_f. For *FS* greater than 1.2, the predicted p_f increases with the increasing variability of the scale of fluctuation. Since the required minimum *FS* in the design against basal-heave using the slip circle method is 1.2 (JSA 1988; PSCG 2000;

TGS 2001), the effect of the variability of the scale of fluctuation is far less significant than the mean scale of fluctuation itself.

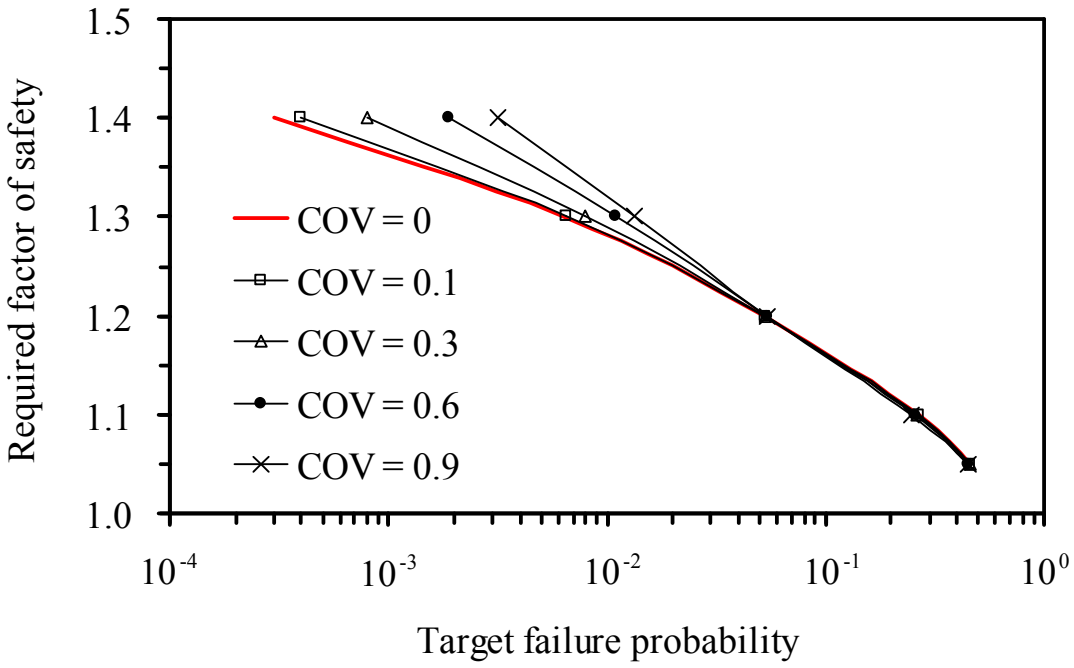

Figure 2.14: Effect of uncertainty in the scale of fluctuation on the probability of failure against basal-heave in a braced excavation in clay (scale of fluctuation = 2.5m, *COV* of $s_u/\sigma'_v = 0.3$).

Practical engineering application

In the reliability-based design against basal-heave considering the effect of spatial variability, it is desirable to facilitate the design procedure with design chart that relates the traditional design index (such as the required factor of safety) to the degree of spatial effect (such as the scale of fluctuation). In this regard, the previous analysis results are further interpreted and the relationship between the required factor of safety and the scale of fluctuation at a certain failure probability can be obtained. Figure 2.15 shows such a

relationship at failure probability of 10^{-3}. It should be noted that 10^{-3} satisfies the expected performance level of *above average* as classified by U.S. Army Corps of Engineers (1997). Similar design charts may be obtained at various levels of target failure probability. Using the design chart such as Figure 2.15, the reliability-based design may be realized by meeting the required factor of safety at a project site that is characterized with a scale of fluctuation through site investigation.

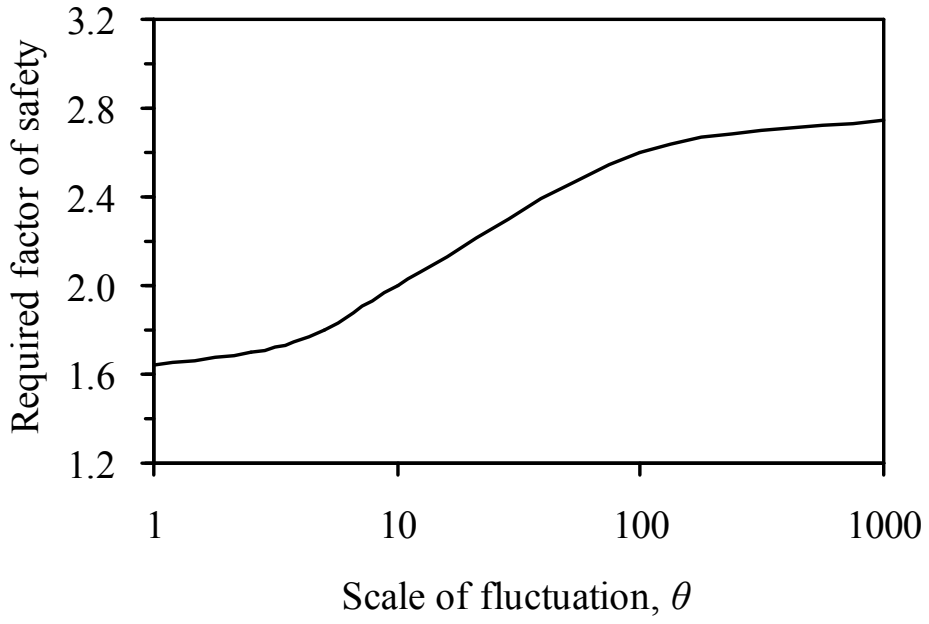

Figure 2.15: Relationship between required factor of safety and scale of fluctuation at failure probability of 10^{-3}.

Procedure for applying the proposed approach

The proposed simplified approach for reliability analysis of basal-heave stability in a braced excavation considering the spatial variability of soils is summarized into the following procedure:

1. Select the analytical model for the basal-heave stability analysis of a braced excavation in clay [for example, slip circle method as per JSA (1988)].
2. Determine the variation of soil parameters (such as undrained shear strength) described with their *COVs* and the spatial variability, defined by the correlation function and scale of fluctuation, based on site investigation, soil testing, and engineering judgment guided by published literature.
3. For the basal-heave stability analysis in a braced excavation in clay, the spatial variability of soil parameters such as undrained shear strength can be modeled with a one-dimensional (vertical) random field as stated previously. In this random field model, the characteristic length is taken as the distance from the final strut to the bottom of the diaphragm wall. The variance reduction factor (Γ^2) is then evaluated using Eq. (2.13) with this characteristic length, and finally the reduced variance (σ_{Γ}^2) for this spatially random soil parameter can be determined with Eq. (2.14).
4. With the reduced variance of the undrained shear strength, reliability analysis can be performed using traditional reliability methods such as FORM for the probability of failure against the basal-heave. The solution can easily be implemented in a spreadsheet as shown in Figure 2.12. Reliability or probability-based design can be realized by meeting a target probability of failure against the basal-heave.

Summary

In this chapter, the influence of one-dimensional spatial variability of soil parameter on the reliability analysis of basal-heave stability is presented. The results of RFM of s_u / σ'_v using the Cholesky decomposition method shows that the model with a smaller scale of fluctuation would yield a greater variance reduction in soil parameters (such as s_u / σ'_v), which in turn would yield a smaller variation in the output responses (for example, *FS* against basal-heave). The computed probability of basal-heave failure can be too high if the spatial variability is not considered in the reliability analysis. Thus, the basal-heave stability design will be too conservative if the effect of spatial variability is ignored.

A variance reduction-based simplified approach for the reliability-based design against basal-heave failure in a braced excavation is presented. The proposed simplified approach with variance reduction technique is shown to be able to produce almost identical results with those obtained using the MCS-based RFM approach, provided that an appropriate characteristic length (and thus the reduction factor) can be determined. For the basal-heave stability case in this study, the appropriate characteristic length for the exponential reduction function is determined to be the distance from the final strut to the bottom of the diaphragm wall, which is the vertical scale of the random field in this case. This approach can be implemented in a spreadsheet and requires far less computational effort than the MCS-based RFM approach, is easy to use, and has potential in geotechnical reliability-based design that deals with spatial variability of soils.

CHAPTER III

RELIABILITY ANALYSIS OF BASAL-HEAVE IN A BRACED EXCAVATION IN A TWO-DIMENSIONAL RANDOM FIELD*

Introduction

As demonstrated in Chapter II, the traditional reliability analysis that does not account for the effect of one-dimensional (1-D) spatial variability tends to overestimate the failure probability in the study on basal-heave stability using the slip circle method. Similar conclusions have also been reported in the literature, e.g., Wu et al. (2010a) reported in their reliability analysis of basal-heave failure, it was found that the failure probability tends to be overestimated if the effect of 1-D spatial variability is neglected. Considering that none of the previous studies consider the effect of the two-dimensional (2-D) random field in the basal-heave problem, the methodology including the simplified approach for the 1-D random field study developed in Chapter II, is employed and extended herein for the 2-D random field study.

In this chapter, a simplified approach to consider the effect of spatial variability in a 2-D random field for reliability analysis of basal-heave in a braced excavation in clay is formulated. This simplified approach is demonstrated through a case study. As the first step, the 2-D RFM analysis is performed in a study of basal-heave stability to provide a benchmark. Then, variance reduction factors for both vertical and horizontal directions, at which the simplified approach yields results that match well with those obtained with

* A similar form of this chapter has been published at the time of writing: Luo Z, Atamturktur S, Cai Y, Juang CH. Reliability analysis of basal-heave in a braced excavation in a 2-D random field. Computers and Geotechnics, doi:10.1016/j.compgeo.2011.08.005.

RFM, are back-calculated. Next, assumptions of the characteristic lengths of both vertical and horizontal directions in the stability analysis are verified based on the back-calculated variance reduction factors. Finally, a simplified approach which combines the first-order reliability method (FORM) and the variance reduction technique to account for spatial variability is proposed for reliability analysis of basal-heave stability. The proposed approach is easy to use, requires less computational effort, and yields results (in terms of probability of basal-heave failure) that are nearly identical to those obtained with the MCS-based RFM method.

Two-Dimensional Random Field Modeling of s_u/σ'_v

Conventional random field modeling of s_u/σ'_v

In this chapter, the slip circle method (JSA 1988; PSCG 2000; TGS 2001) for determining *FS* against basal-heave in soft clay is adopted for its simplicity and suitability for modeling the random field of undrained shear strength. The details of this method is documented in Chapter II [Eqs. (2.1-2.3)]. As reflected in the formulation [Eqs. (2.1-2.3)] of the slip circle method, the undrained shear strength (s_u) of clay plays a critical role in the design of a braced excavation against basal-heave. In other words, *FS* is a function of s_u and other parameters.

As noted previously, the first step toward developing a simplified reliability-based procedure for evaluating the probability of basal-heave failure in an excavation in clay with significant spatial variability is to establish a benchmark using the MCS-based RFM. A two-dimensional RFM approach is deemed especially suitable for the basal-heave

problem analyzed with the slip circle method (Figure 3.1).

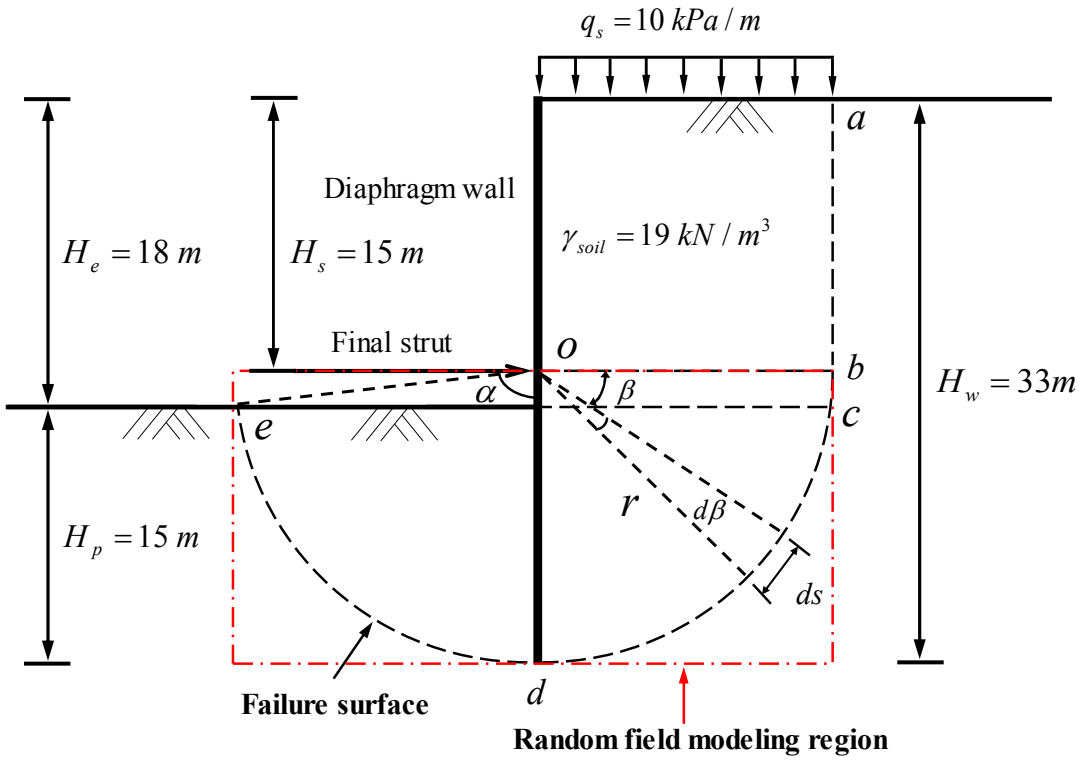

Figure 3.1: Geometry of slip circle method and 2-dimensional random field modeling region for basal-heave stability analysis.

The undrained shear strength generally increases with depth for most normally consolidated clay but the ratio of undrained shear strength over the effective overburden stress (s_u/σ'_v) remains roughly constant (Ladd and Foott 1974). Thus, in this study the parameter s_u/σ'_v is modeled using lognormal random field, and all other input parameters are modeled as *spatially-constant* lognormal variables or constants. The assumption of lognormal distribution for inherent soil variability assures positive soil parameters and has been widely advocated by past studies (e.g., Phoon and Kulhawy

1999b). In RFM, the uncertainty of s_u/σ_v' is represented by its spatially-constant mean $\mu_{\ln}$ and coefficient of variation $COV_{\ln}$ and its scale of fluctuation θ. Thus, the basal heave problem here involves a stationary random field modeling of s_u/σ_v'. The standard deviation and mean of the equivalent normal distribution of s_u/σ_v', denoted as $\ln(s_u/\sigma_v')$, are expressed as:

$$\sigma_n = \sqrt{\ln\left(1+COV_{\ln}^2\right)} \tag{3.1}$$

$$\mu_n = \ln\mu_{\ln} - \frac{1}{2}\sigma_n^2 \tag{3.2}$$

where "*n*" denotes normal distribution and "*ln*" denotes lognormal distribution. The lognormally distributed random field of s_u/σ_v' can be generated through the following transformation (Fenton et al. 2005):

$$s_u/\sigma_v'(x_i) = \exp\{\mu_n + \sigma_n \cdot G_n(x_i)\} \tag{3.3}$$

where x_i is the spatial position at which s_u/σ_v' is modeled; $G_n(x_i)$ is a normally distributed random field with zero mean, unit variance and correlation function $\rho(\tau)$. In this study, the exponential correlation function, which is commonly used in random field modeling, is selected (Jaksa et al. 1999):

$$\rho(\tau) = \exp\left(-\frac{2\tau}{\theta}\right) \tag{3.4}$$

where τ is the absolute distance between any two points in the random field and θ is the scale of fluctuation. As shown in a previous study, the vertical and the horizontal scales of fluctuation in the field for clay are generally different (Phoon and Kulhawy 1999a). In the 2-D RFM, Eq. (3.4) may be modified to consider the unequal scales of fluctuations (Suchomel and Mašín 2011):

$$\rho(\tau) = \exp\left[-2\sqrt{\left(\frac{\tau_v}{\theta_v}\right)^2 + \left(\frac{\tau_h}{\theta_h}\right)^2} \right] \tag{3.5}$$

where τ_v and τ_h are the absolute vertical and horizontal distance between any two points in the random field, respectively; and θ_v and θ_h are the vertical and the horizontal scales of fluctuation, respectively. In this study, the correlation matrix built with the correlation function is decomposed by *Cholesky decomposition* which has been proved simple and effective (Fenton 1997; Suchomel and Mašín 2010):

$$L \cdot L^T = \rho \tag{3.6}$$

With the matrix L, the correlated standard normal random field can be obtained by linearly combining the independent variables as follows (Fenton 1997):

$$G_n(x_i) = \sum_{j=1}^{i} L_{ij} Z_j \qquad i = 1, 2, \cdots, M \tag{3.7}$$

where M is the number of points in the random field; Z_j is the sequence of independent standard normally distributed random variables.

The normalized undrained shear strength s_u/σ'_v at each spatial position in the random field can be obtained with Eq. (3.3) for a specified mean, standard deviation, and scale of fluctuation using Monte Carlo simulation. In each simulation, the same mean, standard deviation, and scales of fluctuation of s_u/σ'_v are used. The statistics of output such as *FS* [Eq. (2.1)] can be obtained after a sufficient number of simulations are carried out. The failure probability p_f is computed as the ratio of the number of simulations that yield failure ($M_R < M_D$ or $FS < 1$) over the total number of simulations *N*. The number of MCS samples should be at least 10 times of the reciprocal of the target failure probability (Ang and Tang 2007; Wang et al. 2011a). In this study, the level of failure probability of interest is greater than 10^{-4}, therefore N is set at 10^5.

Figure 3.2 shows the results of random field modeling at four combinations of θ_v and θ_h given as an example the mean of s_u/σ'_v = 0.3 and coefficient of variation (COV) = 0.3: (a) $\theta_h = \theta_v = 2.5$m; (b) $\theta_h = \theta_v = 10$m; (c) $\theta_h = 2.5$m, $\theta_v = 10$m; and (d) $\theta_h = 10$ m, $\theta_v = 2.5$m. The RFM region shown in Figure 3.2 includes 36 by 18 square elements with element size of 1m. Considering that the aforementioned RFM procedure is defined at the point level, the local averaging over the square element size is performed to obtain the locally averaged statistics. The local averaging is realized through multiplying a variance reduction factor to the variance of a normal variable. Then the statistics of the equivalent lognormal variable are computed (Griffiths and Fenton 2004; Suchomel and Mašín 2011). As shown in Figure 3.2, the darker color represents higher s_u/σ'_v and lighter color represents smaller s_u/σ'_v. The effect of scales of fluctuation is apparent in the 2-D RFM:

either in the vertical or horizontal direction, smaller θ corresponds to more drastic variation of s_u/σ'_v in that direction of the random field; conversely, a larger θ corresponds to more uniform s_u/σ'_v in that direction of the random field. In either direction, the spatial variation in the case of smaller θ is much more significant than that for larger θ.

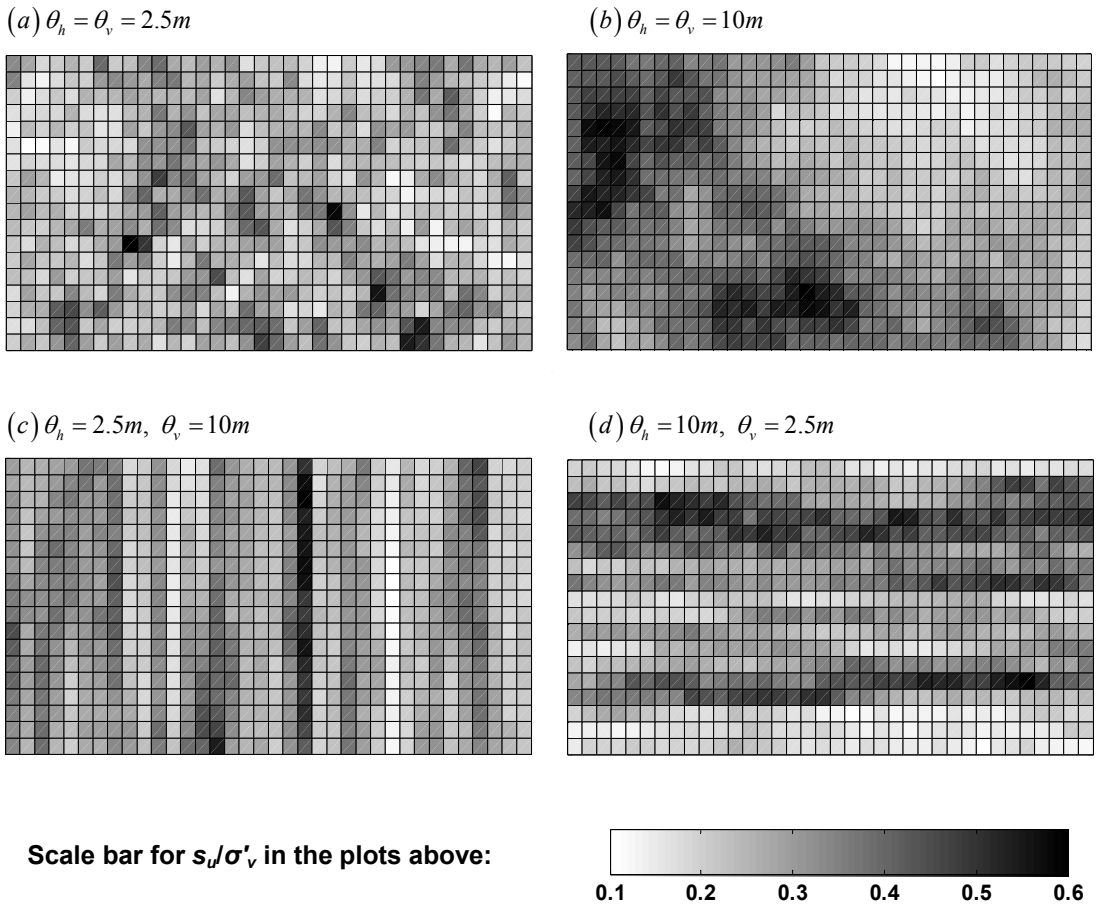

Figure 3.2: Influence of scale of fluctuation on the 2-D random field modeling of s_u/σ'_v at given mean of 0.3 and *COV* of 0.3.

Simplified approach based on equivalent variance technique

The second step toward developing a simplified reliability-based procedure for evaluating the probability of basal-heave failure is to establish a simplified solution that matches closely with the MCS-based RFM solution.

The simplified approach is based on the concept of *spatial averaging* in which the spatial variability of the soil property is averaged in order to approximate a random variable that represents a soil parameter (Vanmarcke 1977). The averaged variability of the soil property over a larger domain can be quantified with an *variance reduction technique* in which the variances of soil parameters may be reduced by multiplying a factor known as *variance reduction factor* (Γ^2). With two inputs: scale of fluctuation and characteristic length, the variance reduction factor that adopts an exponential form is given as follows (Vanmarcke 1983):

$$\Gamma^2 = \frac{1}{2}\left(\frac{\theta}{L}\right)^2\left[\frac{2L}{\theta} - 1 + \exp\left(-\frac{2L}{\theta}\right)\right] \tag{3.8}$$

where θ is the scale of fluctuation and L is the characteristic length.

In the 2-D random field, the variance reduction factor is expressed as the product of the variance reduction factors in the vertical and horizontal directions, computed with respective scales of fluctuation and characteristic length (Vanmarcke 1977):

$$\Gamma^2 = \Gamma_v^2 \cdot \Gamma_h^2 \tag{3.9}$$

where Γ_v^2 and Γ_h^2 are the vertical and horizontal variance reduction factors,

respectively. The reduced variance σ_{Γ}^{2} can be obtained with the following equation:

$$\sigma_{\Gamma}^{2} = \Gamma^{2} \cdot \sigma^{2} \tag{3.10}$$

where σ^{2} is the variance of the soil parameter of concern (s_u / σ_v' in this study). In this study, the positive square root of the variance reduction factor is referred to herein as the *reduction factor* (Γ) to differentiate it from the variance reduction factor (Γ^{2}).

It is noted that if the variance reduction technique is used to simplify the effect of the spatial variability of a lognormal distributed parameter, as is the case in this study, only the variance of its equivalent normal distribution, defined previously, should be reduced through the use of variance reduction factor.

For the simplified approach using the equivalent variance technique, the analysis can be conducted either with MCS or with a reliability method. The latter is preferred, as it requires far less computational effort and is more practical than the MCS-based RFM. Implementation of the reliability methods in a spreadsheet has been demonstrated to be a practical approach to geotechnical problems (e.g., Low and Tang 1997; Juang et al. 2006; Juang et al. 2009). Past investigators (Peschl and Schweiger 2003; Suchomel and Mašín 2010) have shown that reliability analysis with the equivalent variance technique can capture the overall trend of the MCS-based RFM. In this chapter, the two approaches are compared within the context of 2-D random field modeling.

Simplified Reliability Method for Assessing Probability of Basal-Heave Failure in Braced Excavation in 2-D Random Field

RFM approach for probability of basal-heave failure

The probability of basal-heave failure in a braced excavation in clay is first analyzed herein using the conventional random field modeling with *Cholesky* decomposition method. The geometry and input data for the excavation case employed in this study is illustrated in Figure 3.1 and listed in Table 3.1, respectively. The undrained shear strength s_u / σ'_v is modeled as a spatially random variable, and the unit weight of soil and surcharge are modeled as spatially-constant random variables. All other geotechnical and structural parameters are treated as constants for simplicity, since the uncertainties in these parameters are relatively negligible.

Table 3.1: Input parameters for a basal-heave stability problem shown in Figure 3.1.

Parameters	Notations	Values	
		Mean	COV
Unit weight of soil	γ	19 kN/m^3	0.1
Surcharge	q_s	10 kPa/m	0.2
Depth of GWT	D	2m	N/A
Final excavation depth	H_e	18m	N/A
Final strut depth	H_s	15m	N/A
Penetration depth	H_p	15m	N/A

*In this study, many basal-heave problems defined with this set of input parameters and geometry are analyzed. The difference in these problems is in the choice of the mean value of the normalized undrained shear strength (s_u / σ'_v), which results in different factors of safety (*FS*).

Typical *COV* of the undrained shear strength s_u is about 0.3, although it could be as high as 0.8 (Phoon and Kulhawy 1999a). In this study, the *COV* of s_u / σ'_v is first set at 0.3 and the effect of assuming higher *COV*s is examined later. Based on a statistical study by (Phoon and Kulhawy 1999a), the average vertical and horizontal scales of fluctuation for clay are 2.5m and 50.7m, respectively. In a 2-D RFM, both vertical and horizontal spatial variability are considered. It should be noted that for basal-heave analysis, only the random field shown in Figure 3.1 (the box region) needs to be modeled since the resistance moment [Eq. (2.3) in Chapter II] comes only from this region. Here, the RFM region in Figure 3.1 is subdivided into 36 by 18 square elements (horizontal direction by vertical direction). The size of the square elements is 1m. For this 2-D RFM, the total number of elements (648 elements in this case) is comparable to the suggested maximum number by Fenton (1997) for the Cholesky decomposition operation. Although a larger modeling region can be adopted, the region shown in Figure 3.1 is the minimum region that covers the slip circle where the resistance moment M_R is derived.

To provide a reference, the effect of vertical and horizontal scales of fluctuation is first examined *separately* (i.e., treating it like 1-D RFM). Thus, when vertical or horizontal spatial variability is considered, the other direction is assumed to be spatially constant. To study the effect of spatial variability, a series of scales of fluctuation (θ = 1m, 2.5m, 10m, and 100m) for each direction is investigated.

Thus, given a set of input data for a braced excavation (Figure 3.1 and Table 3.1), the probability of basal-heave failure is computed for a design with a given *FS* [say, *FS* = 2.0 as per Eq. (2.1) in Chapter II] and a given scale of fluctuation that reflects the 1-D

random field of s_u/σ'_v. This probability can be calculated using the MCS. For each given scale of fluctuation and design *FS*, 10^5 simulations are conducted. The probability of failure is determined by the ratio of the number of failure cases (defined here as *FS* < 1.0) over the total number (i.e., 10^5). This process is repeated for each series of scale of fluctuation and each series of "designs" (signaled by a series of *FS* values, which was realized by assuming different mean s_u/σ'_v values while keeping the mean values of all other parameters the same). For a single run of MCS, the execution time for 10^5 simulations is approximately 4 minutes on a laptop PC equipped with an Intel Pentium Dual CPU T2390 running at 1.86GHz using MATLAB (MathWorks 2010). The results are shown in Figure 3.3(a) for vertical spatial variability and Figure 3.3(b) for horizontal spatial variability. The results presented in this figure provide the engineer a basis for selecting a factor of safety for design against basal-heave using the slip circle method [Eqs. (2.1-2.3)]. This basis is the target probability of failure that considers the spatial variability of soil parameters. The design, based on the target probability of failure is referred to herein as the probability-based (or reliability-based) design against basal-heave failure.

The effect of scales of fluctuation in a 1-D random field is quite obvious: a smaller scale of fluctuation results in a smaller p_f at the same *FS*. As shown in Figure 3.3(a), if the target p_f is set at 10^{-3}, the required *FS* is about 1.85 at θ_v = 2.5m [note: this θ_v value is the mean of the vertical scale of fluctuation for clay as per Phoon and Kulhawy (1999a)], and is about 2.65 at θ_v = 100m (note: this θ_v value is close to a spatially-constant condition). Similar conclusions may be drawn from Figure 3.3(b) for

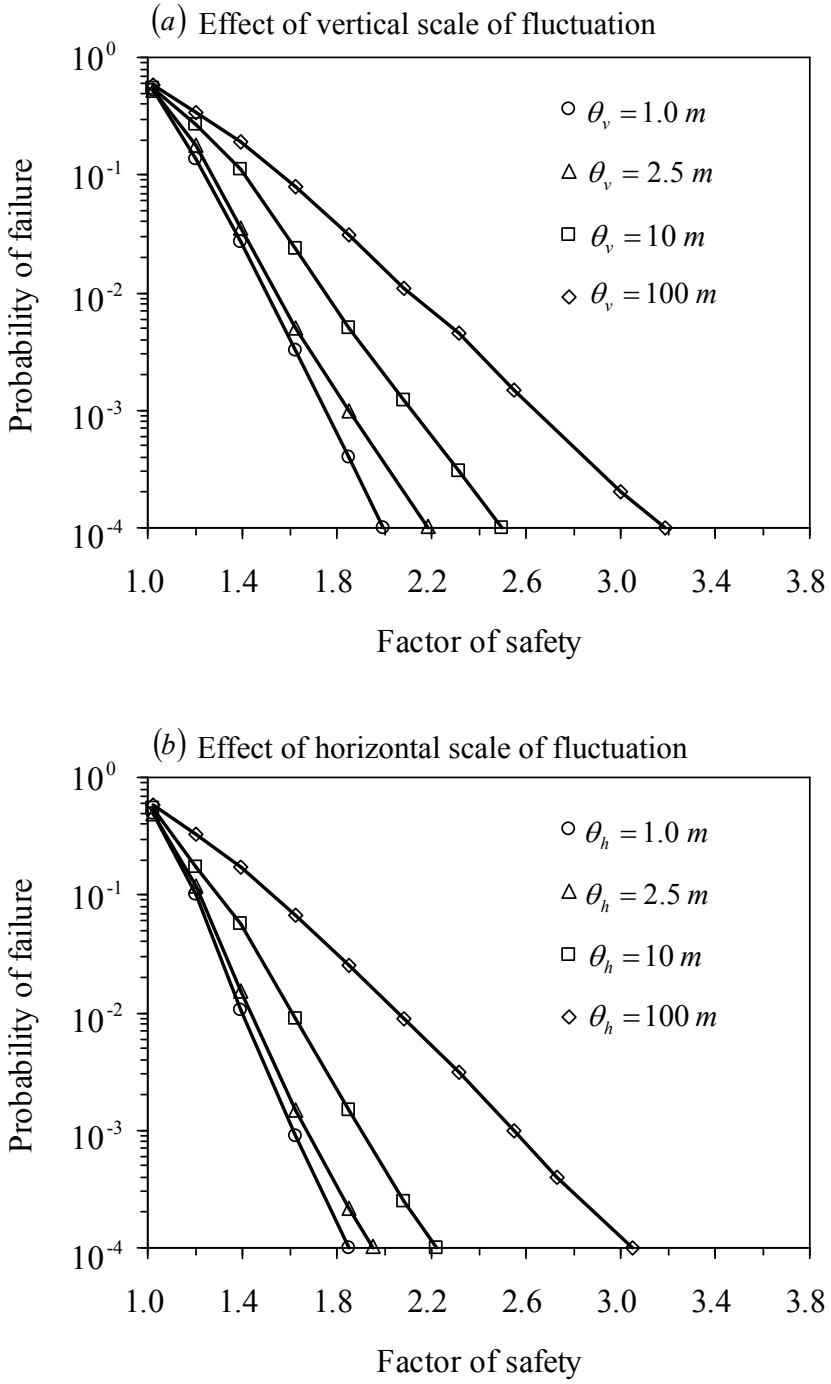

Figure 3.3: Effect of 1-dimensional spatial variability on the relationship between failure probability and factor of safety in the reliability-based design.

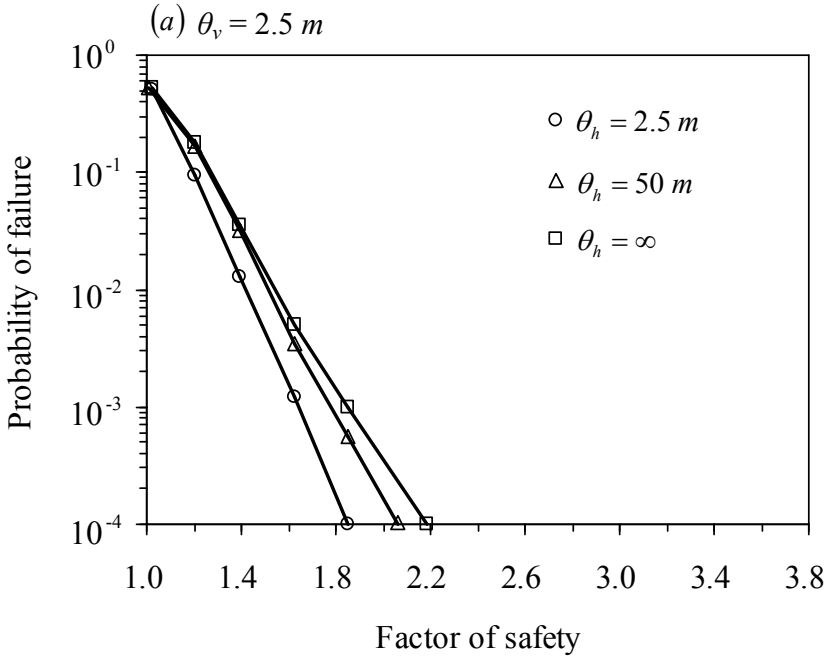

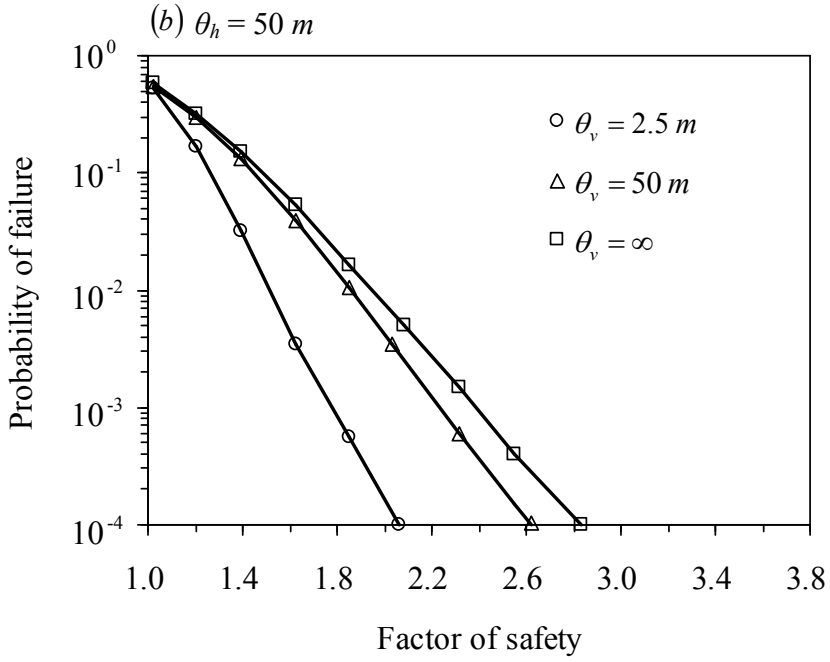

Figure 3.4: Effect of 2-dimensional spatial variability on the relationship between failure probability and factor of safety in the reliability-based design.

the effect of horizontal spatial variability. *The implication is that the required FS will be overestimated for a target* p_f *if the effect of spatial variability is ignored.* Thus, traditional reliability analysis that considers variation of input soil parameters (for example, through *COV*) but not spatial variability exhibited in a random field can over-estimate the probability of failure for a given deterministic-based design (i.e., a given *FS*).

The effect of 2-D spatial variability is examined next. To begin with, three different horizontal scales of fluctuation (θ_h = 2.5m, 50m, and ∞) are considered simultaneously with the average vertical scale of fluctuation [θ_v = 2.5m as Phoon and Kulhawy (1999a)] to study the effect of θ_h at fixed θ_v. The results are shown in Figure 3.4(a). Afterwards, three different vertical scales of fluctuation (θ_v = 2.5m, 50m, and ∞) are considered simultaneously with the average vertical scale of fluctuation [$\theta_h \approx$ 50m as per Phoon and Kulhawy (1999a)] to study the effect of θ_v at fixed θ_h. The results are shown in Figure 3.4(b). The effect of the scales of fluctuation in a 2-D random field is also obvious: at a fixed scale of fluctuation in one direction, a smaller scale of fluctuation in the other direction results in a smaller p_f at the same *FS*. Furthermore, the required *FS* will still be overestimated for a target p_f if the soil parameter is modeled with only a 1-D random field, as opposed to a 2-D random field. Therefore, it is essential to consider 2-D spatial variability in the probability-based (or reliability-based) design against basal-heave failure in a braced excavation.

One concern with traditional reliability-based design in geotechnical practice in the past is that the computed failure probability is often high in a design that satisfies the

minimum *FS* specified in the codes, but failure seldom occurs in such cases. For example, this concern has been reported by Goh et al. (2008) and Wu et al. (2010a) in their study of basal-heave stability in an excavation. Overestimation of variation in soil parameters is often pointed out as a possible cause for having a higher *computed* probability of failure. Based on the results presented (Figures 3.3 and 3.4), it is evident that negligence in the effect of spatial variability of soil parameters can lead to an overestimation, perhaps to a high degree, of the failure probability. Thus, to apply the traditional simplified reliability-based method for evaluating the failure probability, an adjustment is needed to model spatial variability.

Equivalent simplified approach with variance reduction technique

While the RFM analysis generally yields the most accurate results, it requires use of the MCS. On the other hand, the simplified approach can be implemented with reliability-based methods. Past studies have shown that simplified approaches with a proper variance reduction can match well with the RFM solution. In other words, for a RFM solution, an equivalent solution using simplified approach is possible. Therefore, the analysis for the probability of basal-heave failure in a braced excavation in a random field can be performed using traditional reliability-based methods, provided that an equivalent simplified approach can be established first.

The desired equivalency between simplified approach and RFM solutions in this case is "equal" probability of failure, or $p_f = P[M_R < M_D]$. For the basal-heave problem analyzed herein using the *slip circle method* [Eqs. (2.1-2.3)], the undrained shear

strength is the only soil parameter that is treated as spatially random, while all other parameters are set as constants so that the spatially random effect of the undrained shear strength is examined explicitly. Here, in search for the equivalency between the RFM approach and the simplified approach, M_D is treated as a constant and M_R is treated as a random variable. Therefore, the equivalency in the computed failure probability can be achieved if M_R, determined from the two approaches (simplified approach and RFM) agrees with each other at the same level of soil variability (i.e., the same level of *COV* and scale of fluctuation). Because the mean of M_R is approximately the same regardless of which of the two approaches is employed [This is apparent since in this study M_R is linearly correlated with s_u as per Eq. (2.3) and Figure 2.6], it is considered appropriate and adequate to use the variation (or more precisely, the standard deviation) of the computed M_R as a basis for establishing the equivalency.

It should be noted that the mean of M_R (and thus *FS*) may not be independent of the scale of fluctuation θ as observed from the results of the slip circle method, since the shear zone may develop through softer areas (Suchomel and Mašín 2010). If other approaches such as finite element method are employed for basal heave analysis, the computed mean of M_R is likely to change with θ (Suchomel and Mašín 2010). This effect is not accounted with the slip circle method, which is a limitation of the proposed approach. However, this issue is beyond the scope of this study.

Equivalency between simplified approach and RFM solution may be achieved by applying variance reduction to the former, which requires determination of the reduction factor (Γ). For the basal-heave problem, Γ values at various levels of variability (in terms

of standard deviation σ and scale of fluctuation θ of s_u/σ'_v) can be back-calculated using the procedure illustrated in Figure 2.9 in Chapter II. As shown in Figure 2.9, the flow sequence on the left summarizes the procedure of RFM with the *Cholesky decomposition* method [Eqs. (3.1-3.7)]. The standard deviation of M_R, denoted herein as σ_{NS}, is obtained from 10^5 MCS of the basal-heave analysis for a braced excavation in clay with a given pair of standard deviation σ and scale of fluctuation θ of s_u/σ'_v.

In Figure 2.9, the flow sequence on the right summarizes the procedure of simplified approach using the equivalent variance technique. First, an interval of the reduction factor, [Γ_L Γ_U], is assumed for this case (with the same σ and θ of s_u/σ'_v). Γ_L and Γ_U are the assumed lower and upper bounds, which may be set at 0 and 1, respectively. Then the bisection method is used to search for the equivalent variance: the interval is divided into two segments by the midpoint $\Gamma_p = (\Gamma_L + \Gamma_U)/2$, and the variance is reduced with Γ_p. With the reduced variance σ_Γ, MCS may be performed without the Cholesky decomposition. The standard deviation of M_R, denoted herein as σ_S, is then obtained from 10^5 MCS of the basal-heave analysis of the same case, as in the RFM analysis (left side of the flowchart shown in Figure 2.9). If the reduction factor Γ_p is correct, the two standard deviations, σ_{NS} and σ_S, will be equal to each other for the given pair of standard deviation σ and scale of fluctuation θ of s_u/σ'_v. In this study, the Γ value at which $\sigma_{NS} \approx \sigma_S$ (or $|\sigma_{NS} - \sigma_S|/\sigma_{NS} \le 10^{-3}$) is the target reduction factor for a given pair of σ and θ of s_u/σ'_v. As shown in Figure 2.9, if the above

stopping criterion ($\left|\sigma_{NS} - \sigma_S\right| / \sigma_{NS} \le 10^{-3}$) is not satisfied, the interval of Γ is shortened by setting $\Gamma_L = \Gamma_p$ (for $\sigma_{NS} - \sigma_S > 0$) or $\Gamma_U = \Gamma_p$ (for $\sigma_{NS} - \sigma_S < 0$). The new midpoint Γ_p is then computed and the aforementioned procedure is repeated until the final reduction factor for a given pair of σ and θ of s_u / σ'_v is obtained. It should be noted that for this "equivalency" analysis, the simplified approach is implemented with the MCS. As will be shown later, the simplified approach can also be implemented with FORM to further reduce the computational effort.

Through the above back-calculation procedure (Figure 2.9), the reduction factor Γ for an equivalent simplified approach can be obtained. Figures 3.5(a) and 3.5(b) show the *back-calculated* Γ values for various pairs of σ (or *COV*) and θ of s_u / σ'_v, for vertical and horizontal spatial variability, respectively. Two observations are made: (1) the inherent variability rarely influences the variance reduction at the same θ level; (2) the reduction factor Γ depends only on θ at the same *COV* level. These observations are consistent with the variance reduction models presented in literature [e.g., Eq. (3.8) from Vanmarcke (1983)].

Finally, a comparison is made between reduction factors (Γ), computed using the variance reduction function [Eq. (3.8)] and those obtained through the back-calculation procedure discussed above. Note that the evaluation of Eq. (3.8) requires knowledge of the characteristic length. In this study, the vertical characteristic length L_v is assumed to be the vertical distance between the depth of the final strut and the bottom of the diaphragm wall ($L_v = \overline{od}$ = 18m as in Figure 3.1); horizontal characteristic length L_h is

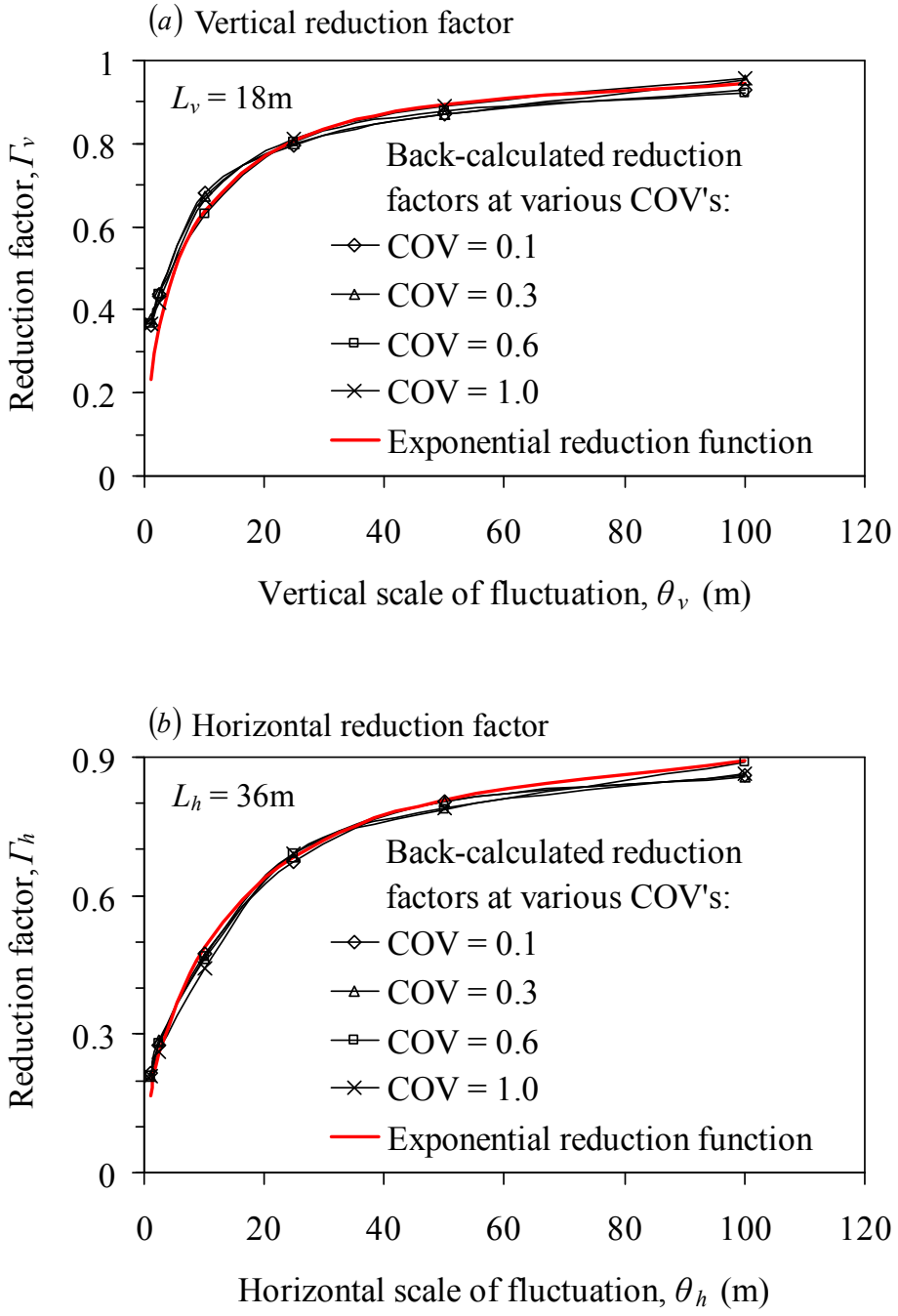

Figure 3.5: Comparison between the reduction factors back-calculated using the MCS-based RFM and those computed using Eq. (3.8) with assumed characteristic lengths (L_v = 18m or L_h = 36m).

assumed to be the horizontal scale of the slip circle ($L_h \approx \overline{ec} \approx$ 36m as in Figure 3.1). The rationale for these assumptions is that these lengths are the vertical and horizontal scales of the region that contributes to the resistance moment in the random field. With the assumed characteristic lengths, reduction factors are computed with Eq. (3.8), and the results are shown in Figure 3.5 for comparisons with those that are back-calculated based on the equivalency analysis presented previously.

As shown in Figure 3.5, the assumptions of L_v = 18m and L_h = 36m yield reduction factors consistent with those that are back-calculated from the equivalency analysis. The implication is that for basal-heave analysis in a 2-D random field using the slip circle method (Figure 3.1), vertical characteristic length L_v can be taken as the vertical distance between the depth of the final strut and the bottom of the diaphragm wall (the length $\overline{od}$ as in Figure 3.1) and horizontal characteristic length L_h can be taken as the horizontal scale of the slip circle (the length $\overline{ec}$ as in Figure 3.1). This follows that variance reduction factor (Γ^2) or reduction factor (Γ) can be computed for a given spatial variability level, and with the concept of spatial averaging, the reduced variation of the random variable for an equivalent simplified approach is obtained. Finally, the simplified reliability analysis can be performed in this equivalent stationary random field.

Practical reliability analysis of basal-heave considering 2-D spatial variability

Based on results presented in the previous sections, a step-by-step procedure is established for the simplified reliability analysis of basal-heave in a braced excavation in clay considering 2-D spatial variability:

1. Select an analytical model for basal-heave analysis (for example, slip circle method).
2. Obtain spatially-constant input parameters and random variables, such as unit weight of soils and applied surcharge.
3. Characterize a spatially random variable (in this case, the normalized undrained shear strength) with its mean, *COV* and horizontal and vertical scales of fluctuation (θ_h and θ_v,) for this 2-D random field.
4. Determine the vertical and horizontal characteristic lengths (L_v and L_h) based on the selected random field region (such as the one shown in Figure 3.1). Apply the equivalent variance technique [Eqs. (3.8-3.10)] to determine the reduced variance (σ_{Γ}^2) of normalized undrained shear strength.
5. When the equivalent variance technique is used to simplify the effect of the spatial variability of a lognormal distributed parameter, the variance of its equivalent normal distribution should be reduced in this process.
6. Conduct FORM analysis (for example, using a spreadsheet implementation as shown in Figure 3.6) using the reduced variance of the normalized undrained shear strength. The reliability index and probability of failure can be determined using FORM.

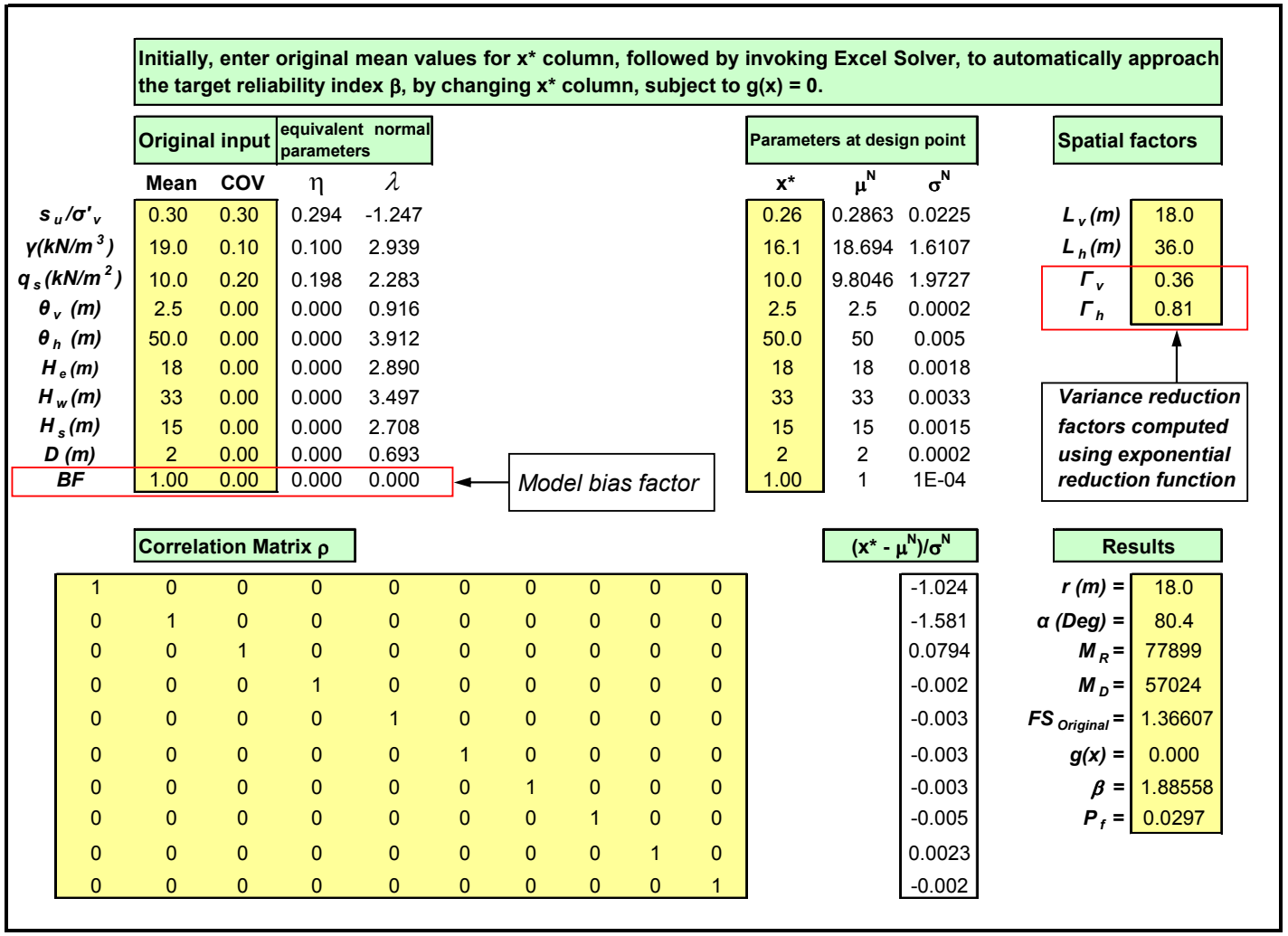

Figure 3.6: Reliability-based procedure for evaluating failure probability of basal-heave.

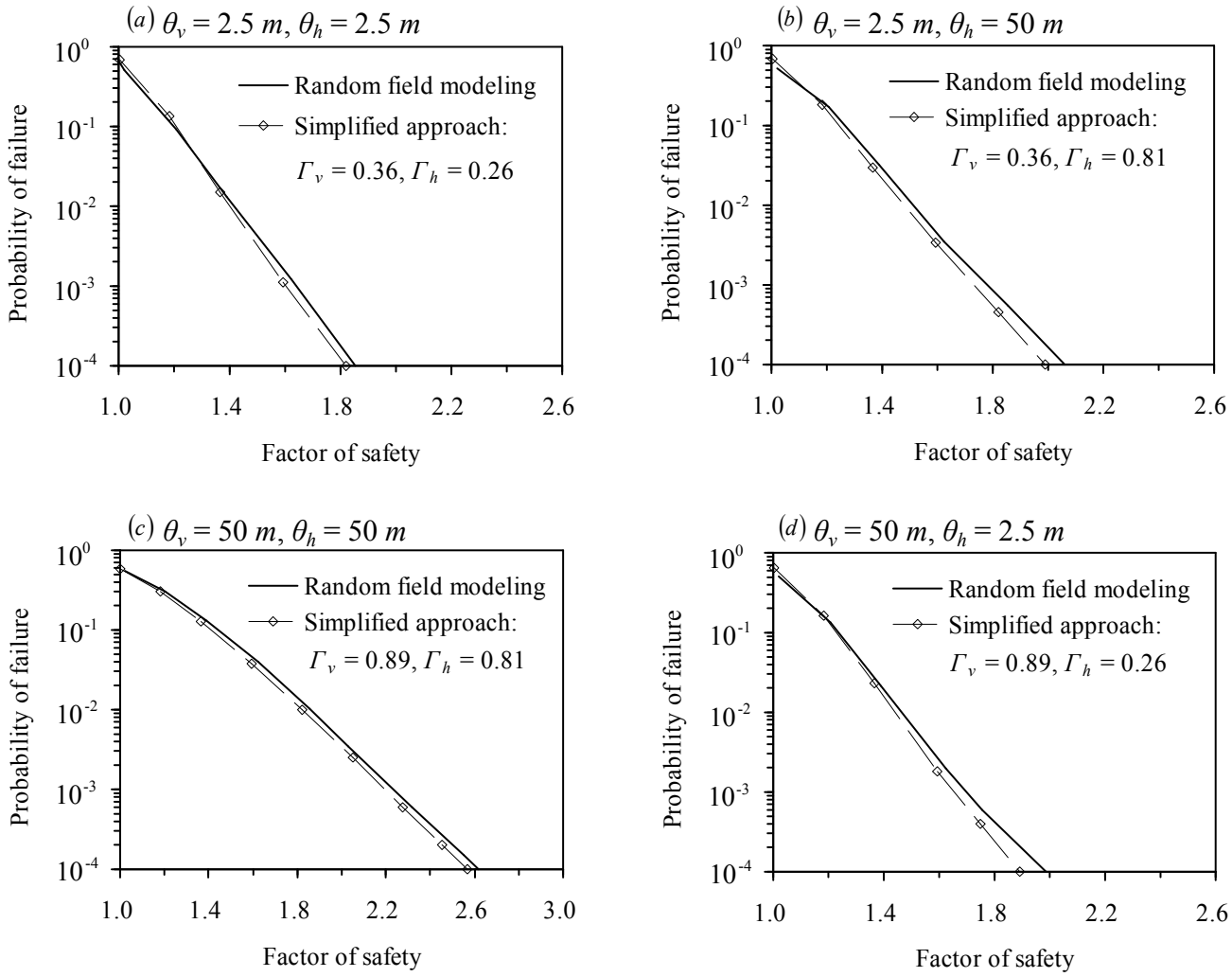

Figure 3.7: Comparison between the MCS-based RFM solutions and those by the simplified approach.

As an example, basal-heave in a braced excavation shown in Figure 3.1 with input parameters listed in Table 3.1 is analyzed. All parameters except s_u/σ'_v are treated as spatially-constant random variables or simply constants. The parameter s_u/σ'_v is modeled with a 2-D random field, and characterized by a mean value of 0.30, a COV of 0.3, and scales of fluctuation θ_h = 2.5 m and θ_v = 50 m. As shown in Figure 3.7, the equivalent simplified approach that considers the spatial variability of s_u/σ'_v is realized using the variance reduction function [Eq. (3.8)] with characteristic lengths L_v = 18 m and L_h = 36 m. The reduced variance of s_u/σ'_v in the equivalent simplified approach is thus obtained. FORM analysis is then performed using the spreadsheet as shown in Figure 3.6, which yields reliability index β = 1.8856 and probability of failure p_f = 0.0297. It should be noted that the model bias (*BF*) of the deterministic slip circle method is ignored at this point [as shown in Figure 3.6, mean value of model bias (denoted as μ_{BF}) is set as 1.0 and the *COV* of the model bias (denoted as COV_{BF}) is set as 0.0); the effect of model bias is examined later].

To further examine the capability of the spreadsheet that implements the FORM procedure with the equivalent variance technique, the basal-heave problems that were analyzed with the MCS-based RFM approach (Figure 3.4), are re-analyzed. Comparisons with the previous results from Figure 3.4 are shown in Figure 3.7 for four different scenarios of constant vertical and horizontal scales of fluctuation: (a) $\theta_v = \theta_h$ = 2.5m; (b) θ_v = 2.5m, θ_h = 50m; (c) $\theta_v = \theta_h$ = 50m; (d) θ_v = 50 m, θ_h = 2.5m. Note that Case (b) represents the mean values for θ_v and θ_h suggested by Phoon and Kulhawy (1999a). As in

Figure 3.4, a series of basal-heave problems (signaled by different *FS* values, which were realized by assuming different mean s_u / σ'_v values while keeping the mean values of all other parameters the same) are analyzed. In Figure 3.7, the results show that regardless of the chosen scales of fluctuation and design safety level (*FS* value), the probabilities of basal-heave failure obtained from the spreadsheet agree very well with those determined with the MCS-based RFM approach. At any given target probability of failure (Figure 3.7), the maximum difference in the required *FS* between the two approaches (RFM vs. simplified approach) is less than 5%. Thus, the simplified approach is deemed effective.

Effect of model bias on the computed probability of failure

The analyses of basal-heave failure presented so far are performed assuming no model bias in the adopted slip circle method. In the reliability analysis shown in Figure 3.6, the model bias is implemented with a bias factor (BF), which is treated as a random variable. To implement the assumption of no model bias, the mean of the model bias factor is taken as unity ($\mu_{BF} = 1.0$) with no variance ($COV_{BF} = 0.0$). Most geotechnical analysis models are biased one way or the other because they often represent a conservative approximation of the actual conditions. If the model bias exists but is not accounted for, the computed probability of failure may be either underestimated or overestimated. This is an additional source of uncertainty that could influence the selection of a required factor of safety for a target failure probability in a reliability-based design.

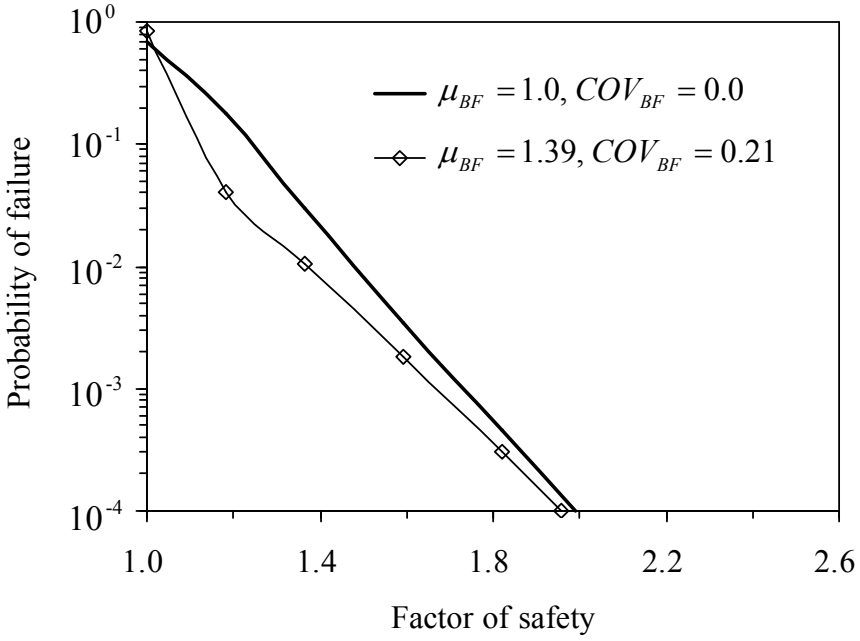

Figure 3.8: Effect of model bias of the slip circle method on the relationship between failure probability and factor of safety derived through reliability analysis.

A recent calibration study on the slip circle method (Wu et al. 2011) reports that the mean value (μ_{BF}) and the *COV* of model bias (COV_{BF}) of the method are 1.39 and 0.21, respectively. To examine the effect of this model bias on the failure probability determined using the FORM-based spreadsheet solution, Case (b) in Figure 3.7(b), in which θ_v = 2.5m, θ_h = 50m, is reanalyzed with this model bias factor. The results with and without this model bias factor are compared in Figure 3.8. It is observed that at the same *FS* level, the failure probability is smaller if the model bias of the slip circle method is considered. Thus, negligence of the model bias in the reliability analysis of basal-heave failure can lead to an overestimation of the failure probability. As shown in Figure 3.8, however, the effect of the model bias is less significant at smaller target probability level (e.g., $p_f = 10^{-3}$ to 10^{-4}). For example, at the target probability of failure $p_f = 10^{-4}$, the

difference in the required *FS* for the basal-heave design between the two conditions (with and without model bias consideration) is less than 1.5%. As a reference, at this target probability of failure, the difference in the required *FS* for the basal-heave design between the two conditions of spatial variability (with and without considerations of spatial variability of the undrained shear strength of clay) is approximately at 50%. Thus, at the generally accepted level of failure probability (p_f = 10^{-3} to 10^{-4}), the need to consider spatial variability in the analysis is clearly demonstrated while the effect of model bias of the slip circle method is relatively insignificant.

Summary

In this chapter, the simplified approach developed in Chapter II to consider the effect of 1-D spatial variability on the reliability analysis of basal-heave in braced excavation in clays, is extended for a 2-D random field. This simplified approach is demonstrated through a case study. As the first step, the 2-D RFM analysis is performed in a study of basal-heave stability to provide a benchmark. The results show that negligence of 1-D or 2-D spatial variability in reliability analysis can significantly overestimate the probability of basal-heave failure for a given deterministic design with a certain factor of safety (e.g., Figures 3.3 and 3.4).

Then, variance reduction factors for both vertical and horizontal directions, at which the simplified approach yields results that match well with those obtained with RFM, are back-calculated. The assumptions of the characteristic lengths of both vertical and horizontal directions in the stability analysis are verified based on the back-calculated

variance reduction factors. This case study found that for basal-heave analysis in a 2-D random field using the slip circle method (Figure 3.1), the vertical characteristic length L_v can be taken as the vertical distance between the depth of the final strut and the bottom of the diaphragm wall (length $\overline{od}$ in Figure 3.1) and the horizontal characteristic length L_h can be taken as the horizontal scale of the slip circle (length $\overline{ec}$ in Figure 3.1).

Finally, a simplified approach which combines the first-order reliability method (FORM) and the variance reduction technique to account for spatial variability is proposed for reliability analysis of basal-heave stability. The proposed approach is implemented in a spreadsheet and thus is easy to use, requires less computational effort. The simplified approach yields results (in terms of probability of basal-heave failure) that are nearly identical to those obtained with the MCS-based RFM method.

CHAPTER IV

PROBABILISTIC SERVICEABILITY ASSESSMENT IN A BRACED EXCAVATION CONSIDERING SPATIAL VARIABILITY*

Introduction

One of the main concerns in a braced excavation in an urban area is the risk of damage to adjacent infrastructures caused by the excavation-induced wall deflections and ground movements. Damage to the adjacent infrastructures caused by ground movements is referred to herein as the *serviceability failure* in a braced excavation. In many excavation projects, the owners or regulatory agencies establish the *limiting* wall and ground responses as a means of preventing excavation failure and damage to adjacent infrastructures. Table 1.1 shows an example of such limiting response criteria from China (PSCG 2000). Thus, it is essential to have the ability to accurately "predict" the maximum wall deflection and ground settlement during the design of braced excavations.

Past experience has shown that construction details can have a great effect on the wall deflection and ground settlement that actually occur in the field. In this study, the effect of construction sequence is simulated in the finite element analysis, as braced excavations are carried out in stages. However, good workmanship is assumed in the excavation and no other construction related effect is considered in the analysis.

To accurately predict the maximum wall deflection and ground settlement, it is essential to properly characterize the site conditions. An appropriate site investigation

* A similar form of this chapter has been published at the time of writing: Luo Z, Atamturktur S, Juang CH, Huang H, Lin PS. Probability of serviceability failure in a braced excavation in a spatially random field: Fuzzy finite element approach. Computers and Geotechnics, doi:10.1016/j.compgeo. 2011.07.009.

program is needed; in particular, design soil parameters must be properly evaluated and selected. For braced excavations in clays, Hsiao et al. (2008) pointed out that normalized undrained shear strength (s_u / σ'_v) and normalized initial tangent modulus (E_i / σ'_v) are the most important soil factors. As in many geotechnical projects, however, it is difficult to determine the values of these parameters with *certainty*, especially with limited test data. Uncertainty in these parameters leads to uncertainty in the computed maximum wall deflection and ground settlement, which makes it more difficult to assess whether the predicted responses are excessive as compared to the specified *limiting* wall and ground responses. This problem could be complicated further with the inherent variability of soils and the spatial correlation. A sensible approach would be to consider all these uncertainties, derive the probabilities of exceeding the *limiting* wall and ground responses, then make the design decisions based on these exceedance probabilities.

The effect of inherent spatial variation of soil properties has been demonstrated in many geotechnical problems, and modeling of this variation with random field theory has already been reported (Griffiths and Fenton 2009). However, a rigorous simulation of the random field using the finite element method (FEM) solution demands a large amount of computation time, which is not practical for analyzing complicated problems such as wall and ground responses in a braced excavation (Schweiger and Peschl 2005). To this end, the proposed approach, consisting of using fuzzy sets (Zadeh 1965) and a variance reduction technique (Vanmarcke 1977) to approximate the effect of a random field, appears to be a feasible alternative for analysis for the probability of serviceability failure.

In summary, this chapter focuses on a simplified approach for estimating the probability of serviceability failure (i.e., exceeding the limiting wall and ground responses) in a braced excavation in a spatially random field. Uncertain soil parameters are represented by fuzzy sets and spatial variability is considered by means of variance reduction. Propagation of the uncertainty of these soil parameters through finite element solution is carried out by the alpha-cut method (Juang et al. 1998). The FEM analysis of the braced excavation is conducted using a finite-element computer code with a constitutive model that can effectively model the small-strain nonlinear soil behavior. The results of the FEM-based fuzzy set approach are fuzzy numbers that represent wall and ground responses. The probability of exceeding a specified response is then computed from the resulting fuzzy numbers. A case study is presented to demonstrate the proposed simplified approach, which is shown to be effective and simple to use.

Finite Element Modeling with a Small-Strain Nonlinearity Soil Model

Numerical methods such as the finite difference method or finite element method are often used to analyze wall deflection and ground settlement in a braced excavation (Whittle and Hashash 1994; Ou et al. 1998; Hsieh et al. 2003; Kung et al. 2007a). In this study, wall and ground responses in a braced excavation in clays are analyzed using a commercially available finite element code, Plaxis^{TM} (Brinkgreve and Vermeer 2002). *It should be noted that use of this software in this study does not represent an endorsement of the software; other FEM codes can be employed.*

Kung et al. (2007a) indicated that wall deflection was relatively easier to predict

accurately than ground settlement and the accuracy of the prediction often depended on the capability of utilized soil models. They showed that proper modeling of *small-strain* nonlinearity soil behavior is essential for accurate predictions of ground settlement in a braced excavation using FEM. This view was shared by many previous investigators (Hsieh and Ou 1997). In the work by Kung et al. (2007a), a small-strain nonlinear soil model, known as the Modified Pseudo Plasticity (MPP) model, was implemented in the computer code AFENA (Hsieh and Ou 1997) for the analysis of braced excavations. The MPP model was developed by Hsieh et al. (2003) for clays, with considerations for anisotropic properties, high stiffness at small-strain, and degradation behaviors. Here, the range of small strain is from 0 to 10^{-5}. Through a series of analyses of laboratory tests (the conventional and small-strain CK_0UC tests) and well-documented case histories of braced excavation, Kung et al. (2007a) demonstrated the validity of the MPP model and the accuracy of the FEM predictions of wall and ground responses in braced excavations using AFENA with the MPP soil model.

Plaxis^{TM} (Brinkgreve and Vermeer 2002) is a proprietary FEM code, but it prescribes a programming format that the user can follow to implement a constitutive law of soils. To follow up on the previous work (Kung et al. 2007a), it is desirable to implement the MPP model as a user-defined model in Plaxis^{TM}. Thus, Plaxis^{TM} with the MPP soil model (implemented by Dang 2009) is used in this study.

To verify the accuracy of the FEM code, we re-analyze the excavation case at Taipei National Enterprise Center (TNEC) that was documented by Ou et al. (1998). The results are compared with those reported previously by Kung et al. (2007a), who analyzed

the same TNEC case using the AFENA code with the MPP model. In that previous study, the capability of the AFENA code with the MPP model for predicting wall and ground responses in a braced excavation was demonstrated. In the present study, we compare the maximum wall deflections and the maximum ground settlements at various stages of excavation of TNEC obtained by the two FEM codes (Plaxis^{TM} with MPP versus AFENA with MPP). Figures 4.1(a) and 4.1(b) compare the results of FEM predictions of the maximum wall deflections and the maximum ground settlements, respectively. The results show that the Plaxis^{TM} solutions in this study are as accurate as those obtained by Kung et al. (2007a) using AFENA, and both agree well with field observations. Thus, Plaxis^{TM} code with the MPP soil model is found to be satisfactory for predicting the wall and ground responses in a braced excavation. Furthermore, in this study, Plaxis^{TM} code with the MPP soil model is further used to study the effect of the spatial variability of soils on the probability of exceeding the limiting responses in a braced excavation. *For convenience, the software Plaxis^{TM} implemented with the MPP soil model is referred to hereinafter as "the FEM code."*

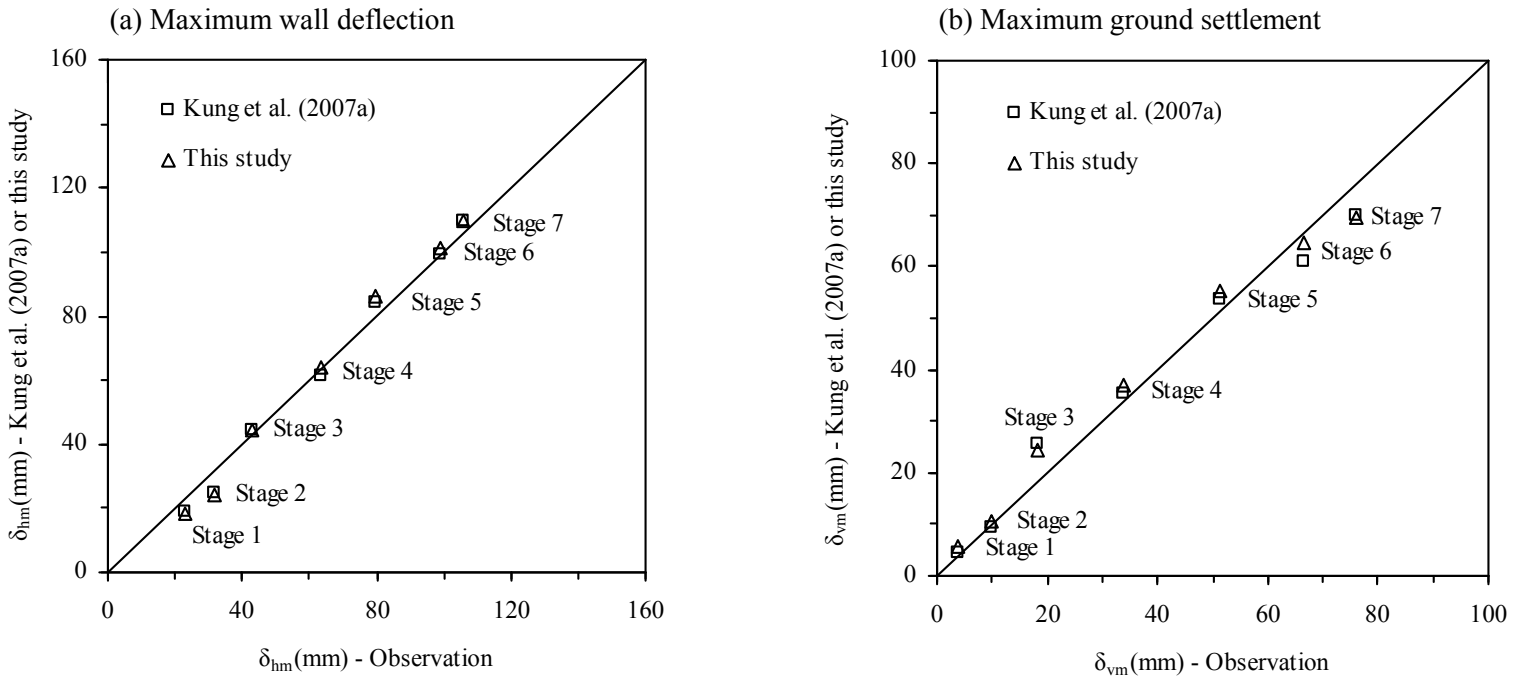

Figure 4.1: Maximum wall deflections and maximum ground settlements at various stages of excavation of the TNEC case – A comparison of the observed values with those obtained by Kung et al. (2007a) using AFENA and in this study using PlaxisTM; both FEM codes implemented with the MPP soil model.

Modeling Spatial Variability in Braced excavations in Clays

Spatial variability

In a traditional deterministic approach, the FEM solution generally assumes soil parameters to be spatially constant. In recent studies using random FEM to consider spatial variability, Griffiths et al. (2009) found the effect of inherent spatial variations of soil properties can be significant in FEM solutions of many geotechnical problems. The random FEM approach, however, is computationally intensive (Schweiger and Peschl 2005). For the complex problem of staged, braced excavations, it can be considered appropriate to use a simplified model of spatial variability. Among the methods dealing with the spatial variability of soil, the spatial averaging of the variation of the soil properties has shown to be an effective tool (for example see, Phoon and Kulhawy 1999a,b; Phoon et al. 2003; Klammler et al. 2010). In this study, the focus is to examine the effect of spatial variability of soil parameters on the wall and ground responses in a braced excavation using *the FEM code*; and to this end, the spatial averaging approach is adopted.

Spatial averaging

The concept of spatial averaging was described by Vanmarcke (1977) as follows: the variability of the average soil properties over a large domain is less than that over a small domain. The reduced variability of soil properties over a large domain can be characterized by the *variance function*, which is related to the autocorrelation function. The exponential model that is widely used in the study of spatial variability is selected

herein:

$$\rho(\Delta z) = \exp\left(-2\frac{|\Delta z|}{\theta}\right) \tag{4.1}$$

where $|\Delta z|$ is the distance between any two points in the field; θ is the scale of fluctuation that is used to normalize $|\Delta z|$.

To consider spatial averaging in a reliability analysis, variances of soil parameters are reduced by multiplying a factor that depends on the scale of fluctuation (Vanmarcke 1983). This factor is the value of the variance reduction function that can be obtained by integration of an autocorrelation function such as Eq. (4.1). Thus, the variance reduction function may be expressed as (Vanmarcke 1983):

$$\Gamma^2 = f(L,\theta) = \frac{1}{2}\left(\frac{\theta}{L}\right)^2\left[\frac{2L}{\theta} - 1 + \exp\left(-\frac{2L}{\theta}\right)\right] \tag{4.2}$$

where L is the characteristic length with respect to a potential failure surface. In general, the value of the variance reduction function is less than 1, and as such, this value is often referred to as the variance reduction factor (Γ^2).

The characteristic length may be assumed to be the length of the sliding surface (failure surface) in the stability analysis of a braced excavation, as suggested by Schweiger and Peschl (2005). A similar assumption was made by Most and Knabe (2010) in their study of bearing capacity of footings using variance reduction technique. Figure 4.2 shows an example of the sliding surface based on the slip circle method (JSA 1988).

In this study, the characteristic length L is taken as the total length of the arc length ***bcd*** and the vertical length ***ab***.

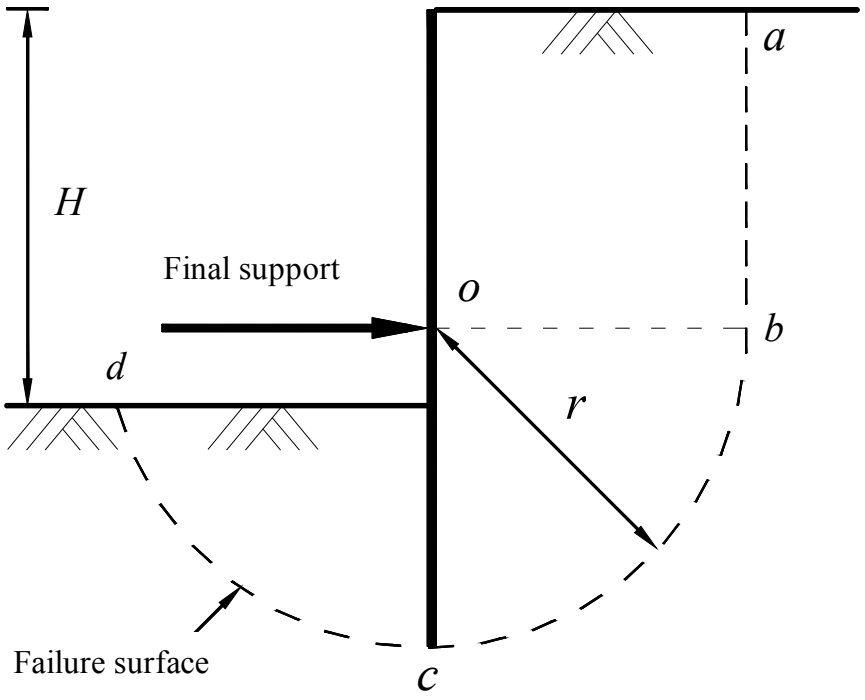

Figure 4.2: An example of failure surface in braced excavation.

With the known characteristic length (L) and the scale of fluctuation (θ), the reduced variance σ_{Γ}^2 can then be obtained with the following equation:

$$\sigma_{\Gamma}^2 = \Gamma^2 \cdot \sigma^2 \tag{4.3}$$

where σ^2 is the variance of the soil parameter, and Γ^2 is the variance reduction factor.

The spatial averaging approach has been shown to be an effective simplification

of the real random field. As pointed out by Schweiger and Peschl (2005), a more rigorous simulation of the random field demands a large amount of computational time, which may not be practical for complicated numerical simulations such as the problem of braced excavation. In this study, the spatial averaging effect is examined using the checkerboard approach (Griffiths and Fenton 2009) and the feasibility of the variance reduction technique to model the spatially randomness within the context of a braced excavation is demonstrated.

Fuzzy Sets Methodology - Modeling and Processing of Uncertain Parameters

Uncertainty modeling with fuzzy sets

Geotechnical engineers almost always have to deal with uncertainty, whether it is formally acknowledged or not (Juang and Elton 1996). When input soil parameters cannot be ascertained due to limited data availability, engineering judgment is often exercised to select a conservative design parameter. Uncertainty in soil parameters may be dealt with by using an appropriate factor of safety. However, in many cases, it is advantageous to assess this uncertainty and to include it in the analysis so that a more informed design decision can be made.

Fuzzy set theory (Zadeh 1965) has been shown effective and suitable for modeling uncertainty in soil parameters (Juang et al. 1991; Juang et al. 1992a,b; Juang and Elton 1996; Juang et al. 1998) when data are insufficient to fully define a probability distribution. A fuzzy set is a set of paired values $[x, \mu_A(x)]$, where an element x belongs to the set A to a degree defined by its membership function $\mu_A(x)$. The membership grade,

ranging from 0 to 1, is used to characterize the degree of belief that x belongs to A. The fuzzy set theory has been widely used in many engineering and non-engineering fields. Examples of the application of fuzzy sets in geotechnical engineering can be found in literature (e.g., Juang et al. 1991; Juang et al. 1992a,b; Valliappan and Pham 1995; Chen and Juang 1996; Juang and Elton 1996; Juang et al. 1998; Dodagoudar and Venkatachalam 2000; Peschl and Schweiger 2003; Saboya et al. 2006).

For routine geotechnical uncertainty modeling, use of a subset of a fuzzy set, called fuzzy number, to represent an uncertain soil parameter may be sufficient (Juang and Elton 1996). A fuzzy number is a fuzzy set that is normal and convex—the shape of the membership function is single humped and has at least one value whose membership grade (or degree of belief) is 1. Figure 4.3(a) shows an example of a fuzzy number. If there is no reason to suggest otherwise (because of lack of data), the shape of the membership function may be assumed to be triangular, as shown in Figure 4.3(a), because of its simplicity in formulation and ease of computation (Juang et al. 1998). The triangular fuzzy number has been shown to be useful in many engineering applications (Elton et al. 2000). A triangular fuzzy number is characterized by three values: a lower bound, an upper bound, and a mode (most probable value). The mode has a membership grade of 1, the highest possibility, to represent uncertain soil parameter. As the value of the parameter departs from the mode, the degree of belief for this value to represent the soil parameter decreases, and when the value reaches the lower bound (or the upper bound), the degree of belief is reduced to zero.

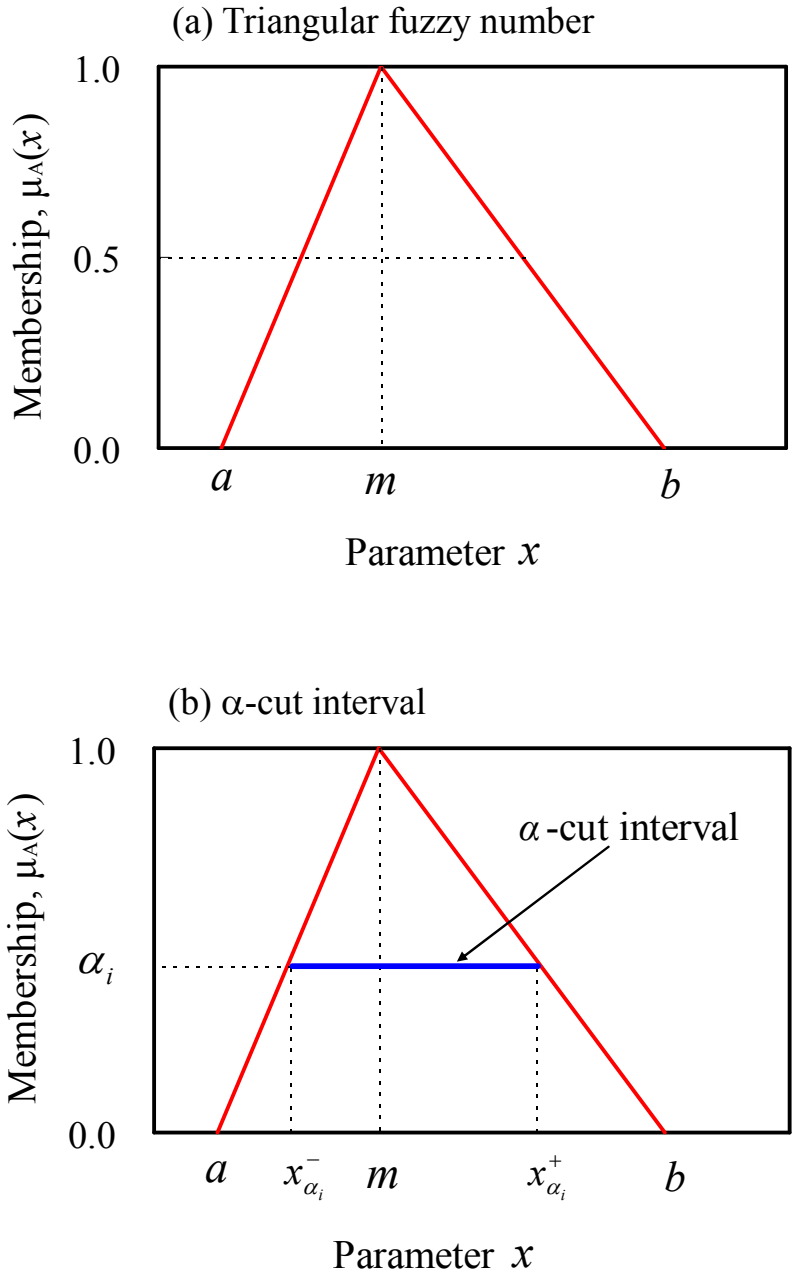

Figure 4.3: Example of triangular fuzzy number and α-cut interval.

The concept of a simple representation of an uncertain soil parameter is not new. In a widely cited paper, Duncan (2000) proposed the concept of the *highest conceivable*

value and *lowest conceivable* value as a way to estimate the uncertainty of a soil parameter. He initially suggested that the standard deviation (σ) of a soil parameter may be estimated by taking the difference between the highest conceivable value and the lowest conceivable value and dividing it by 6. However, in the field of geotechnical engineering, lack of sufficient number of observations is often a norm rather than exception; as such, the variation of soil parameters can often be underestimated. Thus, it would be more appropriate to adopt a divider of less than 6 [for example, 4, as later recommended by Duncan (2001)].

In many cases, the standard deviation may also be estimated by adopting the published coefficients of variation (COV) on a given soil parameter (e.g., Harr 1987; Phoon and Kulhawy 1999a). Of course, these COV values may not be accurate for local soils and some adjustment may be needed. Furthermore, the mean (μ) of the parameter of concern may be computed from a limited number of data points or simply estimated as the *most probable* value. With knowledge of the standard deviation and mean, simple reliability methods such as the first order second moment (FOSM) method can be used to compute the probability of "failure."

In this study, however, a different approach is employed. Assuming the engineer can estimate a soil parameter with three values, the highest conceivable value (upper bound), the lowest conceivable value (lower bound), and the most probable value (mode), then a triangular fuzzy number as illustrated in Figure 4.3(a) can be readily defined. Generally, the most probable value (mode) can be fairly accurately estimated by taking the mean of the available data (even with only a few data points). The upper and lower

bounds can be estimated based on published coefficient of variation (which yields standard deviation), for example, by taking ±2 standard deviations from the mean. *The estimate of the mode and the upper and lower bounds with very limited data should be guided by local experience and engineering judgment.* With the estimate of the mode, lower bound, and upper bound, the soil parameter can be modeled with a triangular fuzzy number.

If the data are lacking or insufficient to fully define a probability distribution, as in many geotechnical engineering projects due to cost constraints, then as an approximation, use of a triangular fuzzy number to model uncertain soil parameter is considered appropriate. Such use of a fuzzy number allows us to analyze the effect of uncertainty and compute the probability of serviceability failure in an efficient way. Of course, probabilistic analysis of braced excavations can also be effectively analyzed using the probability theory (e.g., Baroth and Malécot 2010).

Fuzzy data processing by means of vertex method

Almost all routine geotechnical analyses are performed with deterministic models. If the input soil parameters are uncertain and take fuzzy numbers as their values, the output of the deterministic model will be a fuzzy number (or fuzzy numbers). In this case, uncertainties in the input parameters are propagated through the solution processes; and in this study, the processes primarily involve the finite element solution of wall and ground responses in braced excavations.

The fuzzy finite element approach (FFEA) is taken in this study to handle the

uncertainty propagation through the finite element solution. To propagate fuzzy input through the FEM code, the vertex method proposed by Dong and Wong (1987) is adopted. This method is based on the α-cut concept. As shown in Figure 4.3(b), at a membership grade of α_i, an interval with a lower bound of $x_{\alpha_i}^-$ and an upper bound of $x_{\alpha_i}^+$ can be formed. Mathematically, it can be shown that any fuzzy number can be represented by a set of α-cut (or α-level) intervals with α ranging from 0 to 1. Thus, to propagate fuzzy input through the FEM code, fuzzy numbers are first discretized into a set of α-cut intervals (for example, taking $\Delta\alpha$ at 0.2 for α ranging from 0 to 1 yields 6 different levels, α = 0, 0.2, 0.4, 0.6, 0.8, and 1.0). This changes the analysis from the operation of fuzzy numbers into the operation of intervals. However, the traditional interval analysis cannot handle complex computation processes that are involved in finite element solutions. The vertex method removes this difficulty with an effective "sampling" technique.

At each α-level, the intervals of the fuzzy input variables are obtained and the combinations of vertexes (i.e., the lower bounds and the upper bounds of the α-cut intervals of all fuzzy input) are determined. Given n fuzzy input variables, the number of combinations of vertexes is 2^n. Each vertex represents a set of fixed values of input variables that can be readily entered into the FEM code for a deterministic analysis. Each of the 2^n combinations of vertexes are used one-by-one in the FEM analysis, which yields a set of 2^n solutions. Taking the minimum and the maximum of these solutions, an interval is obtained at the specified α-level. Dong and Wong (1987) has proven mathematically that at a given α-level, the interval solution obtained with this vertex method is an exact solution. Repeating the above process for a set of α values, a set of

interval solutions are obtained. Recalling that a fuzzy set is defined by a set of paired values $[x, \mu_A(x)]$, thus the lower bounds and the upper bounds of these intervals along with the corresponding α values define a fuzzy number that represents the outcome of the fuzzy FEM analysis.

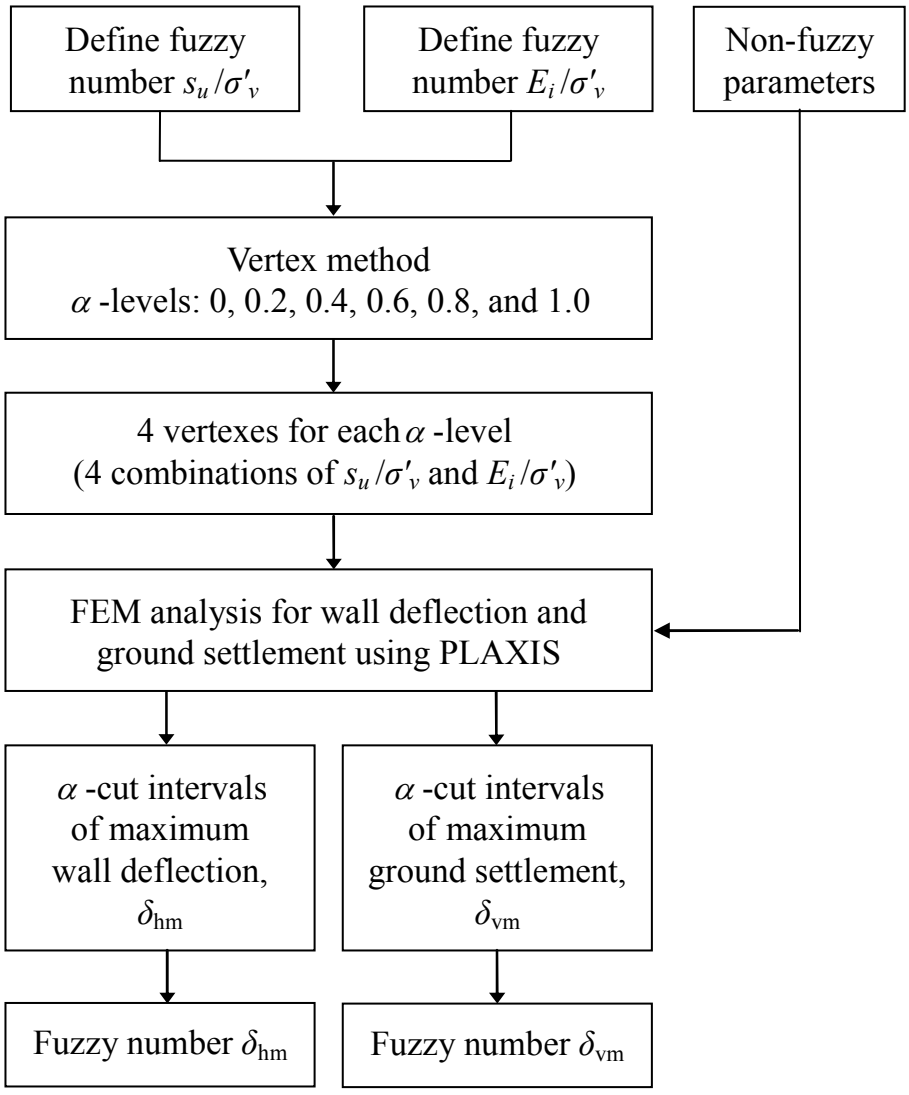

Figure 4.4: Vertex method for fuzzy FEM analysis of braced excavation.

It is noted that the output fuzzy number is generally not sensitive to the number of α-levels, which depends on the magnitude of $\Delta\alpha$, adopted for discretization of fuzzy input variables. For most geotechnical problems, use of $\Delta\alpha = 0.2$ is adequate (see Figure 4.4). If in doubt, however, a sensitivity analysis can be performed using smaller $\Delta\alpha$ values to confirm the convergence in the solution.

In previous studies by Hsiao et al. (2008), wall and ground responses are reported to be strongly affected by variation in the normalized undrained shear strength (s_u / σ'_v) and the normalized initial tangent modulus (E_i / σ'_v). In this study, to deal with uncertain parameters using the proposed methodology, these two parameters are treated as fuzzy parameters and all other factors such as the stiffness of wall and strut, the excavation depth and width, etc. are treated as non-fuzzy parameters. Figure 4.4 shows a flowchart depicting the process of fuzzy data propagation through the FEM code by means of the vertex method.

Interpretation of the resulting fuzzy number

The resulting fuzzy number, obtained by applying the vertex method to a deterministic approach (such as Plaxis^{TM} solution), reflects the uncertainty in the model output. In this study, the model output is the maximum wall deflection and the maximum ground settlement in a braced excavation. An important design consideration is to ensure the probability of exceeding the maximum wall deflection (or ground settlement) is less than a threshold value. To this end, a simple way to compute such probability from the resulting fuzzy number is needed. Using the resulting fuzzy number shown in Figure 4.5

as an example, the probability of exceeding a limiting value can be computed as follows:

$$p_E = p(x > x_{\text{lim}}) = \frac{A_E}{A_F} \tag{4.4}$$

where A_E is the shade area depending on the limiting value x_{lim} and A_F is the entire area under the "curve" of the fuzzy number.

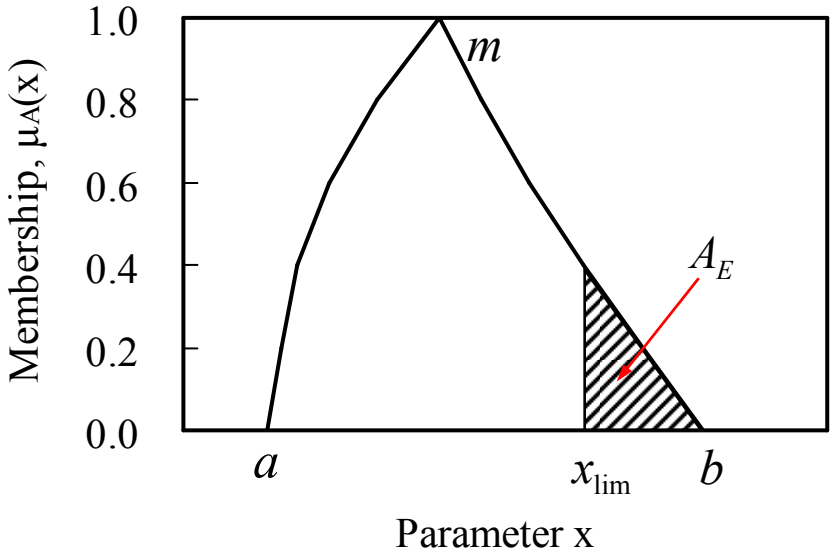

Figure 4.5: Fuzzy number that represents the model output. The shaded area normalized to the full area under the shape is the probability of exceeding the limiting response (x_{lim}).

It is noted that in Figure 4.5, normalization of the shade area with respect to the entire area under the curve is needed as the latter is not necessarily equal to 1. Although a more elegant formulation of the failure probability can be found in the literature (for example, Guo and Lu 2003), Eq. (4.4) is easy to follow and implement.

Case Study – TNEC Excavation Case

The TNEC excavation case in Taiwan (Ou et al. 1998) is used herein as an example to illustrate the fuzzy finite element approach (FFEA) for the analysis of wall and ground responses in braced excavations in clay with a consideration for its spatial variability.

In this case, the excavation width is 41.2 m and the length of the diaphragm wall is 35 m. The excavation is carried out using a top-down construction method in seven stages with support provided by steel struts and floor slabs. Excavation depths and support locations are detailed in Table 4.1. Soil parameters used in *the FEM code* are shown in Table 4.2. In this study, the undrained condition for clay layers is modeled. It is noted that the second layer (8 m – 33m) in the soil profile is a clay layer that dominates the maximum wall and ground responses in this excavation. Hsiao et al. (2008) estimated the coefficient of variation (COV) of the strength and stiffness parameters of Taipei clay as 0.16. In the present study, we consider the uncertainty in soil parameters as well as their spatial variability in the FEM solution. To model the uncertainty of this clay soil, the normalized undrained shear strength (s_u / σ'_v) and normalized initial tangent modulus (E_i / σ'_v) are treated as fuzzy parameters and all other factors such as the stiffness of the wall and strut, the excavation depth and width, etc. are treated as constant parameters in the analysis.

Table 4.1: Propping arrangement for the excavation and the stiffness of struts and floor slabs in the FEM analysis in TNEC case (after Kung et al. 2007a).

Stage	Excavation depth H (m)	Depth of struts H_p (m)	stiffness of struts and slab floor, EA [kN/(m·m^{-1})]
1	2.8	2.0*	8240
2	4.9	3.5**, 0**	125568
3	8.6	7.1**	125568
4	11.8	10.3**	125568
5	15.2	13.7**	125568
6	17.3	16.5*	24035
7	19.7	17.1**	125568

Note: *Steel strut; **Floor slab.

Table 4.2: Soil profile and soil model parameters used in FEM analysis (from Kung et al. 2007a).

Depth(m)	Soil type	Soil model	γ (kN/m^3)	s_u / σ'_v	E_i / σ'_v	ϕ' (º)	K=K_{ur}	n
8.0-33.0	CL	MPP	18.9	0.32	672			
37.5-46.0	SM	Duncan-Chang	19.6			32	2500	0.5
0-5.6	CL	MPP	18.3	0.32	672			
35.0-37.5	CL	MPP	18.2	0.34	714			
5.6-8	SM	Duncan-Chang	18.9			31	750	0.5
33.0-35.0	SM	Duncan-Chang	19.6			31	2500	0.5

Note:

ϕ' = effective friction angle; K_{ur} = elastic modulus of unloading-reloading stages; n = elastic modulus exponent; MPP = Modified Pseudo Plasticity model.

Averaging the effect of spatial variation – A checkerboard study

The effect of spatial variation of soil parameters may be analyzed with a checkerboard analysis (Griffiths and Fenton 2009). In this approach, the random field is

meshed to many small square areas where the upper bound and the lower bound of the soil parameters alternate in the two-dimensional array. The soil parameters in the horizontal direction have much larger scales of fluctuation and are generally spatially correlated when compared with the vertical direction (Phoon and Kulhawy 1999a). Therefore, for simplicity, only the variability through the excavation depth is considered in this study. The upper and lower bounds of the soil parameters (s_u / σ'_v and E_i / σ'_v) are assumed to be the mean, plus and minus one standard deviation respectively, and they only vary vertically on the checkerboard, as shown in Figure 4.6.

Five scenarios are examined in the checkerboard study using *the FEM code*. In the "base" scenario (denoted as S0), the entire clay layer is assigned the mean soil parameters (s_u / σ'_v and E_i / σ'_v) as in a deterministic analysis. In the first scenario (S1), the scale of fluctuation is assumed to be infinite and the two soil parameters, s_u / σ'_v and E_i / σ'_v, are taken as the mean, minus and plus one standard deviation [S1(a) and S1(b), respectively]. In the second scenario (S2), the clay layer is subdivided into four sub-layers. The upper bound and lower bound of s_u / σ'_v and E_i / σ'_v alternate on the checkerboard and thus there are two sub-scenarios in the following sequence: "upper-lower-upper-lower bound sequence" [S2(a)] and "lower-upper-lower-upper bound sequence" [S2(b)]. In the third and fourth scenarios [S3 and S4], the clay layer is subdivided into eight and sixteen sub-layers respectively, with a similar alternating sequence of lower and upper bound. Examples of scenarios S3(a) and S4(a) are shown in Figures. 4.6(a) and 4.6(b), respectively, to illustrate the schematic of the checkerboard

study on the TNEC excavation case.

(a) Scenario Three: 8 sub-layers, Case (a) [denoted as S3(a)]

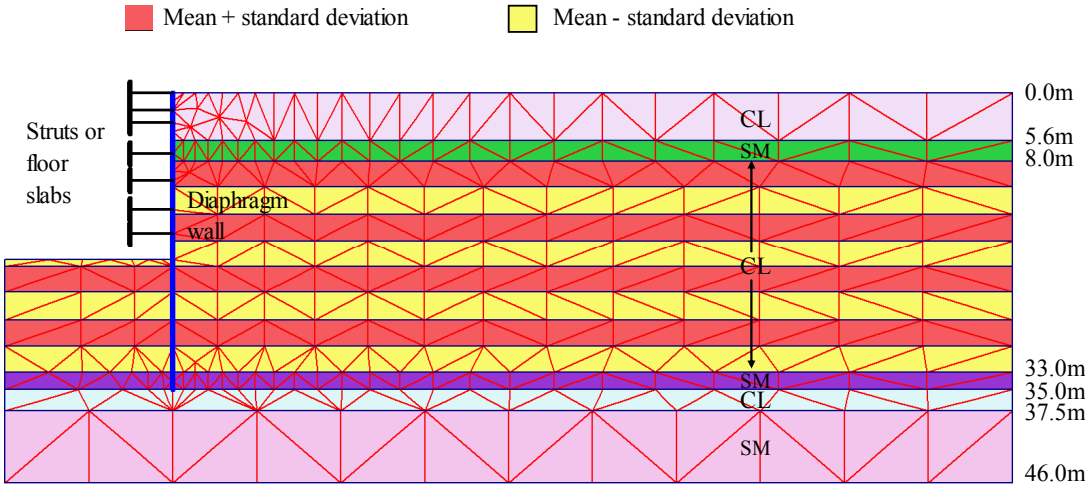

(b) Scenario Four: 16 sub-layers, Case (a) [denoted as S4(a)]

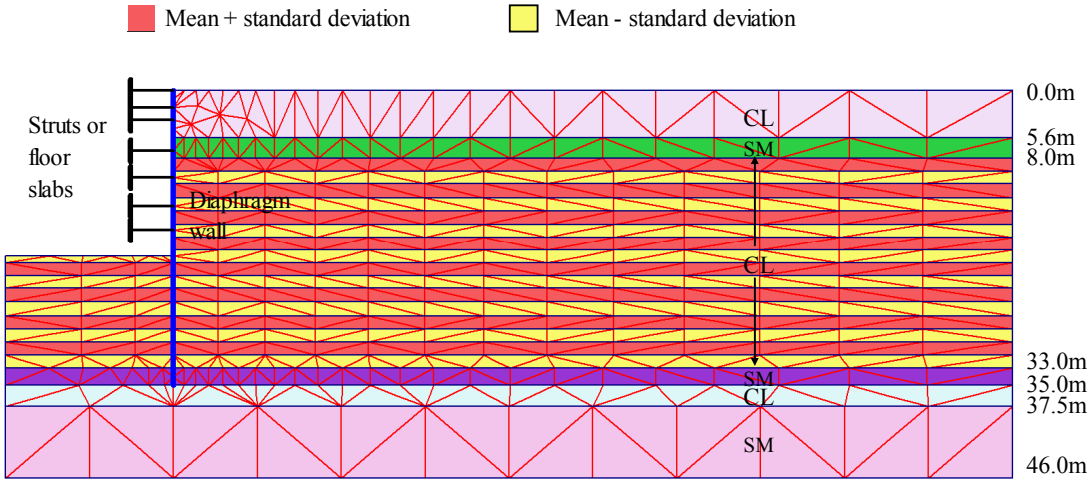

Figure 4.6: Schematic of checkerboard study on the variation of soil parameters in an FEM model of TNEC case.

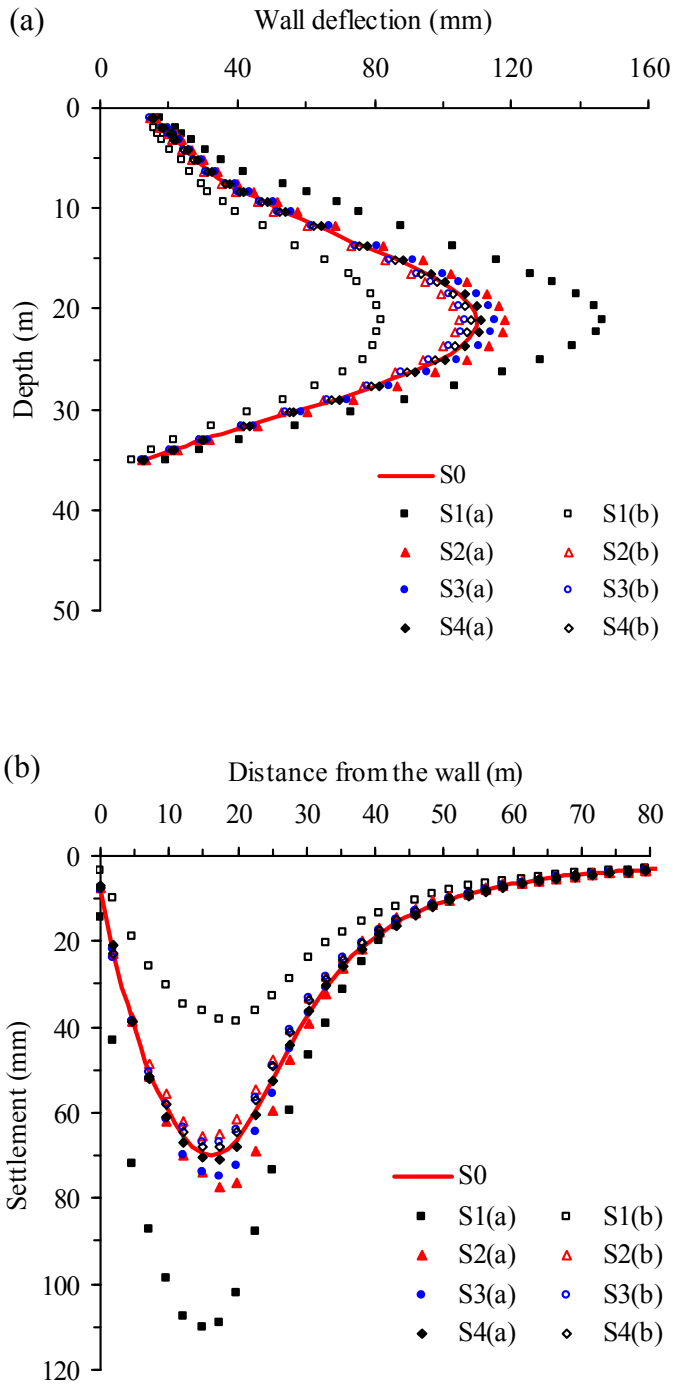

Figure 4.7: Influence of scale of fluctuation on wall deflection and ground settlement.

In reference to the "base" scenario, the other four scenarios are set up so that the scale of fluctuation decreases gradually from S1 to S4. Here, S1 is viewed as equivalent to the spatially-constant condition, while S4 has the smallest scale of fluctuation among all the scenarios with soil parameters varying drastically from sub-layer to sub-layer in the vertical direction. The rationale behind the division of the clay layer in the checkerboard study as described previously is consistent with the random field analysis conducted by Griffiths et al. (2006) –as the scale of fluctuation approaches to infinity, the shear strength at each point in the random field becomes uniform; on the other hand, as the scale of fluctuation approaches zero, the shear strength at each point in the random field becomes independent and fluctuates rapidly from point to point.

The finite element analysis under different scenarios is aimed at investigating the averaging effect of spatial variation. The results of wall and ground responses through the checkerboard study are shown in Figures 4.7(a) and 4.7(b), respectively. The responses computed with the "base" scenario are shown with solid curves in these figures. The variations in wall deflection and ground-surface settlement for other scenarios are observed [for example, comparing the difference between S1(a) and S1(b), and between S2(a) and S2(b), and so on]. The variation in responses is the greatest under scenario S1, in which the scale of fluctuation is assumed to be infinite (and thus the soil parameters are spatially constant). The variation in responses decreases from S1 to S4 as the spatial variability increases (or the scale of fluctuation decreases). In conclusion, as the scale of fluctuation becomes smaller, the variation of wall and ground responses becomes smaller.

Since the results from the previous geotechnical random field studies have shown

that variation of the output increases with variability of the input (e.g., Griffiths et al. 2006), the conclusion from the checkerboard study in this study is consistent with the concept of the spatial averaging effect: a smaller scale of fluctuation results in a larger variance reduction in soil parameters, which would yield a smaller variation of wall and ground responses.

The results of the checkerboard study show a strong averaging effect of the spatially random soil parameters exists in the braced excavation problem. Even though the checkerboard analysis is a simplified simulation of the real random field of soils, it ascertains the validity of the variance reduction technique in the finite element analysis of braced excavation in clays. This provides the basis for the proposed FFEA approach that takes into account the spatial variability of soil parameters.

Fuzzy FEM analysis of TNEC case considering spatial variability

As noted previously, the goal of this study is to demonstrate the proposed procedures for computing the probabilities of exceeding the limiting wall and ground responses in a braced excavation while taking into account spatial variability in key soil parameters. For this case study, the TNEC excavation, the normalized undrained strength s_u / σ'_v and the normalized initial tangent modulus E_i / σ'_v of the clay are s_u / σ'_v = 0.32 and E_i / σ'_v = 672, respectively (Kung et al. 2007a). The standard deviations of the two parameters are estimated to be 0.05 and 108 respectively, based on a reported coefficient of variation (COV) of 0.16 (Hsiao et al. 2008). The two soil parameters are treated here as triangular fuzzy numbers, since the available data are not sufficient to

characterize them in terms of probability distributions.

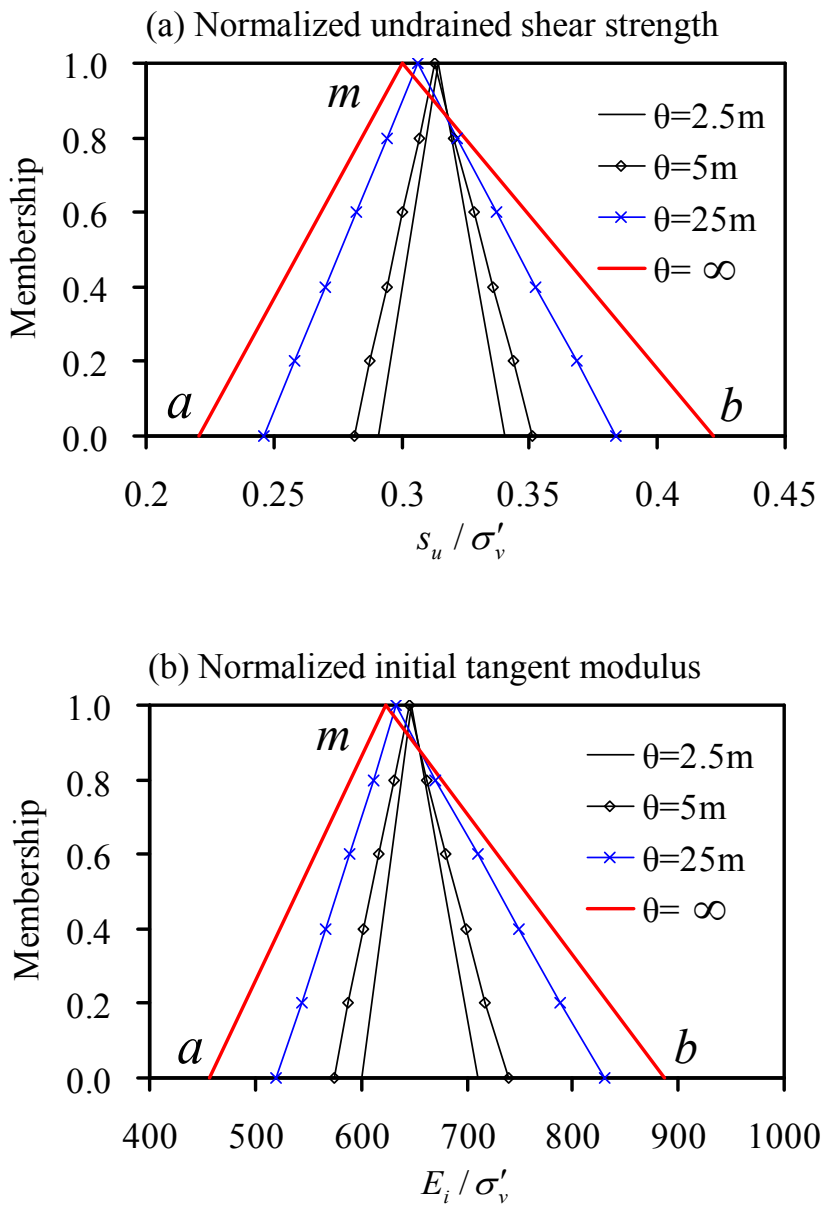

Figure 4.8: Fuzzy input parameters at different scales of fluctuation.

To consider the effect of spatial variability, let's *first* assume that the field has an

infinite scale of fluctuation. The variance reduction factor (Γ^2) in this case is equal to 1 (i.e., no reduction) and thus the standard deviations for s_u / σ'_v and E_i / σ'_v would be 0.05 and 108, respectively. If we assume the mean plus and minus 2 times the standard deviation for the lower and upper bound, and *conservatively* assume the mode to be slightly less than the mean, then the fuzzy numbers for s_u / σ'_v and E_i / σ'_v can be readily constructed [see the triangular membership function labeled *a-m-b* in Figures 4.8(a) and 4.8(b), respectively]. Of course, slightly different fuzzy numbers may be obtained by different individuals based on their own experience. This is the nature of geotechnical practice, due to limited data availability. Fortunately, similar conclusions are usually reached even with some differences in the assumed fuzzy numbers. When in doubt, however, a series of sensitivity analyses with different assumed fuzzy numbers should be performed to remove or reduce the uncertainty in the solution.

Analysis of the braced excavation in the TNEC case is carried out using *the FEM code*. To deal with the fuzzy input, the vertex method is employed using the algorithm shown previously in Figure 4.4. The resulting fuzzy numbers obtained from *the FEM code*, as shown in Figure 4.9, represent the maximum wall deflection (δ_{hm}) and ground-surface settlement (δ_{vm}). Under this scenario of an infinite scale of fluctuation, the computed maximum wall deflection (δ_{hm}) is described by the triangular membership function labeled *a-m-b* in Figure 4.9(a), and the computed ground-surface settlement (δ_{vm}) is described by the triangular membership function labeled *a-m-b* in Figure 4.9(b).

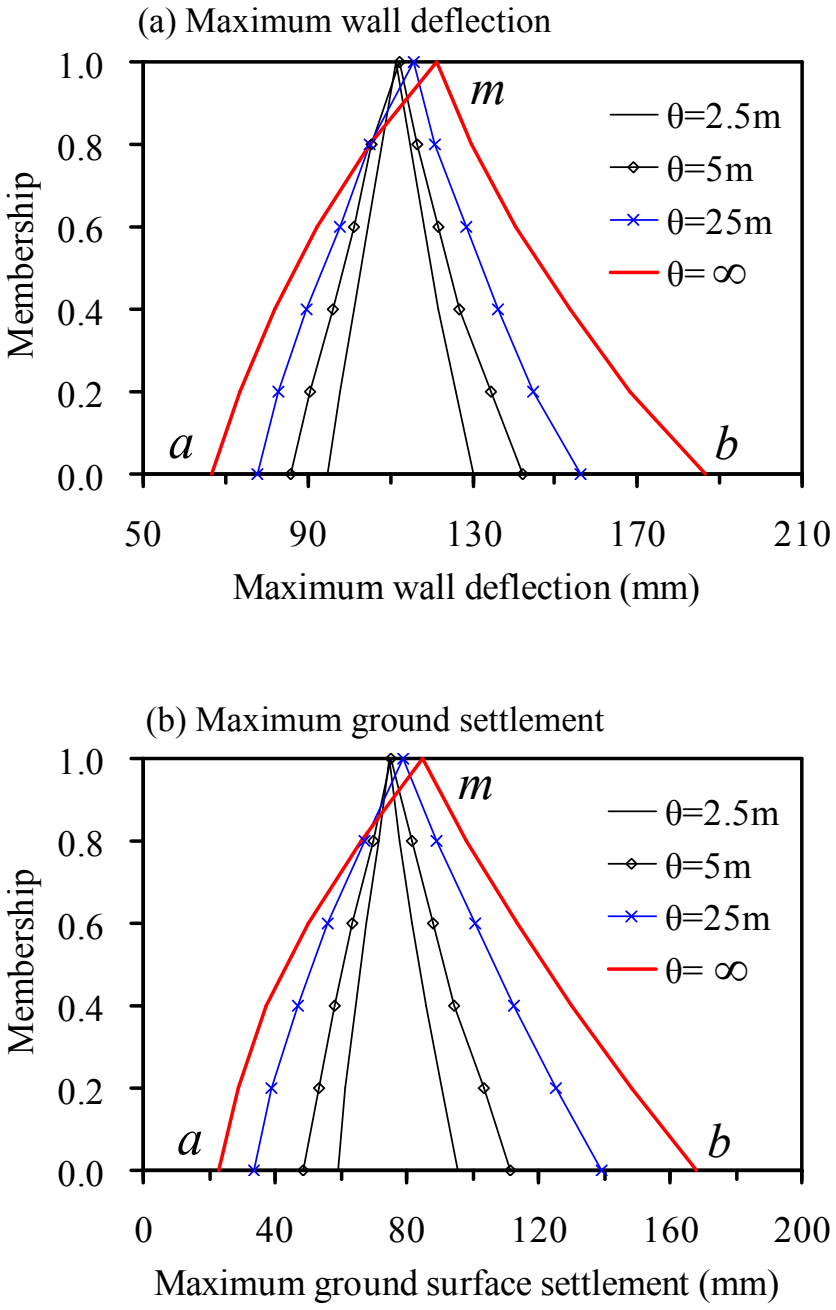

Figure 4.9: Resulting fuzzy numbers for maximum wall deflection and ground-surface settlement.

It should be noted that the results shown in Figure 4.9 were obtained using the

vertex method with discretization increment $\Delta\alpha = 0.2$ (Figure 4.4). A series of analyses were also carried out using $\Delta\alpha = 0.1$ and 0.05 for discretization of the input fuzzy variables. The output fuzzy numbers for maximum wall deflection (δ_{hm}) and ground-surface settlement (δ_{vm}) for this TNEC case remain nearly the same with smaller $\Delta\alpha$ values. Thus, in this case, the analysis of wall deflections of ground settlement in an excavation, the use of $\Delta\alpha = 0.2$ is adequate.

The entire processes described in the above FFEA analysis can be repeated for any assumed scale of fluctuation. For simplicity, we can assume the scales of fluctuation of the two soil parameters in this TNEC case are the same; that is, $\theta = \theta_{s_u/\sigma'_v} = \theta_{E_i/\sigma'_v}$. For demonstration purposes, let's repeat the FFEA analysis for three additional scales of fluctuation (2.5m, 5m, and 25m). For each scenario involving a different scale of fluctuation, the variance reduction factor (Γ^2) is first computed with Eq. (4.2), which requires knowledge of the characteristic length, *L*. At the TNEC site, and within the length of the diaphragm wall, the deposit consists primarily of a clay layer, the thickness of which is approximately equal to 90% of the wall length. Sensitivity analysis using *the FEM code* shows the clay layer dominates the wall and ground responses in this excavation, as expected. Therefore, it is considered appropriate to estimate the characteristic length *L* according to the procedure described previously (in reference to Figure 4.2). Following this argument, *L* is estimated to be 71 m in this case.

Once the variance reduction factor is estimated for a given scale of fluctuation, the "reduced" standard deviations of the soil parameters (s_u/σ'_v and E_i/σ'_v) are then

computed with Equation (4.3). Thus, the fuzzy numbers that represent s_u / σ'_v and E_i / σ'_v for any given scale of fluctuation can be constructed with the results shown in Figures 4.8(a) and 4.8(b), respectively. Next, the analyses with *the FEM code* in the framework of the vertex method (Figure 4.4) proceeds. The resulting fuzzy numbers that represent maximum wall deflection (δ_{hm}) and ground-surface settlement (δ_{vm}) are shown in Figures 4.9(a) and 4.9(b), respectively.

As shown in Figures 4.9(a) and 4.9(b), the variability of maximum wall deflection and ground-surface settlement increase *significantly* with the scale of fluctuation. The variance reduction in cases of smaller scales of fluctuation are reflected in reduced variability of the computed δ_{hm} and δ_{vm}. Thus, neglecting spatial variability of input soil parameters (by assuming $\theta = \infty$) can lead to an overestimation of variation of computed wall and ground responses in a braced excavation.

Probabilities of exceeding the specified limiting wall and ground responses

Because the predicted wall and ground responses in a braced excavation are fuzzy numbers, the assessment of whether predicted responses are excessive and intolerable can best be expressed in a probability term. In fact, the probability of exceeding a limiting value, such as limiting wall deflection ($\delta_{\lim,hm}$) or limiting ground-surface settlement ($\delta_{\lim,vm}$), can be computed easily with Eq. (4.4).

For illustration purposes, the probabilities of exceedance are computed for the TNEC case under a few assumed limiting wall and ground responses. The results are

plotted in Figures 4.10(a) and 4.10(b) for the probabilities of exceeding the chosen limiting wall deflection and ground settlement, respectively. The probability of exceedance is seen to decrease with the chosen limiting deformation (either wall deflection or ground settlement) which is consistent with the previous study (Hsiao et al. 2008). The effect of the scale of fluctuation on the probability of exceedance is clearly observed. When relatively smaller limiting $\delta_{\lim,hm}$ and $\delta_{\lim,vm}$ are adopted, the scenario with a smaller scale of fluctuation yields a higher probability of exceedance. The trend reverses when relatively larger limiting $\delta_{\lim,hm}$ and $\delta_{\lim,vm}$ are adopted. For the probability of exceeding the limiting wall deflection, the reversal of the trend occurs when $\delta_{\lim,hm} \approx 108$ mm is adopted. Similarly, for the probability of exceeding the limiting ground settlement, the reversal of the trend occurs when $\delta_{\lim,vm} \approx 72$ mm is adopted. Of course, this observation may not be generalized as it may be specific to the TNEC case. Further studies are needed to confirm this observation. Nevertheless, the results show that neglecting spatial soil variability in the analysis can lead to either overestimation or underestimation of the probability of exceedance, depending on the chosen limiting wall and ground responses. Thus, it is important to assess spatial variability during site investigation and to incorporate this variability in the probability analysis.

(a) Wall deflection

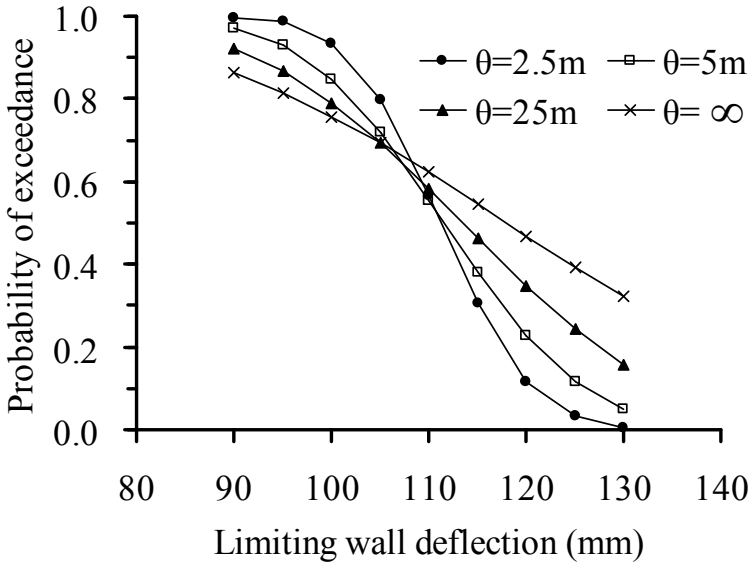

(b) Ground surface settlement

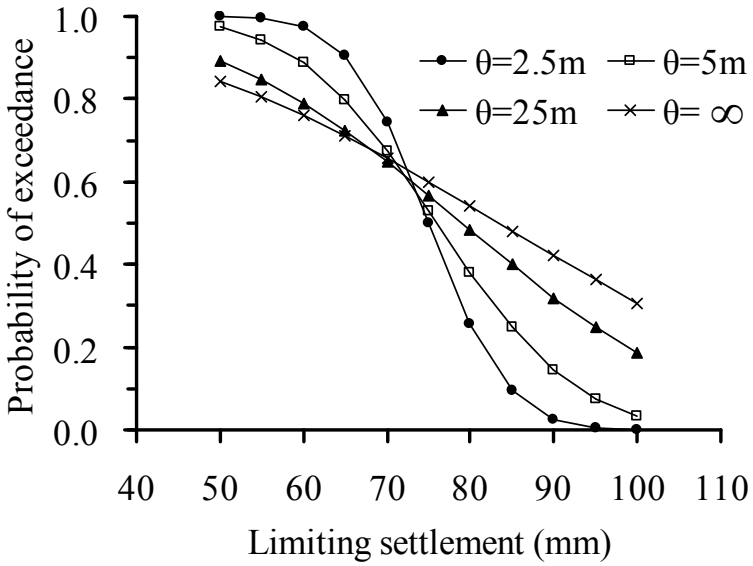

Figure 4.10: Probability of exceedance computed at various levels of limiting wall deflection and ground surface settlement.

Summary and limitations of the proposed framework

The proposed framework allows for evaluation of the probability of serviceability failure (i.e., the probability of exceeding limiting wall and ground responses) in a braced excavation. This framework consists of the following elements: 1) finite element method (FEM) for analyzing the wall and ground responses in a braced excavation, 2) fuzzy set modeling of parameter uncertainty, 3) spatial averaging technique for handling soils spatial variability, 4) vertex method for propagating fuzzy input through FEM model, and 5) interpretation of fuzzy output. The proposed framework represents an efficient use of various existing methods for solving a complex braced excavation problem.

The limitations of the proposed framework stem mostly from the limitations of component methods employed in this framework and the assumptions that are made in using these methods. These limitations are briefly discussed in the following.

1) The accuracy of the computed probability of exceedance (i.e., exceeding limiting wall and ground responses) depends on the accuracy of the FEM model and the accuracy of the derived soil parameters. We assume that the two-dimensional (2-D) FEM solutions for wall and ground movements in a braced excavation obtained with Plaxis^{TM} are reasonably accurate.
2) Fuzzy set modeling of parameter uncertainty represents an approximation that stems from the use of insufficient number of data that necessitates an exercise of engineering judgment. The accuracy of the computed probability of exceedance can certainly be affected by this approximation. On the other hand, fuzzy set modeling allows for an estimation of the probability of exceedance

with limited data. Furthermore, the fuzzy FEM analysis is well-defined and introduces no additional error, once uncertain parameters are properly modeled with fuzzy sets.

3) The computed probability of exceedance can also be affected by the assumptions made in modeling spatial variability. In this study, the variance function is defined with an assumption that the autocorrelation function takes the form of a single exponential model. Although the effect of the type of autocorrelation function (for example, constant, triangular, or exponential) was found insignificant in a recent study of bearing capacity problems (Most and Knabe 2010), this issue needs further investigation. Furthermore, in this study the soil variability is considered only in the vertical direction. Although the horizontal scale of fluctuation for clay is generally much greater than the vertical scale of fluctuation (Phoon and Kulhawy 1999a), and thus, its effect is far less significant, the effect of the spatial variability assumption on the computed probability of exceedance needs further investigation (by considering 2-D or 3-D spatial variability models).

Summary

The focus of this chapter is to demonstrate a simplified approach for evaluating the probability of exceeding the specified limiting wall and ground response in a braced excavation as a means to prevent the excavation failure or damage to the adjacent infrastructures. This approach (FFEA) consists of the following elements: 1) finite

element method (FEM) for analyzing the wall and ground responses in a braced excavation, 2) fuzzy set representation of parameter uncertainty, 3) spatial averaging technique for handling soil variability, 4) vertex method for propagating fuzzy input through FEM model, and 5) fuzzy probabilistic interpretation of the fuzzy output. A well-documented case history is analyzed to demonstrate this simplified approach. The results show that the proposed framework is effective for assessing probability of exceeding the limiting wall and ground responses in a braced excavation.

Neglecting spatial variability of input soil parameters can lead to an overestimation of variation of wall and ground responses in a braced excavation. The effect of the scale of fluctuation on the "probability of exceedance" (exceeding the specified limiting response) is also observed in this study. Neglecting spatial variability in the FFEA analysis can lead to either overestimation or underestimation of the probability of exceedance, depending on the specified limiting response. Thus, it is important to assess spatial variability during site investigation and to incorporate this variability into the FFEA analysis of braced excavation.

The results presented in this chapter are limited to one-dimensional (1-D) spatial variability with an assumed exponential autocorrelation function. The effects of adopting other autocorrelation functions and/or considering 2-D (or 3-D) spatial variability on the computed probability of exceedance is beyond the scope of this study; however, further investigation of these issues is warranted.

CHAPTER V

EFFECT OF SMALL SAMPLE SIZE ON THE PROBABILISTIC SERVICEABILITY ASSESSMENT [*]

Introduction

An accurate calculation of the probability of exceeding a limiting deformation requires an accurate analysis model for the wall and ground responses (which can lead to a well-characterized and proper limit state or performance function) and an accurate statistical characterization of the input soil parameters. In this chapter, the KJHH model (Kung et al. 2007b), a semi-empirical model that was generated with hundreds of finite element simulations and validated with well-documented case histories, will be used for computing the excavation-induced wall and ground responses in an excavation in clays. The KJHH model is well characterized, and thus, the focus of this chapter is on parameter uncertainty and its effect on the computed probability of exceedance.

The sources of parameter uncertainty include inadequate site investigation, measurement errors, as well as inherent and spatial variability of soil. Statistical methods have long been used for characterization of parameter uncertainty in geotechnical engineering (e.g., Lee et al. 1983; Harr 1987; Baecher and Christian 2003; Ang and Tang 2007; Fenton and Griffiths 2008). Reliability analysis offers a means to *explicitly* account for the uncertainty in soil parameters (Harr 1987; Ang and Tang 2007). Previous studies on reliability analysis of excavation-induced deformation showed that uncertainties in

[*] A similar form of this chapter has been submitted at the time of writing: Luo Z, Atamturktur S, Juang CH. Bootstrapping for characterizing the effect of uncertainty in sample statistics – A case study of the serviceability failure probability in a braced excavation.

soil parameters can have a significant effect on the probability of serviceability failure in a braced excavation (e.g., Hsiao et al., 2008).

Many reliability analyses are based on sample statistics of soil parameters that are derived from very limited data. These sample statistics are often assumed, out of necessity, to be the population statistics. Thus, the accuracy of a reliability analysis is affected by: (1) the accuracy of sample statistics (including mean and standard deviation in most applications) of the uncertain soil parameters, and also (2) type of the probability distribution of these parameters that often has to be assumed (Schweiger and Peschl 2005). It is noted, however, that most soil parameters can be adequately modeled with a lognormal distribution (Phoon and Kulhawy 1999b) or truncated normal distribution (Most and Knabe 2010). Thus, the focus of this study is to examine the effect of *uncertain* sample statistics on the result of the reliability analysis.

Because of budget constraints, the geotechnical engineer often has to derive sample statistics from a small sample (i.e., a small data set), which can lead to uncertainty in these statistics. Thus, the effect of this uncertainty on the probability of failure should be examined. In this study, we investigate this effect using the bootstrapping technique (Efron 1979). To demonstrate this technique, a case study investigating the effect of uncertain sample statistics of soil parameters on the computed probability of serviceability failure in a braced excavation is presented. Unlike traditional reliability analysis, where a single fixed probability is obtained with a set of *fixed* sample statistics, reliability analysis with the bootstrap method explicitly considers the uncertainty in the derived sample statistics. The latter approach enables an interval estimate of the failure

probability at a specified confidence level. The information gained through this approach is in the form of a confidence interval and can enable the engineer to make a more informed design decision.

Performance Function for Probability of Exceedance

As noted previously, the KJHH model (Kung et al. 2007b) is employed herein to compute the maximum wall deflection (δ_{hm}) and maximum ground-surface settlement (δ_{vm}) in a braced excavation in clays. This model was derived based on multivariate nonlinear regression analysis with data derived from thirty-three excavation histories and hundreds of numerical simulations using finite element method (FEM). This model consists of a set of equations that collectively can be used to compute δ_{hm} and δ_{vm} based on the following parameters: excavation depth (*H*); excavation width (*B*); the system stiffness [$S = EI/\gamma_w h_{avg}^4$ as defined in Clough and O'Rourke (1990), where *E* is the Young's modulus of wall material, *I* is the moment of inertia of the wall section, γ_w is the unit weight of water, and h_{avg} is the average support spacing]; the normalized clay layer thickness $\Sigma H_{clay} / H_{wall}$ [where H_{wall} is the wall length and ΣH_{clay} is the total thickness of all clay layers within the wall length; in a clay only deposit, this ratio is equal to 1]; the normalized undrained shear strength (s_u/σ'_v); and the normalized initial tangent modulus (E_i / σ'_v). The maximum lateral wall deflection (δ_{hm}) is determined as:

$$\delta_{hm} = a_0 + a_1X_1 + a_2X_2 + a_3X_3 + a_4X_4 + a_5X_5 + a_6X_1X_2 + a_7X_1X_3 + a_8X_1X_5 \qquad (5.1)$$

where $X_1 = t(H)$, $X_2 = t\left(\ln\left(EI/\gamma_w h_{avg}^4\right)\right)$, $X_3 = t(B/2)$, $X_4 = t(s_u/\sigma_v')$, $X_5 = t(E_i/\sigma_v')$. The mean and standard deviation of the model uncertainty or bias factor (*BF*) of this model are estimated to be at 1.0 and 0.25, respectively (Kung et al. 2007b). The coefficients for Eq. (5.1) determined through the least-square regression are as follows: a_0 = –13.41973, a_1 = –0.49351, a_2 = –0.09872, a_3 = 0.06025, a_4 = 0.23766, a_5 = –0.15406, a_6 = 0.00093, a_7 = 0.00285 and a_8 = 0.00198. Variables $X_i\ (i = 1, 5)$ are obtained through transformation:

$$X_i = t(x_i) = b_1 x_i^2 + b_2 x_i + b_3 \tag{5.2}$$

where $x_i\ (i = 1, 5)$ is the corresponding input parameter. The coefficients for the transformations in this model are summarized in Table 5.1.

Table 5.1: Coefficients for transformation of input variables (Kung et al. 2007b).

Variables x	Coefficients in Eq. (5.2)		
	b_1	b_2	b_3
H (m)	-0.4	24	-50
$\ln(EI/\gamma_w h_{avg}^4)$	11.5	-295	2000
$B/2$ (m)	-0.04	4	90
s_u/σ_v'	3225	-2882	730
E_i/σ_v'	0.00041	-1	500

To compute the maximum ground-surface settlement (δ_{vm}), the KJHH model employs a deformation ratio *R* defined as follows:

$$R = c_0 + c_1 Y_1 + c_2 Y_2 + c_3 Y_3 + c_4 Y_1 Y_2 + c_5 Y_1 Y_3 + c_6 Y_2 Y_3 + c_7 Y_3^3 + c_8 Y_1 Y_2 Y_3 \quad (5.3)$$

where $Y_1 = \sum H_{clay} / H_{wall}$, $Y_2 = s_u / \sigma'_v$, $Y_3 = E_i / 1000\sigma'_v$, and the coefficients for Eq. (5.3) determined through the least-square regression are as follows: c_0 = 4.55622, c_1 = –3.40151, c_2 = –7.37697, c_3 = –4.99407, c_4 = 7.14106, c_5 = 4.60055, c_6 = 8.74863, c_7 = 0.38092 and c_8 = –10.58958. Then, the maximum ground-surface settlement (δ_{vm}) is obtained:

$$\delta_{vm} = R \cdot \delta_{hm} \quad (5.4)$$

The mean and standard deviation of the model uncertainty or bias factor (*BF*) of this model are estimated to be at 1.0 and 0.34, respectively (Kung et al. 2007b).

With the above set of equations [Eqs. (5.1) through (5.4)], the maximum wall deflection (δ_{hm}) and maximum ground-surface settlement (δ_{vm}) in an excavation in clays can be computed. These equations provide a fairly accurate estimate of the wall and ground responses. If so desired, more sophisticated methods such as well-calibrated FEM models can be used for determining the wall and ground responses. Nevertheless, the simplified approach using the above set of equations allows us to easily set up a performance function for evaluating the probability of exceeding the specified limiting wall and ground response:

$$G(x) = y_{\lim} - y = 0 \tag{5.5}$$

where $G(x)$ is the limit state or performance function, x is a vector of parameters, y is the response (the maximum wall deflection or ground settlement) computed with the KJHH model, and $y_{\lim}$ is the specified limiting response.

Point Estimate Method for Uncertainty Propagation and Probability of Exceedance

For a *given* braced excavation in clay, Hsiao et al. (2008) found that among all input parameters of the KJHH model, the wall and ground responses are most sensitive to the variation in s_u/σ'_v and E_i/σ'_v. Thus, for a *given design* of a braced excavation, all parameters but s_u/σ'_v and E_i/σ'_v may be considered as fixed variables, and as such, the wall and ground responses become only a function of these two soil parameters and the bias factor. For simplicity, the two random variables s_u/σ'_v and E_i/σ'_v are denoted as x_1 and x_2 respectively; meanwhile, the model bias factor (*BF*) of the KJHH model is denoted as x_3. Thus, the response y, either as the maximum wall deflection δ_{hm} or the maximum ground settlement δ_{vm}, can be written as $y = f(x_1, x_2, x_3)$. Many different methods may be used to compute the mean and standard deviation of the response y. In this study, the point estimate method (PEM; see Rosenblueth 1975; Harr 1987; Christian and Baecher 1999) is chosen for this task for its simplicity and ease in Excel® implementation. With the PEM approach, the m^{th} moment for y can be readily expressed as (Harr 1987):

$$E[y^m] = p_{+++}y^m_{+++} + p_{++-}y^m_{++-} + p_{+-+}y^m_{+-+} + p_{+--}y^m_{+--} + p_{-++}y^m_{-++} + p_{-+-}y^m_{-+-} + p_{--+}y^m_{--+} + p_{---}y^m_{---} \tag{5.6}$$

where

$$y_{\pm\pm\pm} = f\left(\overline{x_1} \pm \sigma[x_1],\ \overline{x}_2 \pm \sigma[x_2],\ \overline{x}_3 \pm \sigma[x_3]\right) \tag{5.7}$$

$$p_{\pm\pm\pm} = \frac{1}{8}\left(1 \pm \rho_{x_1,x_2} \pm \rho_{x_1,x_3} \pm \rho_{x_2,x_3}\right) \tag{5.8}$$

and where $\overline{x}_1$, $\overline{x}_2$, $\overline{x}_3$, $\sigma[x_1]$, $\sigma[x_2]$, $\sigma[x_3]$ are the mean values, and the standard deviations, for random variables x_1, x_2 and x_3, respectively; $\rho_{i,j}$ is the correlation coefficient between random variables *i* and *j*; sign preceding $\rho_{i,j}$ is determined by the sign of the multiplication of *i* and *j*. In this study, no correlation between *BF* and each soil parameter is assumed, while soil parameters s_u/σ'_v and E_i/σ'_v are positively correlated (Hsiao et al. 2008).

Once the first and second moments are obtained, the mean μ_y and the standard deviation σ_y of the response *y* can be computed as follows (Ang and Tang 2007):

$$\mu_y = E[y] \tag{5.9}$$

$$\sigma_y = \sqrt{E[y^2] - \left(E[y]\right)^2} \tag{5.10}$$

Although both *y* and $y_{\lim}$ in Eq. (5.5) can be treated as a random variable, in this study $y_{\lim}$ is treated as a constant, as it is almost always specified as a constant in an applicable

design code (for example, see Table 1.1). Thus, the reliability index β can be computed as follows:

$$\beta = \frac{y_{\lim} - \mu_y}{\sigma_y} \tag{5.11}$$

Then, the probability of exceeding the limiting response (p_f) can be computed as:

$$p_f = P[y > y_{\lim}] = 1 - \Phi(\beta) \tag{5.12}$$

where Φ is the cumulative standard normal distribution, and in Excel®, it is implemented with a built-in function NORMSDIST.

Variation of Sample Statistics Determined by Bootstrapping

Because of the uncertainties in the adopted analysis model and the input parameters, the answer to the question of whether the maximum wall or ground response will exceed the specified limiting value in a given excavation design cannot be expressed as a simple "yes" or "no" with certainty. A logical, and more appropriate, answer would be a probability of exceedance, which gauges the likelihood of exceeding the specified limiting values. In other words, the uncertainty leads us to the use of probability as an answer. Of course, the probability is an estimate of the likelihood before the "event;" after the event, it can only be equal to either 0 or 1.

In the procedure and formulation presented previously, the knowledge of mean and standard deviation of the two key soil parameters, s_u / σ_v' and E_i / σ_v', is needed.

Because geotechnical parameters, such as s_u / σ_v' and E_i / σ_v', are typically evaluated with a small sample size, the derived sample statistics (such as mean and standard deviation) are subjected to error. Therefore, the variation from the "true" mean and standard deviation (i.e., those of the population) is expected. As a result of this inevitable uncertainty in sample statistics, the probability of exceedance evaluated with the previous procedure can no longer be adequately expressed as a single, fixed value. By considering the effect of the variation of the derived sample statistics (mean and standard deviation), an estimate of the variation of the computed probability of exceedance (through an evaluation of reliability index), in the form of a confidence interval, can be made. To derive the confidence interval of the probability of exceedance, it is first necessary to estimate the variation of the derived sample statistics.

Bootstrapping (Efron 1979) is a technique that can be used to estimate the variation of the sample statistics derived from a small sample. To begin with, the original set of observations (e.g., soil test data) are denoted as X_1, X_2, $\cdots$, X_n and a bootstrap sample set B_j with n_b samples is denoted as $B_{1,j}$, $B_{2,j}$, $\cdots$, $B_{n_b,j}$. The number of samples n_b in a single bootstrap re-sampling is chosen to be equal to the number of observations n in our study. Then, a bootstrap sample set is constructed by random re-sampling with replacement from the original observations as illustrated in Figure 5.1.

With the constructed re-sampling set, the sample statistics of concern (e.g., mean value and variance) can be obtained as follows:

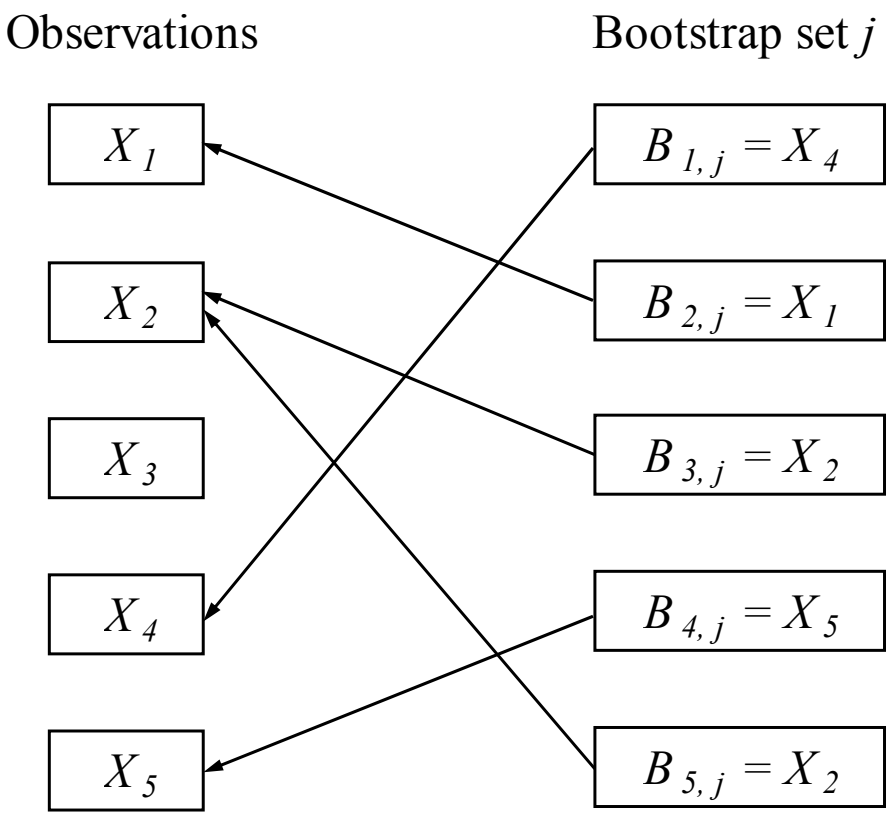

Figure 5.1: Generation of one bootstrap sample from the original observations through random choice with replacement (adapted from Most and Knabe 2010).

$$\overline{B}_{n,j} = \frac{1}{n}\sum_{i=1}^{n} B_{i,j} \tag{5.13}$$

$$S^2_{n,j} = \frac{1}{n-1}\sum_{i=1}^{n}\left(B_{i,j} - \overline{B}_{n,j}\right)^2 \tag{5.14}$$

The procedure for re-sampling described above is repeated many times and the estimated mean and variance are calculated for each bootstrap sample. To this end, each of statistics investigated can be estimated using its mean value, variance, and histogram.

Thus, the bootstrap mean and variance estimates of the sample mean value M_n can be expressed as follows:

$$M_{n,mean} \approx \frac{1}{n_s}\sum_{j=1}^{n_s}\overline{B}_{n,j} \tag{5.15}$$

$$\sigma^2_{M_n} \approx \frac{1}{n_s-1}\sum_{j=1}^{n_s}\left(\overline{B}_{n,j} - M_{n,mean}\right)^2 \tag{5.16}$$

Similarly, the bootstrap mean and variance estimates of the sample variance S_n^2 can be expressed as follows:

$$S_{n,mean} \approx \frac{1}{n_s}\sum_{j=1}^{n_s}S_{n,j} \tag{5.17}$$

$$\sigma^2_{S_n} \approx \frac{1}{n_s-1}\sum_{j=1}^{n_s}\left(S_{n,j} - S_{n,mean}\right)^2 \tag{5.18}$$

in which, n_s is the number of bootstrap sets and is generally chosen very large (e.g., 10^4) to obtain converged results in the statistical analysis (Most and Knabe 2010).

With the bootstrap method, the variation of the sample statistics of soil parameters can be estimated, and their effect on the computed probability of exceedance can be determined and expressed in terms of confidence intervals.

Case Study – TNEC Excavation Case

The Taipei National Enterprise Center (TNEC) case is a well-documented

excavation case history (Ou et al., 1998). This excavation in soft to medium clays in the Taipei basin was completed in seven stages with the support of steel struts and floor slabs. The excavation width is 41.2 m, the final excavation depth is 19.7 m, and the length of diaphragm wall is 35 m. The soil profile and the excavation depth of each stage are depicted in Figure 5.2.

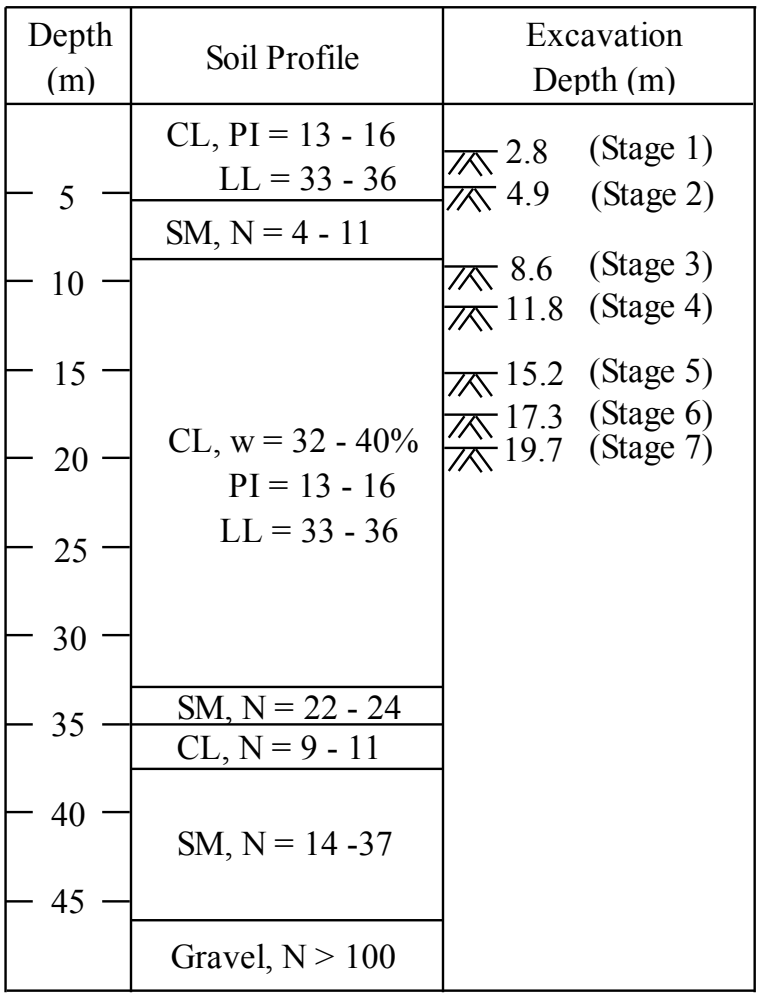

Figure 5.2: Soil profile and excavation depth of TNEC case: LL,liquid limit; N, blow count; PI, plasticity index; w, moisture content (adapted from Kung et al. 2007a).

Reliability analysis based on the KJHH model

The procedure described previously, formulated with Eqs. (5.1) through (5.12), is readily applicable for computing the probability of serviceability failure (p_f), defined herein as the probability of exceeding a specified limiting wall deflection or ground settlement. This probability of exceedance can be obtained once the mean and standard deviation of the response (i.e., maximum wall deflection and ground settlement) are determined. Thus, the key step in this solution process is to determine the mean and standard deviation of the response given uncertain soil parameters.

Assuming that the mean values of s_u / σ'_v and E_i / σ'_v, denoted as μ_S and μ_E respectively, and the standard deviation of s_u / σ'_v and E_i / σ'_v, denoted as σ_S and σ_E respectively, are available, the mean value and standard deviation of the maximum wall deflection δ_{hm} (or the maximum ground settlement δ_{vm}) can be determined with the PEM approach.

For the TNEC case, the sample mean and sample standard deviation of s_u / σ'_v and E_i / σ'_v are given in Table 5.2, based on the 17 small-strain triaxial test data on the reconstituted and undisturbed clay samples reported by Kung (2003). Taking μ_S = 0.31, σ_S = 0.038, μ_E = 581.7 and σ_E = 129.8, the mean of δ_{hm}, denoted as $\mu[\delta_{hm}]$, is computed to be: $\mu[\delta_{hm}]$ = 108.8 mm, and the standard deviation of δ_{hm}, denoted as $\sigma[\delta_{hm}]$, is computed to be: $\sigma[\delta_{hm}]$ = 38.5 mm. If the limiting wall deflection is taken at $0.7\%H_f$ (PSCG 2000), where H_f is the final excavation depth (H_f = 19.7 m in this

case), the probability of exceeding this limiting wall deflection for the final excavation stage can be computed with Eq. (5.12), which yields p_f = 0.22. Similarly, the probability of exceeding the specified limiting ground settlement is determined to be p_f = 0.24. These results of the PEM analysis for the probability of exceedance are summarized in Table 5.3.

Table 5.2: Small-strain triaxial test results for Taipei clay (adapted from Kung 2003).

Test No.	Type	s_u / σ'_v	E_i / σ'_v
1	Reconstituted	0.30	735.0
2	Reconstituted	0.31	606.7
3	Reconstituted	0.30	531.0
4	Reconstituted	0.29	652.5
5	Reconstituted	0.31	573.5
6	Reconstituted	0.33	528.0
7	Reconstituted	0.28	638.1
8	Reconstituted	0.32	501.4
9	Reconstituted	0.31	542.5
10	Undisturbed	0.357	686.2
11	Undisturbed	0.23	404.6
12	Undisturbed	0.37	822.1
13	Undisturbed	0.31	617.2
14	Undisturbed	0.35	765.5
15	Undisturbed	0.35	512.4
16	Undisturbed	0.318	448.1
17	Undisturbed	0.235	324.8
Mean		0.31	581.7
Std. deviation		0.038	129.8

Table 5.3: Probability of exceedance in the TNEC excavation using PEM and bootstrapping method with 17 data points.

Ground or wall response		δ_{hm}	δ_{vm}
Limiting wall or ground responses*		$0.7\%H_f$	$0.5\%H_f$
Probability of exceedance -- PEM results with mean and standard deviation of soil parameters derived from 17 data points		0.22	0.24
Probability of exceedance -- based on bootstrapping analysis	Mean	0.22	0.23
	Standard deviation	0.07	0.08
	95% confidence interval	0.08-0.36	0.07-0.39

*Level III requirements (PSCG 2000); H_f = final excavation depth (19.7 m).

Bootstrapping to consider effect of the variation of sample statistics

As an example, let's consider the 17 pairs of small-strain triaxial test data listed in Table 5.2 (note: an analysis based on fewer data points is presented later). Here, the s_u / σ'_v values range from 0.23 to 0.37, and the E_i / σ'_v values range from 324.8 to 822.1. Figure 5.3 shows the histograms of s_u / σ'_v and E_i / σ'_v, respectively. These histograms do not seem to suggest a normal or lognormal distribution. However, no conclusion can be made regarding the distribution type as the sample size is rather small. For the same reason, there is also uncertainty regarding the derived mean and standard deviation of s_u / σ'_v and E_i / σ'_v.

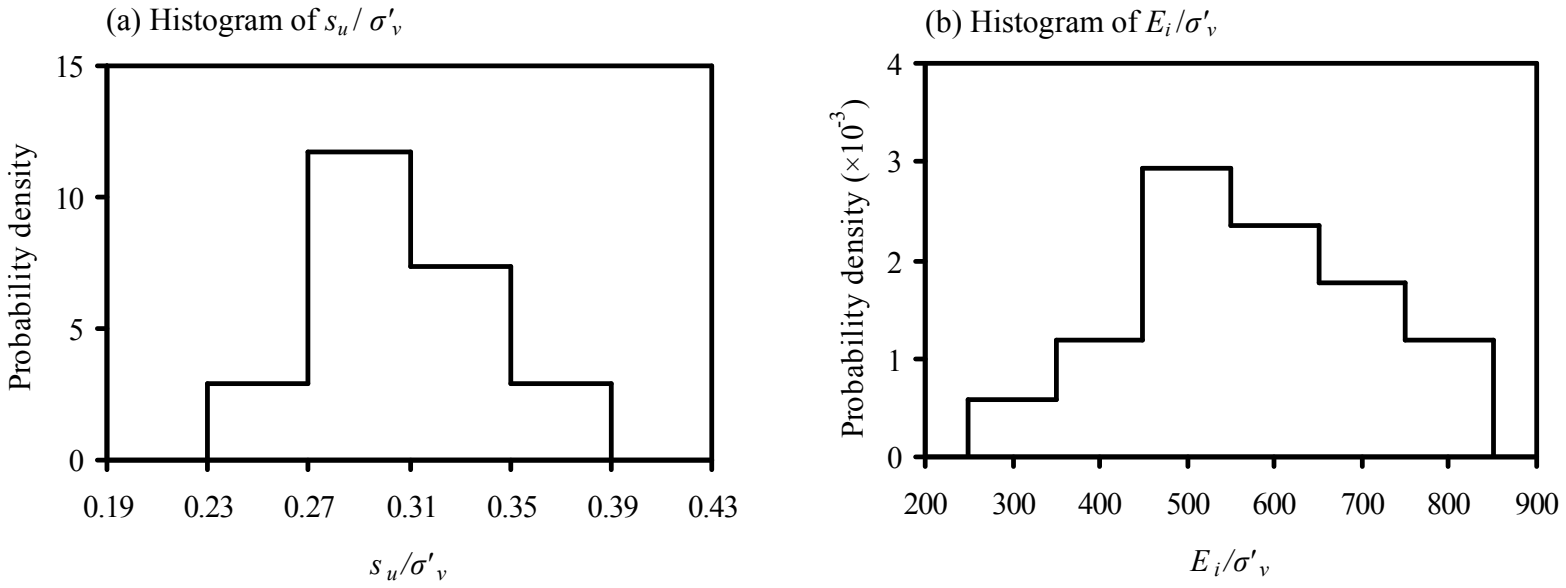

Figure 5.3: Probability distribution of the small-strain triaxial test results listed in Table 5.2.

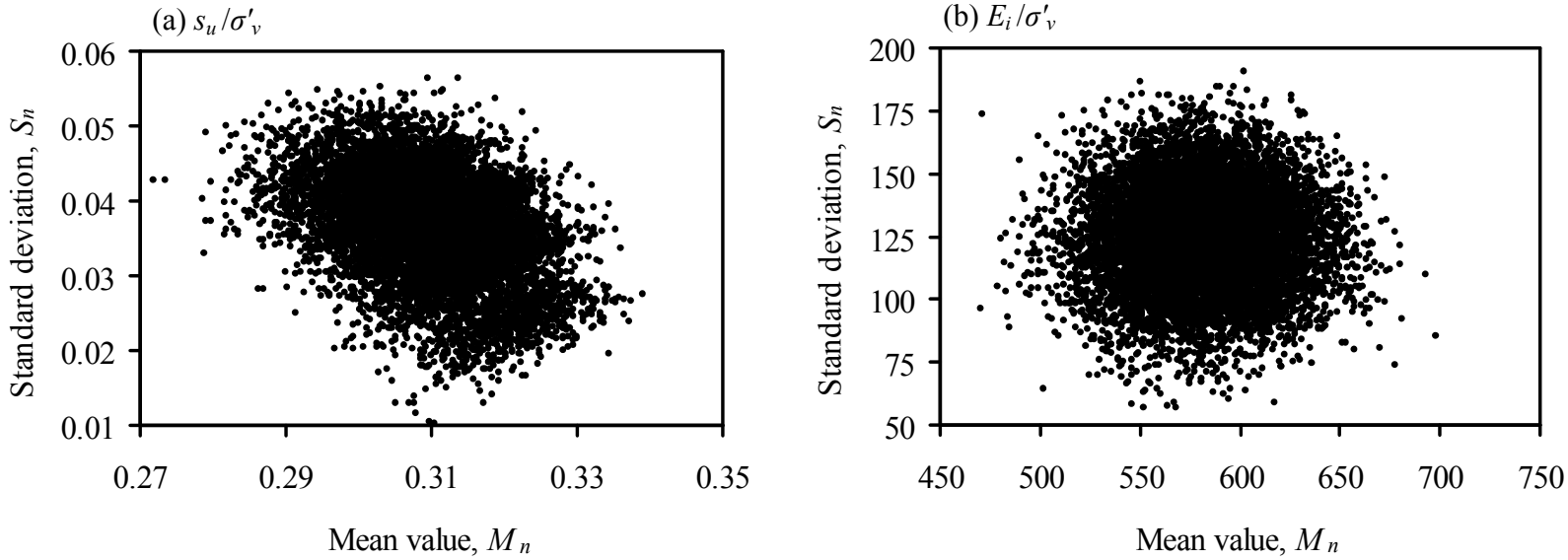

Figure 5.4: Bootstrap samples generated from the original test data listed in Table 5.2.

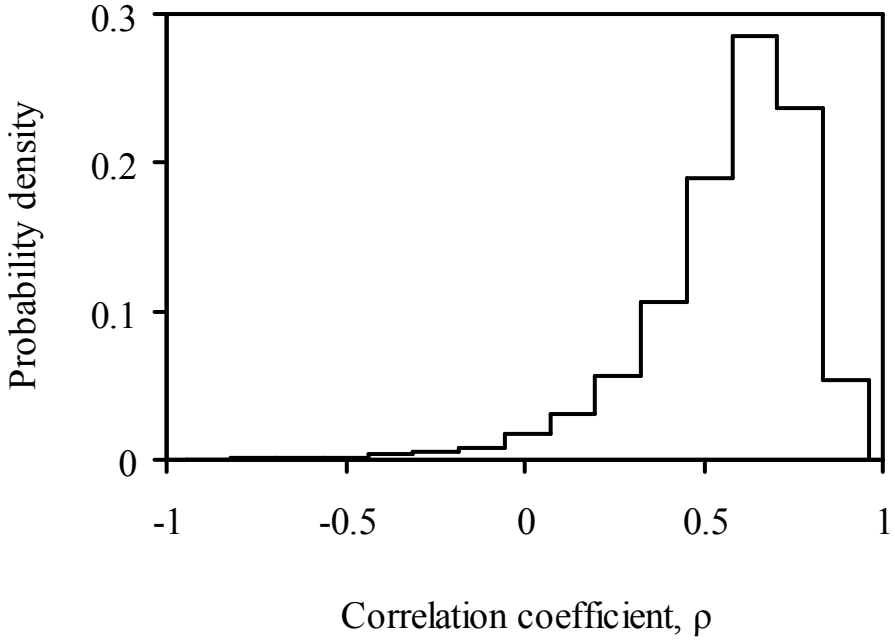

Figure 5.5: Probability distribution of the correlation coefficients for the generated bootstrap samples in Figure 5.4.

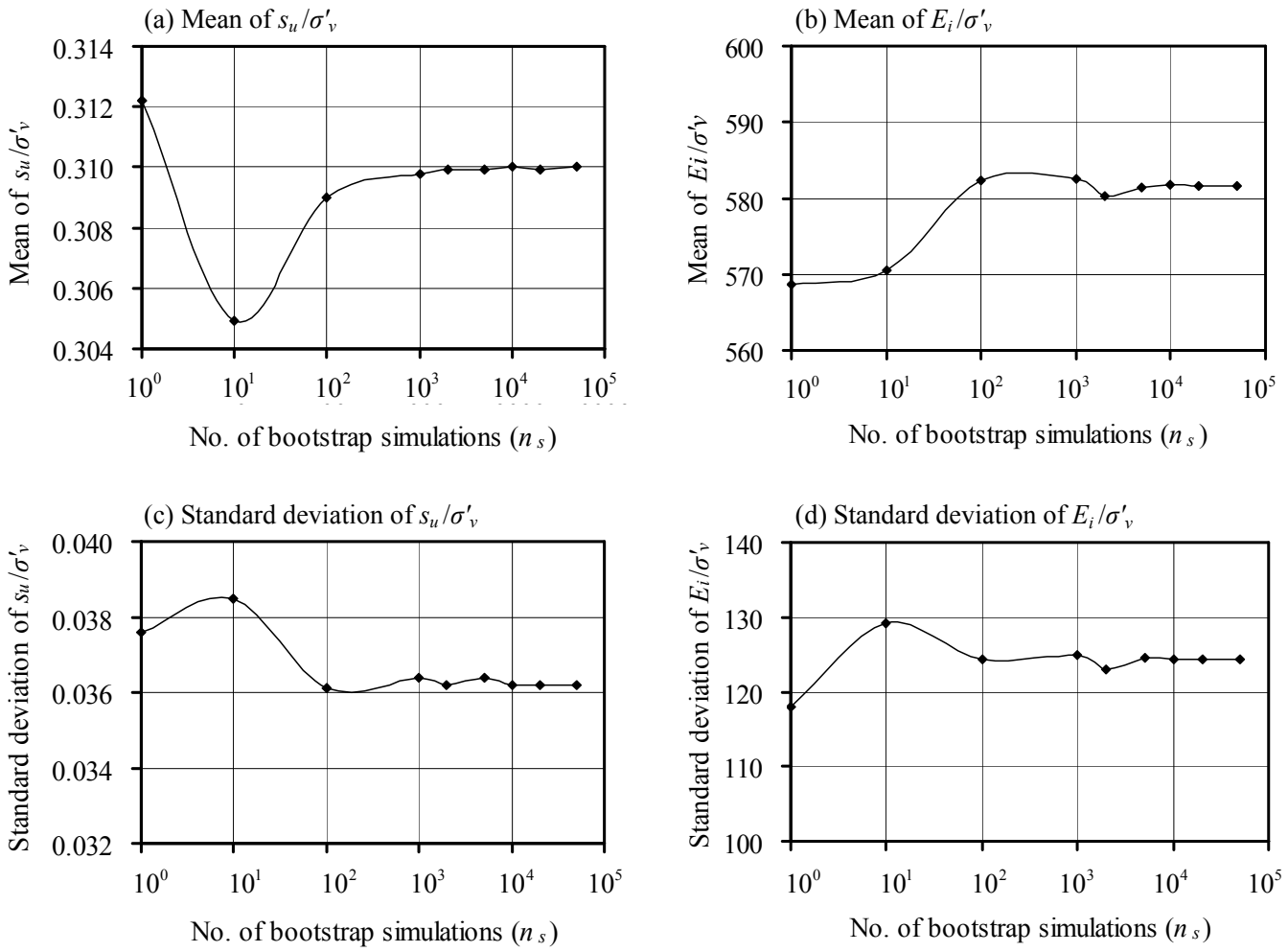

Figure 5.6: Bootstrap mean and standard deviation of s_u/σ'_v and E_i/σ'_v with respect to number of bootstrap simulations.

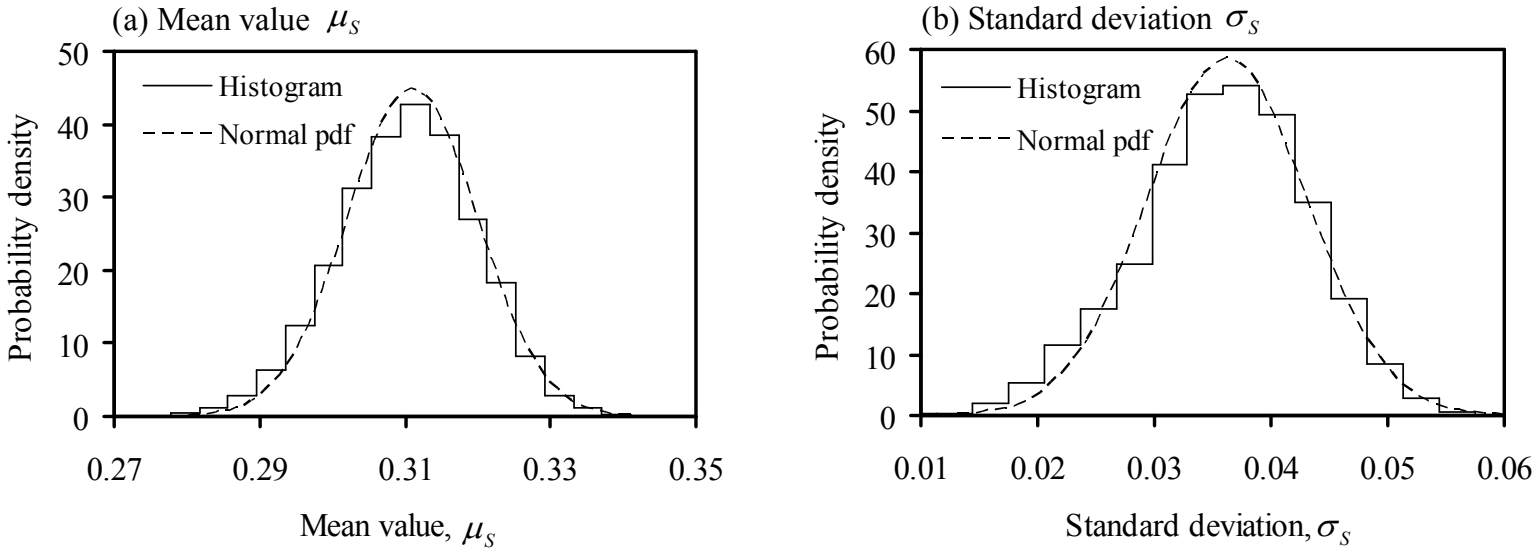

Figure 5.7: Probability distribution of the mean value and standard deviation of s_u / σ'_v.

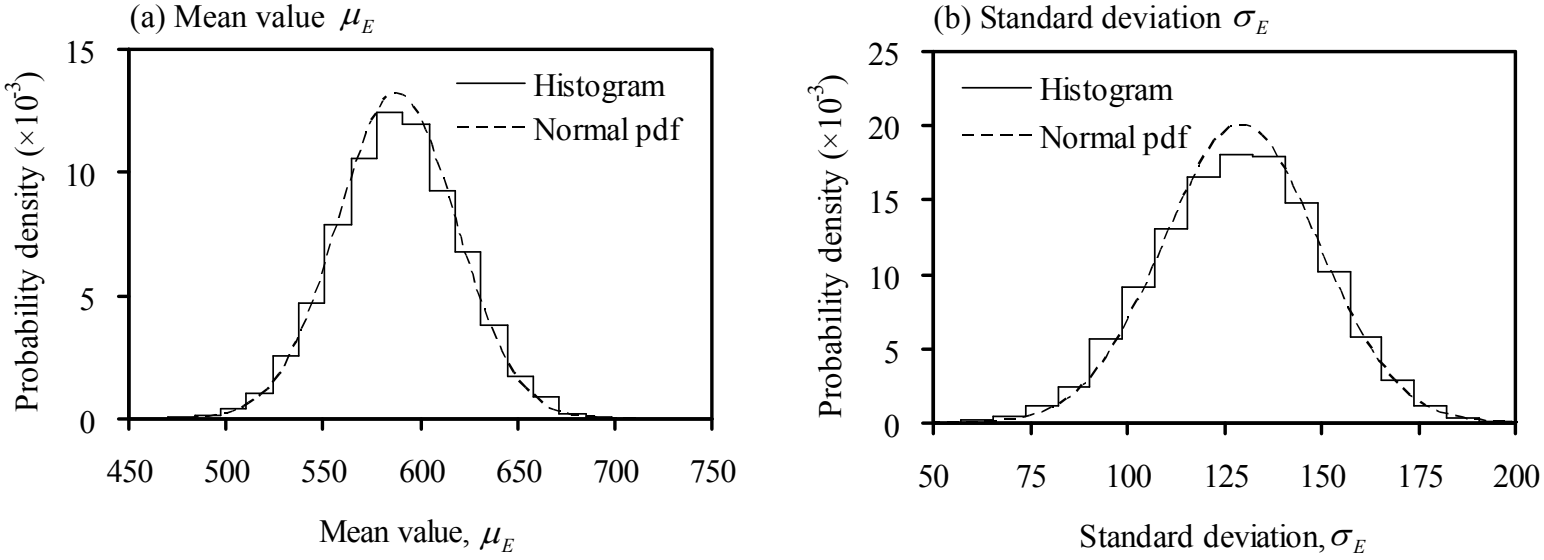

Figure 5.8: Probability distribution of the mean value and standard deviation of E_i / σ'_v.

Thus, the bootstrapping analysis is performed to better characterize these soil parameters and their sample statistics. Figure 5.4 shows 10,000 bootstrap simulations of the small-strain triaxial test results following the procedure described previously. Here, each bootstrap simulation (sample) yields a mean and a standard deviation. Because s_u / σ_v' and E_i / σ_v' are determined from the same soil sample, they are treated as a pair of data when they are re-sampled. Figure 5.5 shows the probability density of the correlation coefficients between s_u / σ_v' and E_i / σ_v' for the 10,000 bootstrap samples. The distribution of the correlation coefficient is heavily left-skewed and almost all the values are positive, which indicates the positive correlation between s_u / σ_v' and E_i / σ_v'.

The selection of 10,000 bootstrap simulations is based on a sensitivity analysis. The statistical fluctuation of the bootstrapped mean and standard deviation of s_u / σ_v' and E_i / σ_v' with the number of bootstrap sets n_s is shown in Figure 5.6. As seen, converged results of the estimated means and standard deviations are observed at 10,000 bootstrap simulations.

With the 10,000 sets of the mean (μ_S) and standard deviation (σ_S) of s_u / σ_v' being secured through bootstrapping (Figure 5.4), the histograms of μ_S and σ_S can be derived (Figure 5.7). Both the mean (μ_S) and the standard deviation (σ_S) are found to essentially follow a normal distribution. The bootstrapped mean and standard deviation are 0.310 and 0.036, respectively. These numbers match well with the sample mean and sample standard deviation shown in Table 5.2, which indicates that the bootstrapped histograms reflect main characteristics of the original data set (sample). Furthermore, an

additional knowledge is gained from bootstrapping: the standard deviations of the mean (μ_S) and standard deviation (σ_S), denoted respectively as $\sigma[\mu_S]$ and $\sigma[\sigma_S]$, are obtained. Thus, an interval estimate of the mean and standard deviation of this uncertain parameter at a specified confidence level (say 95%) is readily available. In other words, there is 95% chance that "true" values for the mean and standard deviation fall within the respective confidence intervals. Finally, an observation can be made regarding the uncertainty or variation of the mean (μ_S) and standard deviation (σ_S) from Figure 5.7. The variation, in terms of coefficient of variation, of the mean (μ_S), as shown in Figure 5.7(a), is much smaller than the variation of the standard deviation (σ_S), as shown in Figure 5.7(b). This confirms the expectation that the variation in the standard deviation due to small sample size is greater than the variation in the mean.

Similarly, Figure 5.8 shows the histograms of the mean (μ_E) and the standard deviation (σ_E) of E_i / σ_v' respectively; both the mean (μ_E) and the standard deviation (σ_E) essentially follow a normal distribution. The bootstrap mean and standard deviation of E_i / σ_v' are 581.9 and 124.3, respectively, which match well with the sample statistics shown in Table 5.2. This indicates, again, that the bootstrapped histograms reflect main characteristics of the original data set. Furthermore, an additional knowledge is gained from bootstrapping: the standard deviations of the mean (μ_E) and standard deviation (σ_E), denoted respectively as $\sigma[\mu_E]$ and $\sigma[\sigma_E]$, are obtained. Similarly, the variation, in terms of coefficient of variation, of the mean (μ_E), as shown in Figure 5.8(a), is much

smaller than the variation of the standard deviation (σ_E), as shown in Figure 5.8(b). Again, this confirms the expectation that the variation in the standard deviation due to small sample size is greater than the variation in the mean.

The effect of the uncertainty or variation of the sample statistics on the computed probability of exceedance is investigated next. For each bootstrapped sample, the mean and standard deviation of the two critical soil parameters, s_u / σ'_v and E_i / σ'_v, are determined. With the known means (μ_S and μ_E) and standard deviations (σ_S and σ_E), the PEM analysis can be conducted to determine the mean and standard deviation of the response *y* based on the KJHH model. This follows that the reliability index (β) and the probability of exceedance (p_f) can be determined with Eq. (5.11) and (5.12) respectively. For demonstration purposes, the limiting wall deflection and ground settlement are set respectively at $0.7\%H_f$ and $0.5\%H_f$ (where H_f is the final excavation depth). These limiting values are specified for excavation protection Level III in the design code adopted in Shanghai (PSCG 2000). Other criteria may be adopted depending on the local design codes or requirements of the client. Furthermore, also for demonstration purposes, the analysis is carried out at the final excavation stage in the TNEC case, as this stage is often the most critical. For each sample, a reliability index (and thus a probability of exceedance) is obtained.

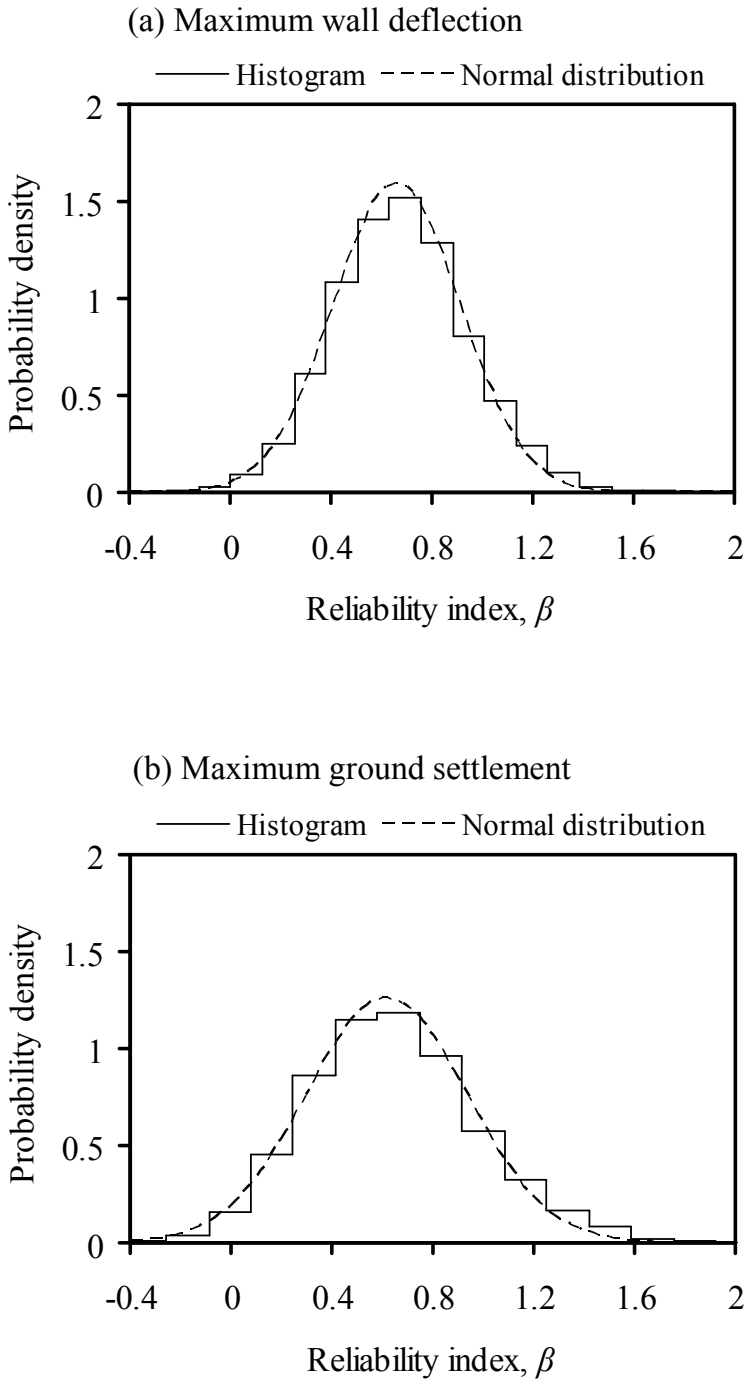

Figure 5.9: Distribution of the reliability indices computed with the specified limiting (a) wall deflection and (b) ground settlement (at final excavation stage).

After repeating the analysis with all 10,000 bootstrapped samples, the same number of β is obtained. Figure 5.9(a) shows a distribution of β when the limiting wall deflection is set at $0.7\%H_f$; and Figure 5.9(b) shows a similar plot of the distribution of β when the limiting ground settlement is set at $0.5\%H_f$. The variation in the computed reliability index due to the variation in the sample statistics can be observed. Assuming a normal distribution for the computed β, a confidence interval at, say, 95% level can be derived; this follows that the probability of exceedance can be expressed in terms of a confidence interval at the 95% level. The results, the probability of wall deflection exceeding $0.7\%H_f$ in the TNEC case ranging from 0.08 to 0.36 at 95% confidence level, and the probability of ground-surface settlement exceeding $0.5\%H_f$ in the TNEC case ranging from 0.07 to 0.39, are also shown in Table 5.3. The knowledge of the variation of the sample statistics, which is derived through bootstrapping, allows us to infer the probability of exceedance in terms of a confidence interval, instead of a single fixed probability.

Further Discussions

Effectiveness of bootstrapping method

The analyses presented previously are based on a sample of 17 small-strain triaxial test data. In many instances, the available data may be fewer than this number. To get a preliminary estimate of this effect and to examine the effectiveness of the bootstrapping method, all of the previous analyses are repeated with only 8 data, taking

only those data from undisturbed samples as shown in Table 5.2.

Based on the 8 data points of small-strain triaxial tests on the undisturbed clays, the sample statistics are determined as follows: μ_S = 0.32, σ_S = 0.055, μ_E = 572.6 and σ_E = 178.5. The mean values are found to be comparable to those computed with 17 data, while the standard deviations are found to be greater than those computed with 17 data. Using the new data, the mean of the maximum wall deflection δ_{hm}, denoted as $\mu[\delta_{hm}]$, is computed to be: $\mu[\delta_{hm}]$ = 107.3 mm, and the standard deviation of δ_{hm}, denoted as $\sigma[\delta_{hm}]$, is computed to be: $\sigma[\delta_{hm}]$ = 37.8 mm. If the limiting wall deflection is taken at $0.7\%H_f$ (PSCG 2000), where H_f is the final excavation depth (H_f = 19.7 m), the probability of exceeding this limiting wall deflection at the final excavation stage will be p_f = 0.21. Similarly, the probability of exceeding the specified limiting ground settlement is determined to be p_E = 0.21, as listed in Table 5.4.

To consider the variation of sample statistics due to use of a small sample (in this case, sample consisting of only 8 data points), bootstrapping is again applied and all the previous analyses are repeated. The new results are summarized in Table 5.4. The probability of the maximum wall deflection exceeding $0.7\%H_f$ in the TNEC case ranges from 0.06 to 0.34 at the 95% confidence level; and the probability of the maximum ground settlement exceeding $0.5\%H_f$ in the TNEC case ranges from 0.04 to 0.36 at the 95% confidence level. These results (Table 5.4) that relied on 8 data points are

comparable with the previous results (Table 5.3) that relied on 17 data points. Thus, bootstrapping is shown to be an effective technique to estimate the variation of sample statistics, as demonstrated with two different sizes of small samples.

Table 5.4: Probability of exceedance in the TNEC excavation using PEM and bootstrapping method with only 8 data points.

Ground or wall response		δ_{hm}	δ_{vm}
Limiting wall or ground responses*		$0.7\%H_f$	$0.5\%H_f$
Probability of exceedance -- PEM results with mean and standard deviation of soil parameters derived from 8 data points		0.21	0.21
Probability of exceedance -- based on bootstrapping analysis	Mean	0.20	0.20
	Standard deviation	0.07	0.08
	95% confidence interval	0.06-0.34	0.04-0.36

* Level III requirements (PSCG 2000); H_f = final excavation depth (19.7 m).

The implication is that the bootstrap method can be an effective tool in geotechnical engineering to capture the variation of sample statistics due to the use of a small sample. Considering that it is a norm in geotechnical practice to have limited data availability, it is essential to estimate the variation of the derived sample statistics, and to assess the effect of this variation. In this regard, the bootstrap method has potential to be indispensible tool in geotechnical engineering. The case study presented in this study shows that additional information (such as the confidence interval of the probability of serviceability failure, as opposed to a single, fixed probability) can be "gained" through bootstrapping analysis. The gained information enables the engineer to make a more

informed decision.

Predicting performance of an excavation design

In this section, the predicted performance of the previously discussed excavation design for the TNEC case is re-assessed considering the Level I and II design requirements for urban excavation protection in Shanghai, China (PSCG 2000). The probabilities of exceedance presented previously were computed for Level III scenario where no important infrastructures or facilities exist within a distance of $2H_f$ from the excavation. An excavation with Level III scenario requires that $\delta_{hm} \leq 0.7\% H_f$ and $\delta_{vm} \leq 0.5\% H_f$. Herein, the probabilities of exceedance are also analyzed for Level II scenario where important infrastructures or facilities such as gas mains and water drains exist within a distance of 1 to $2H_f$ from the excavation, and for Level I scenario where metro lines and important facilities such as gas mains and water drains exist within a distance of $0.7H_f$ from the excavation. As summarized in Table 1.1, an excavation with Level II scenario requires that $\delta_{hm} \leq 0.3\% H_f$ and $\delta_{vm} \leq 0.2\% H_f$, and an excavation with Level I scenario requires that $\delta_{hm} \leq 0.14\% H_f$ and $\delta_{vm} \leq 0.1\% H_f$. The computed probabilities of exceedance in the TNEC case for all three protection levels are summarized in Table 5.5.

Table 5.5: Probability of exceedance in the TNEC excavation under three excavation protection scenarios.

Excavation protection level (PSCG 2000)	Level I		Level II		Level III	
Limiting criterion	$\delta_{hm} \leq 0.14\% H_f$	$\delta_{vm} \leq 0.1\% H_f$	$\delta_{hm} \leq 0.3\% H_f$	$\delta_{vm} \leq 0.2\% H_f$	$\delta_{hm} \leq 0.7\% H_f$	$\delta_{vm} \leq 0.5\% H_f$
Mean of probability of exceedance	0.98	0.91	0.90	0.79	0.20	0.20
Standard deviation of probability of exceedance	0.007	0.02	0.02	0.04	0.07	0.08
95% confidence interval of probability of exceedance	0.97-0.99	0.87-0.95	0.86-0.94	0.71-0.87	0.06-0.34	0.04-0.36

* H_f = final excavation depth = 19.7 m.

For the TNEC excavation case, the maximum wall deflection δ_{hm} predicted using the deterministic KJHH model is 107.3 mm, which is less than $0.7\%H_f$ (137.9 mm) and is greater than $0.3\%H_f$ (59.1 mm) or $0.14\%H_f$ (27.6 mm). Thus, in terms of the maximum wall deflection, the excavation design would be satisfactory under a Level III protection scenario ($\delta_{hm} \le 0.7\%H_f$) and unsatisfactory under a Level II scenario ($\delta_{hm} \le 0.3\%H_f$) or a Level I scenario ($\delta_{hm} \le 0.14\%H_f$). Similar assessment and conclusion can be reached when the TNEC case is evaluated based on the maximum ground settlement δ_{vm}.

Although the deterministic solutions appear to be able to offer a clear-cut answer to the question of whether the excavation design would satisfy design code requirements, as shown in the previous analysis, the uncertainties in the analysis model (the KJHH model in this case) and the input parameters (s_u / σ'_v and E_i / σ'_v in this case) can hinder such ability. In many cases, it would be difficult to judge whether the limiting wall deflection or ground settlement would be exceeded because of the uncertainty in the computed wall and ground responses. Facing such uncertainties, the probabilities of exceedance (or the probability of failure to meet the criterion of a limiting maximum wall deflection or ground settlement) offer a complementary tool to assess the likelihood of unsatisfactory design. As shown in Table 5.5, the confidence intervals of the probability of exceedance at the 95% confidence level are obtained for all three excavation protection levels. If an excavation design with the probability of exceedance of less than 0.35 is considered “acceptable” (note: the acceptable probability should be determined based on

an additional study of risk and agreeable among the parties involved), the TNEC case under Level III scenario would be satisfactory as far as the maximum wall deflection or ground settlement is concerned. Under Level II and Level I scenarios, however, the TNEC case would be unsatisfactory because of the high probability of exceedance even at the lower end of the confidence interval.

The gained knowledge (i.e., the confidence interval of the probability of exceedance in this case) enables the engineer to make a more informed decision. Furthermore, this knowledge may be carried over to the task of evaluating the risk of damage to the adjacent infrastructures and facilities. The latter task, however, is beyond the scope of this study which focuses on the estimate of confidence intervals of the probability of exceedance using bootstrapping method.

Finally, an interesting observation is made of Table 5.5, in which the range of the confidence interval can be relatively small or large, depending on the value of the chosen limiting wall deflection or ground settlement relative to the mean of the computed response. To further elaborate this observation, the probability of exceedance in the TNEC excavation is computed for a series of limiting wall deflection and ground settlement values. Figure 5.10 shows the confidence intervals of the probability of exceedance obtained for various limiting wall deflection values (Figure 5.10a) and ground settlement values (Figure 5.10b). When the limiting wall deflection or ground settlement values are either very small or very large (relative to the mean of the computed responses), the confidence interval of the computed probability of exceedance is very narrow. This phenomenon is easily understood because when the chosen limiting

response approaches to the left tail or the right tail of the probability distribution of the computed response, the variation of the probability of exceedance caused by the uncertainties in the mean and standard deviation of the computed response is naturally small. On the contrary, the range of the confidence interval increases as the chosen limiting response approaches to the mean of the computed response. For example, when the limiting wall deflection is at approximately 110 mm, which is close to the mean of the computed wall deflection (107.3 mm in TNEC), the range of the confidence interval is the widest, as shown in Figure 5.10(a), indicating the greatest variation in the computed probability of exceedance. Similar observation can be made from Figure 5.10 (b) regarding the confidence interval of the probability of exceedance with respect to the computed maximum ground settlement.

Figure 5.10 can also be treated as a case-specific design curve. For a given excavation design at a given site (with limited number of data on key soil parameters), the curve presents the confidence intervals (at 95% level) of the probability of exceedance at a range of limiting wall deflection or ground settlement. This curve enables the designer to make a more informed decision. For example, the designer can easily see the change in the probability of exceedance when a different limiting response value is selected. This is significant because in an assessment of the risk of damage to adjacent infrastructures, the engineer would want to explore the probability of exceedance for a range (however narrow it should be) of limiting responses, rather than for a fixed level of responses.

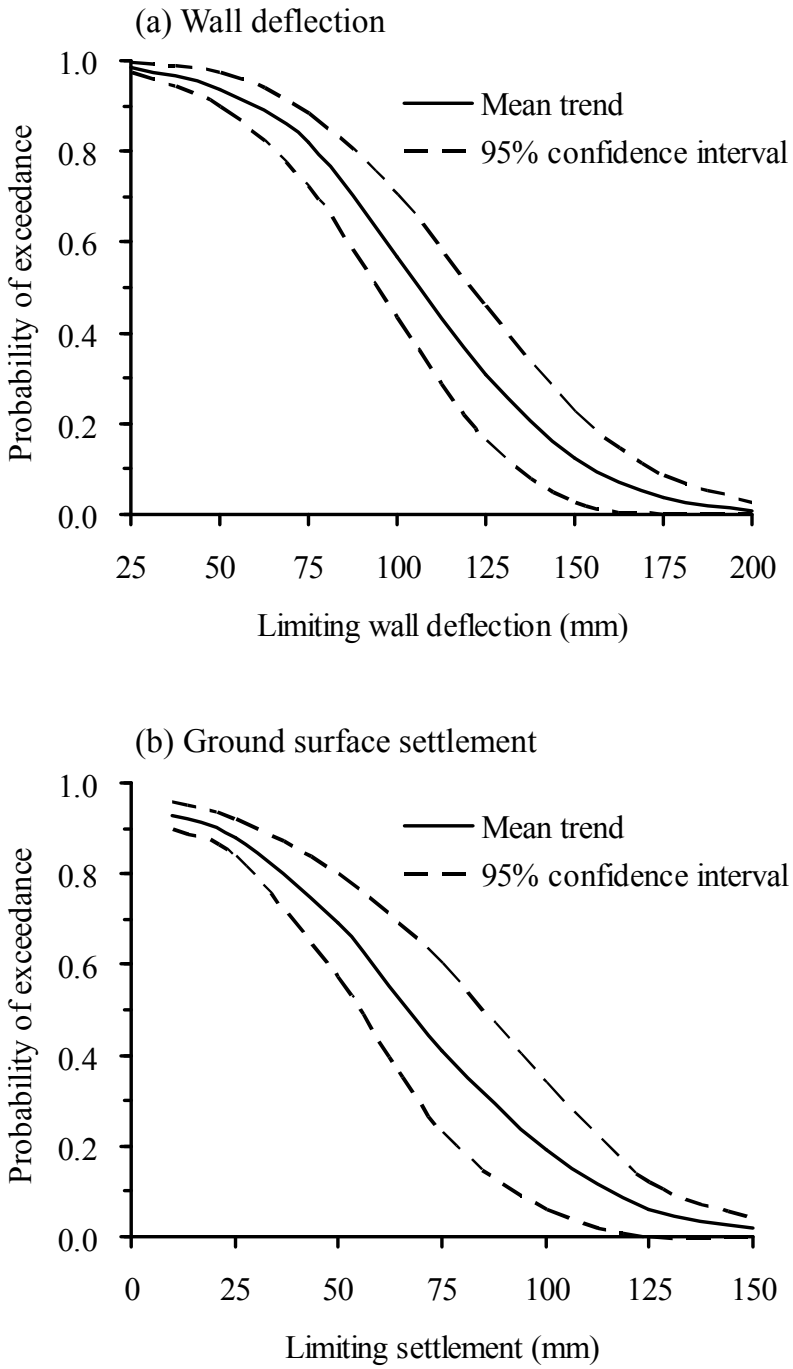

Figure 5.10: Confidence intervals for probability of exceedance in the TNEC excavation computed with various levels of limiting wall deflection and ground surface settlement.

Summary

This chapter focuses on the effect of small sample size of soil parameters on the reliability analysis of the serviceability failure in braced excavation in clays. A simple procedure for assessing the probability of serviceability failure, is presented and demonstrated with a case study. This simple procedure consists of the following components: (1) simulation of performance function using the well-established model KJHH (Kung et al. 2007b) as a response surface; (2) uncertainty propagation using the point estimate method; (3) characterization of the uncertainty of sample statistics using bootstrap method (Efron 1979); (4) confidence interval analysis of the probability of serviceability failure. This simple procedure is demonstrated through a case study to be effective for assessing the effect of small sample size of soil parameters on the probability of serviceability failure.

CHAPTER VI

BAYESIAN UPDATING OF SOIL PARAMETERS IN BRACED EXCAVATIONS [*]

Introduction

Back analysis or inverse analysis based on field observations (or measurements) in a braced (or supported) excavation process has been widely reported (e.g., Whittle et al. 1993; Calvello and Finno 2004; Hashash et al. 2004; Chua and Goh 2005; Hsiao et al. 2008; Tang and Kung 2009; Hashash et al. 2010). Back analysis with field observations is usually performed for important and/or difficult excavation projects only. Since braced excavations are generally carried out in stages, back analysis to update "key" soil parameters (such as the normalized undrained shear strength and the normalized initial tangent modulus in an excavation in clays) is generally realized in multiple stages: before the first excavation stage, the wall and ground responses are predicted with limited field tests and/or laboratory data. Since such data often involve significant uncertainty, the predictions of the wall and ground responses, even those made with the more advanced finite element method (FEM), often fail to match the observed responses at the end of this excavation stage. After the first-stage excavation is completed and wall and/or ground responses are measured, the key soil parameters can be updated with the observed responses to "refine" the knowledge of the soil parameters. With the updated soil parameters, the wall and/or ground responses in the subsequent excavation stages may be predicted with improved fidelity. This process can be repeated stage by stage until the

[*] A similar form of this chapter has been submitted at the time of writing: Juang CH, Luo Z, Atamturktur S, Huang H. Bayesian Updating of Soil Parameters in Braced Excavations Using Markov Chain Monte Carlo Simulation with Metropolis-Hastings Algorithm.

final excavation depth is reached.

The soil parameters updated with field observations through back analysis are not necessarily the "true" values of these parameters, since the wall and ground responses in a supported excavation may also be affected by construction quality (workmanship) and other environmental factors (such as temperature variation), in addition to soil-structure interaction mechanism. Nevertheless, updated soil parameters allow for more accurate predictions of the wall and ground responses in the subsequent stages of excavation, which can be critical in some projects for developing remedial measures for preventing damage to adjacent buildings and infrastructures.

It should be noted that in the early stages (the first or second stage) of excavation using diaphragm wall, the deformation of the wall generally assumes a cantilever shape, and then changes into a concave shape at latter stages (e.g., after the first or second stage). Thus, back analysis in the early stages may not be as effective or necessary as in latter stages. Furthermore, the responses (wall deflection and ground settlement) in an excavation with good workmanship are generally negligible in these early stages.

Many approaches are available for back analysis of soil parameters, e.g., least squares method (Xu and Zheng 2001), maximum likelihood method (Ledesma et al. 1996), Bayesian method (Zhang et al. 2009), and so on. The Bayesian probabilistic framework is demonstrated to be a robust approach for updating input parameters and response predictions (Beck and Au 2002; Zhang et al. 2009) and it offers a procedure to update the probability distribution function of input parameters provided that the observations are available (Miranda et al. 2009). Many successful applications of

Bayesian updating approach in geotechnical engineering have been reported, e.g., pile capacity analysis (Kay 1976), study on embankment on soft clay (Honjo et al. 1994), serviceability assessment of braced excavations in clay (Hsiao et al. 2008), and slope stability study (Zhang et al. 2010). In the work reported by Hsiao et al. (2008), the Bayesian observational method is implemented with a semi-empirical model known as KJHH (Kung et al. 2007b) for predicting wall and ground settlement, and the refinement of settlement predictions are realized in a stage-by-stage manner through updating of the bias factor of the prediction model.

The goal of this chapter is to develop a framework that combines the Bayesian analysis and the observational method for updating soil parameters in a braced excavation in clay. The updated soil parameters are represented by their posterior distributions and sample statistics. In this framework, the updating process starts with an assumption for the prior distributions for soil parameters. After the initial excavation stage is conducted, the maximum wall deflection and maximum ground settlement are observed (or measured). Those observations are used to update the soil parameters through comparison with the predictions, and the updated soil parameters are then used to predict the responses in the subsequent stages. This procedure is repeated stage-by-stage as the excavation proceeds, and the soil parameters are updated accordingly.

It should be noted that in the traditional back analysis, the focus is on finding a set of fixed values for the input parameters of concern. Because of the high degree of uncertainty involved in a braced excavation, the fixed parameter values may not be feasible or physically meaningful. In the present study, parameters of concern are treated

as random variables and the updated parameters are expressed in terms of posterior distributions. To update these parameters, Markov chain Monte Carlo (MCMC) simulation is carried out using Metropolis-Hastings algorithm. In this solution process, a prior distribution of each of the parameters of concern is needed. The prior distribution may be assumed based on prior knowledge (i.e., published literature and/or local engineering experience). As is shown later, converged results can be obtained even the prior knowledge is imperfect. Finally, the proposed framework for updating soil parameters can be implemented with one type of field response observations (in this study, either the maximum wall deflection or maximum settlement observation) or multiple types of observations. While use of Bayesian updating with MCMC method is not new in geotechnical engineering (for example, Zhang et al. 2010), updating with multiple types of observations presented herein is a new contribution. The proposed framework, which deals with updating of multiple soil parameters using multiple response observations from multiple stages of a braced excavation, a complex soil-structure interaction problem, is considered significant. The comprehensive updating analyses of braced excavations through MCMC simulations in this study produce many critical insights.

Framework of Bayesian Updating with Markov Chain Monte Carlo Simulation

Updating soil parameters using one type of response observation

In this study, the Bayesian updating framework is adapted for the KJHH model. The implementation starts with expressing the KJHH model for predicting the maximum

wall deflection or maximum settlement as follows:

$$y = c \cdot \delta(\theta) \tag{6.1}$$

where y is the predicted δ_{hm} or δ_{vm} in a braced excavation; $\delta(\theta)$ denotes the prediction model for either δ_{hm} or δ_{vm} [Eq.(5.1) or Eq.(5.4) in Chapter V]; θ is the vector of the soil parameters (s_u / σ'_v and E_i / σ'_v in this study); c is the model *bias factor* (c_h for δ_{hm} model, c_v for δ_{vm} model), which represents the model uncertainty. For both δ_{hm} and δ_{vm}, the previous study (Kung et al. 2007b) showed that c can be approximately modeled as a normally distributed random variable with a mean value of 1.0; for the adopted δ_{hm} prediction model, the standard deviation of c_v (denoted as σ_{c_v}) is found to be 0.25; for the adopted δ_{vm} model, the standard deviation of c_h (denoted as σ_{c_h}) is found to be 0.34.

Based on Eq. (6.1), the likelihood that the prediction (y) is equal to the observation (Y_{obs}) can be expressed as a conditional probability density function (PDF) of θ:

$$L(\theta | y = Y_{obs}) = N(Y_{obs} / \delta(\theta)) \tag{6.2}$$

where $L(\theta | y = Y_{obs})$ is the likelihood; and the notation N denotes a normal PDF which is a function of $[Y_{obs} / \delta(\theta)]$. It is noted that at a given Y_{obs}, the term

$N\left(Y_{obs}/\delta(\theta)\right)$ is a function of θ only. Recalling that $c = y/\delta(\theta)$, this normal PDF can be characterized with a mean of μ_c and a standard deviation of σ_c. In a Bayesian framework, given a prior PDF, $f(\theta)$, the posterior PDF of θ can be obtained as follows (Wang et al. 2010; Zhang et al. 2010):

$$f\left(\theta|y = Y_{obs}\right) = m_1 \cdot N\left(Y_{obs}/\delta(\theta)\right) \cdot f(\theta) \tag{6.3}$$

where m_1 is a normalization factor that guarantees a unity for the cumulative probability over the entire range of θ.

Updating soil parameters using two types of response observations

To update the soil parameters with the observations of both δ_{hm} and δ_{vm} (denoted herein as Y_{obs1} and Y_{obs2}, respectively), we note that the likelihood that the predicted wall deflection y_1 and the predicted settlement y_2 are equal to the corresponding observations is a conditional probability density function (PDF) of θ:

$$L\left(\theta|y_1 = Y_{obs1}, y_2 = Y_{obs2}\right) = N_2\left(\left[Y_{obs1}/\delta_1(\theta), Y_{obs2}/\delta_2(\theta)\right]\right) \tag{6.4}$$

where $\delta_1(\theta)$ and $\delta_2(\theta)$ denote Eqs. (1) and (4) respectively; N_2 denotes the PDF of a bivariate normal distribution with a mean vector $[\mu] = [\mu_{c_h}, \mu_{c_v}]$ and a covariance matrix of:

$$\left[\sigma^2\right] = \begin{bmatrix} \sigma_{c_h}^2 & \sigma_{c_{hv}}^2 \\ \sigma_{c_{vh}}^2 & \sigma_{c_v}^2 \end{bmatrix} \tag{6.5}$$

where $\sigma_{c_{hv}}^2 = \sigma_{c_{vh}}^2 = \rho\,\sigma_{c_h}\sigma_{c_v}$ and ρ is the correlation coefficient between the two model bias factors c_h and c_v. The above formulation is simply an extension of the formulation presented in Eq. (6.2) from using one type of observation to using two types of observation. Similarly, the posterior PDF of θ updated with two types of observations can be obtained as follows:

$$f\left(\theta \middle| y_1 = Y_{obs1}, y_2 = Y_{obs2}\right) = m_2 \cdot N_2\left(\left[Y_{obs1} / \delta_1(\theta), Y_{obs2} / \delta_2(\theta)\right]\right) \cdot f(\theta) \tag{6.6}$$

where m_2 is a normalization factor that guarantees a unity for the cumulative probability over the entire range of θ.

The posterior distribution may be obtained through optimization or sampling techniques. In this study, Markov chain Monte Carlo (MCMC) simulation method, an efficient sampling technique that can yield samples of a posterior distribution (Beck and Au 2002), is adopted. One advantage of MCMC is that the computation of the normalization factor may be avoided, which is generally difficult for multiple dimensional problems (Gamerman 1997). Furthermore, the Metropolis-Hastings algorithm (Hastings 1970) is adopted in this study for its efficiency to implement MCMC sampling of key parameter θ for its posterior PDF [see Eq. (6.6)].

Procedure of MCMC simulation using Metropolis-Hastings algorithm

The procedure for MCMC simulation (or sampling) of θ for its posterior PDF using the Metropolis-Hastings algorithm can be summarized as follows:

1. At Stage k = 1, determine the first point θ_1 in the Markov chain. This first instance θ_1 may be obtained by random selection from the prior distribution or may simply be assigned the mean value.
2. At next stage k (k starts from 2), randomly generate a new θ_p from a proposal distribution $T\left(\theta_p \middle| \theta_{k-1}\right)$ which is assumed to be a multivariate normal distribution where the mean is set to be the current point θ_{k-1} in the Markov chain and the covariance matrix is equal to $s \cdot C_\theta$, where s is a scaling factor and C_θ is the covariance matrix of the prior distribution of θ. The multivariate normal distribution is chosen for its good convergence properties in the Bayesian inference (Draper 2006).
3. Generate a random number u from a uniform distribution $U(0,1)$.
4. Compute the ratio of densities r:

$$r = \frac{q\left(\theta_p \middle| y = y_{obs}\right)}{q\left(\theta_{k-1} \middle| y = y_{obs}\right)} \leq 1 \tag{6.7}$$

where $q\left(\theta \middle| y = y_{obs}\right)$ is the un-normalized posterior PDF. In this study, $q\left(\theta \middle| y = y_{obs}\right)$ is essentially Eq. (6.3) or Eq. (6.6) without the normalization factor. Note that $q\left(\theta \middle| y = y_{obs}\right)$ is $q(\theta)$ evaluated at $y = y_{obs}$.

5. Determine whether θ_p is acceptable (and thus yields a new point in the Markov chain) with the follow acceptance rule: if $u \le r$, then θ_p is acceptable and set $\theta_k = \theta_p$; otherwise, set $\theta_k = \theta_{k-1}$. Then go back to Step 2.
6. Repeat Step 2 to Step 5 until the target number of samples (i.e., Markov chain "length") is reached.

The Metropolis-Hastings algorithm randomly samples from the posterior distribution. Typically, initial samples are not completely valid because the Markov Chain has not stabilized. These initial samples may be discarded as burn-in samples. Several factors influence the efficiency of sampling posterior distribution with MCMC approach, such as the proposal distribution, Markov chain length, and number of "burn-in" samples. Therefore, the construction of a Markov chain is problem-specific and needs to be examined case by case. We do not impose which MCMC algorithm is used as long as efficient Markov chains can be guaranteed.

Example Application: TNEC Excavation Case

A well-documented excavation case, known as TNEC case in Taiwan (Ou et al. 1998) is used herein as an example to illustrate the Bayesian framework for updating soil parameters using observed wall and/or ground responses in the staged excavation. At TNEC, the excavation width is 41.2 m and the length of diaphragm wall is 35 m. The excavation was performed using top-down construction method in seven stages with the support of steel struts and floor slabs. The soil profile and excavation depths are shown in

Figure 5.2, which is basically a clay site. Thus, the maximum wall and ground responses in this excavation are mainly influenced by the normalized shear strength (s_u / σ'_v) and normalized initial tangent modulus (E_i / σ'_v) of the clay (Hsiao et al. 2008). In this study, the focus is to update these parameters with field observations in the staged excavation using the Bayesian framework.

Parametric study on the construction of Markov chains

Effectiveness and efficiency of the MCMC approach depend on the parametric setting. First, the prior distribution of soil parameter θ (i.e., vector of soil parameters) must be assumed. As an example, *Prior distribution 1*, listed in Table 6.1, is assumed in the parametric analysis presented herein. The effect of choosing other prior distributions on the MCMC solutions is examined later.

Table 6.1: Statistics of four prior distributions used in the Bayesian updating scheme.

Parameter	s_u / σ'_v		E_i / σ'_v	
	Mean	COV*	Mean	COV*
Prior distribution 1	0.25	0.16	500	0.16
Prior distribution 2	0.31	0.16	650	0.16
Prior distribution 3	0.27	0.16	550	0.16
Prior distribution 4	0.35	0.16	750	0.16

*COV suggested by Hsiao et al. (2008) for Taipei clays. Effect of assuming other COVs is examined separately.

Next, proper selection of the scaling factor *s* is deemed critical to an efficient MCMC simulation. To test this notion, three Markov chains are simulated using the following scaling factors: (a) *s* = 0.01; (b) *s* = 3; (c) *s* = 20. For this analysis, the updating

of soil parameters is based on two types of response observations (both maximum settlement and maximum wall deflection observations). The first 2000 samples of s_u / σ'_v in the Markov chains are shown in Figure 6.1. It is apparent that *s* has a significant effect on the efficiency of the MCMC simulation. The low efficiency of the MCMC simulation is observed when *s* is either too small or too large as shown in Figures 6.1(a) and 6.1(c), respectively: in Figure 6.1(a) the overall trend of the samples fluctuates drastically which means longer time is needed to reach a steady state of the generated samples; and in Figure 6.1(c) a large number of the simulated samples are of the same values since many horizontal segments are observed, which also indicates low efficiency in the sampling process (as many rejections occurred). As a comparison, when $s = 3$, the Markov chain samples shows an active simulation behavior as in Figure 6.1(b).

To further examine the effect of scaling factor *s* on the Markov chain construction, Figure 6.2 shows the relationship between the acceptance rate and the scaling factor. Gelman et al. (2004) suggested that the Markov chain simulation is most efficient when the acceptance rate is between 20% and 40%. In our case, the acceptance rate falls within 20% to 40% if *s* is equal to 3 for each of the excavation stages. Therefore, in this study the scaling factor is set as 3 when updating with both observed maximum settlement and observed maximum wall deflection. It is found that when the soil parameters are updated with just one type of field observation (either observed maximum settlement or observed maximum wall deflection), a scaling factor of 2 yields most efficient Markov chain construction. However, determination of *s* should be carefully evaluated for other excavation cases.

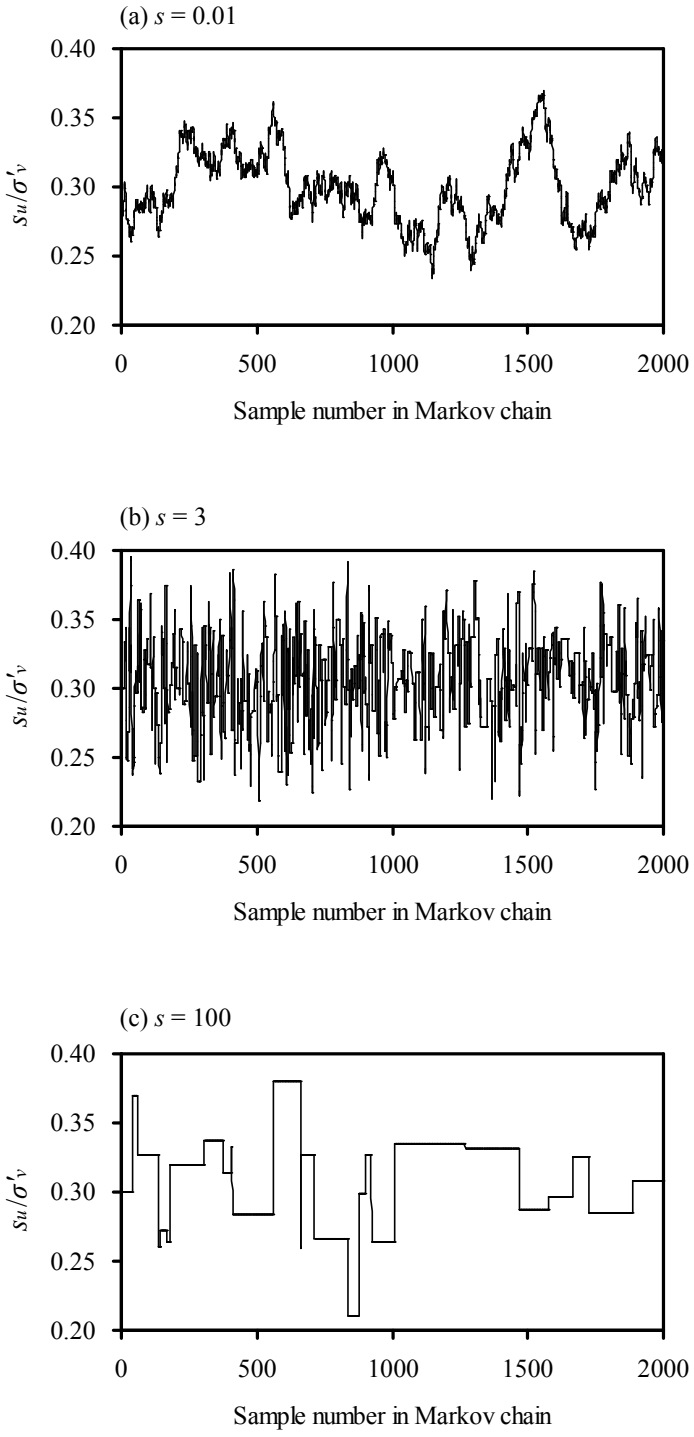

Figure 6.1: Effect of scaling factor on the efficiency of Markov chain sampling: (a) s = 0.01, (b) s = 3, (c) s = 20.

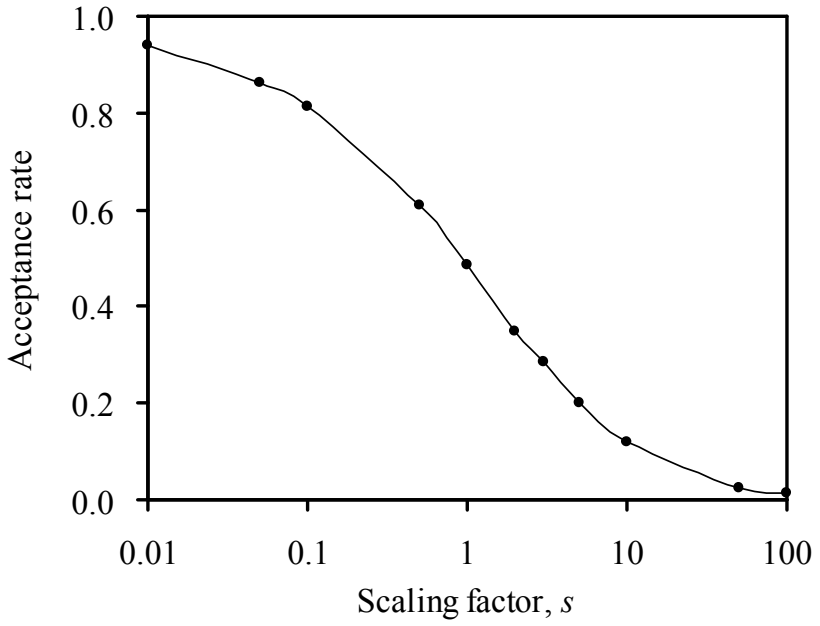

Figure 6.2: Relationship between acceptance rate and scaling factor updated with both observed δ_{hm} and δ_{vm}.

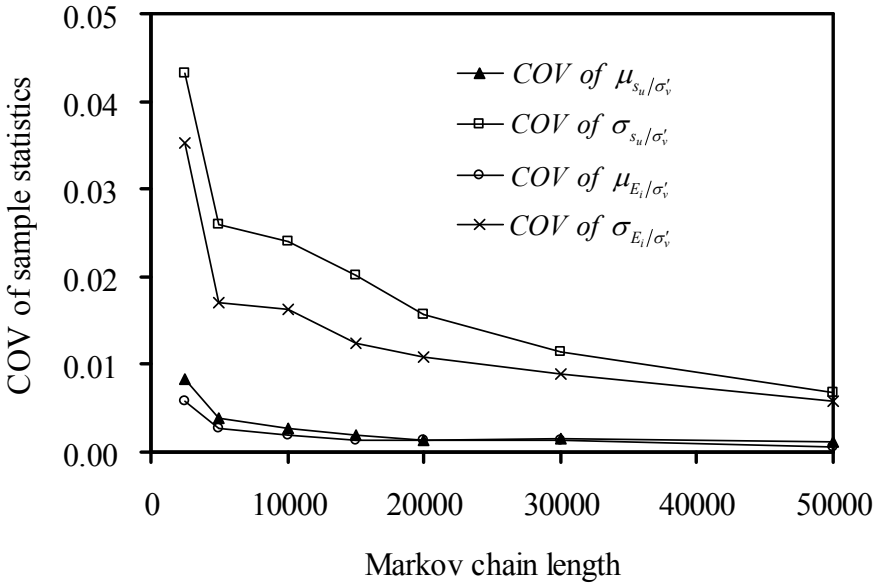

Figure 6.3: Influence of Markov chain length on the mean values and standard deviations of the posterior distributions estimated from 30 different Markov chains with $s = 3$.

With a properly selected scaling factor (s = 3), the soil parameters can be updated stage by stage with the observations. In this study, the first 100 samples in the Markov chains are discarded as the "burn-in" samples. The updated probability density and sample statistics are obtained after the burn-in samples are discarded. The MCMC samples should be continuously generated until the sample statistics of the posterior distribution has converged within a preset tolerance (Wu et al. 2010b; Zhang et al. 2010). Figure 6.3 shows an example of the variation of the sample statistics with the chain length obtained with 30 different Markov chains that were performed with s = 3. As can be seen from the results, at a Markov chain length of 50000, the coefficient of variation (*COV*) for all statistics of the posterior distribution of θ from the 30 Markov chains is less than 1%, the preset tolerance in this study. Therefore, it is concluded that robust posterior statistics can be achieved with the aforementioned parametric settings (e.g., scaling factor, burn-in sample, chain length) in the MCMC simulation.

Based on the selected parametric settings, the updating of soil parameters is carried out using the MCMC simulation with field observations in the TNEC excavation. As an example, Figure 6.4 shows the MCMC sampling process with a Markov chain length of 50000 based on the observations from Stage-6 excavation at TNEC (when the excavation reached the depth of 17.3 m, which is prior to the start of Stage-7 excavation). Figure 6.5 shows the histograms of the Markov chain samples in Figure 6.4. It is observed that the posterior distributions of both s_u / σ'_v and E_i / σ'_v are very close to a normal distribution. The updated distributions of these soil parameters from other stages of excavation all follow approximately a normal distribution.

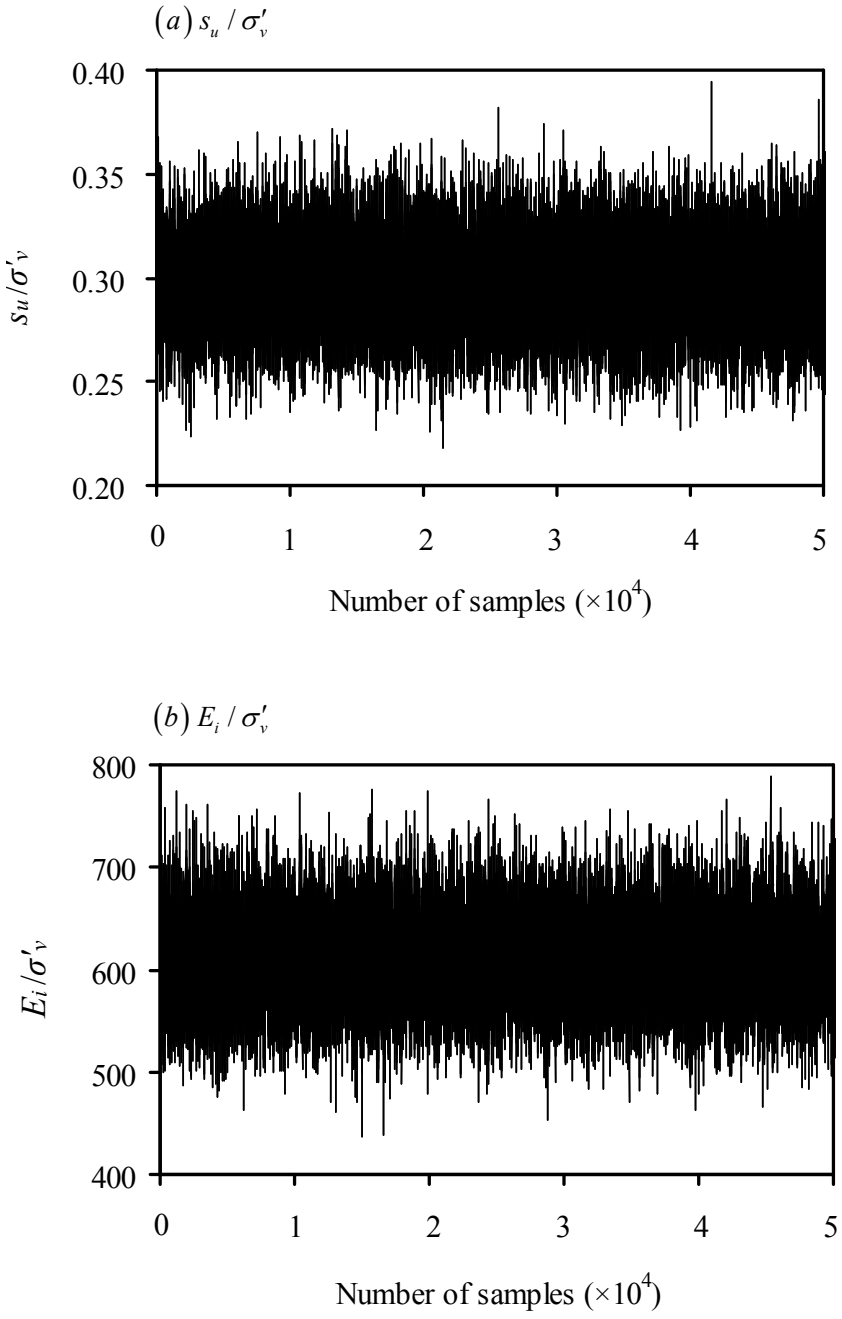

Figure 6.4: Sampling process of MCMC simulations with the observations from the 6th excavation stage (s = 3).

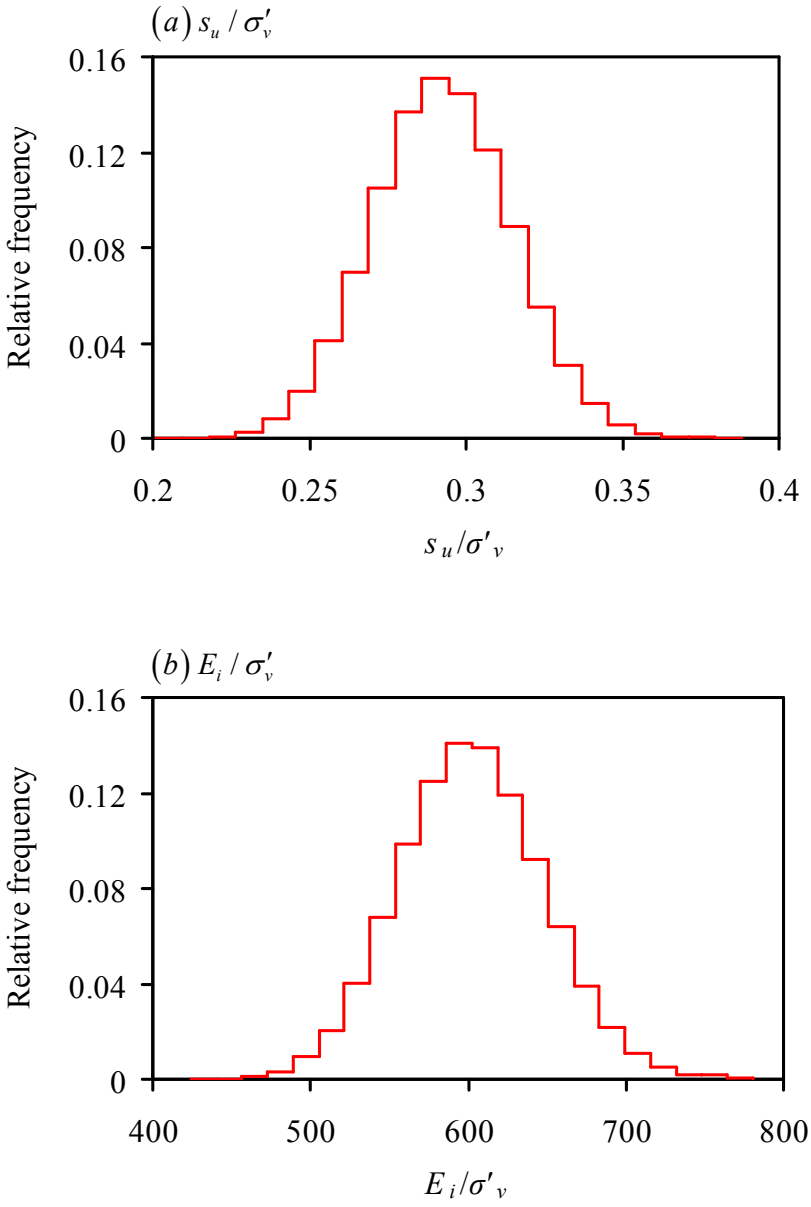

Figure 6.5: Histograms of posterior distribution for s_u/σ'_v and E_i/σ'_v with data from Figure 6.4.

Previous reliability analysis of braced excavations using KJHH model as a performance function shows that the discrepancy between normal and lognormal assumptions has a negligible influence on the predicted excavation-induced serviceability

failure probability (Hsiao et al. 2008). Furthermore, the MCMC sampling using prior distributions as listed in Table 6.1 seldom generates negative numbers. The very rarely generated negative numbers may be disregarded and a truncated normal distribution may be used (Most and Knabe 2010). Thus, normal distribution is assumed for both prior and posterior distributions of soil parameters in this study. For simplicity, the predictions of the wall and ground responses in the subsequent stages can be realized with the mean values of the posterior distributions, and the reliability assessment of the wall and ground responses can be evaluated with the obtained posterior distribution and its statistics.

Updating soil parameters using one type of response observation

As noted previously, back analysis in the early stages (the first or second stage) of excavation may not be effective because of the change of deformed shape of the wall from the cantilever to concave-type shape and because the responses in these early stages under normal workmanship are generally negligible (Kung et al. 2007c; Hsiao et al. 2008).

In this section, the updating is carried out with only one type of response observation. First, the soil parameters are updated using the observed settlements only. Prior to Stage-3 excavation (starting from the depth of 4.9 m; see Figure 5.2), the predicted maximum settlement for the current stage is 47 mm based on the mean values of the assumed *Prior distribution 1* (s_u / σ'_v = 0.25 and E_i / σ'_v = 500) using the KJHH model. The predicted maximum settlements at various target depths are shown in Figure 6.6 (a). As an example, the predictions made prior to Stage-3 excavation (with a target

depth of 8.6 m; see Figure 5.2) are labeled with a square symbol "□" in Figure 6.6(a). As can be seen in this figure, the predictions at this point using the assumed prior information are far away from the 1:1 line (predicted settlement versus observed settlement). After Stage-3 excavation is completed, the maximum settlement at the depth of 8.6 m is observed to be at 18 mm. Using this new observation and the Bayesian updating framework presented earlier, the MCMC samples for posterior distributions of parameters s_u / σ'_v and E_i / σ'_v are generated. For simplicity, sample statistics (mean and *COV*) of these posterior distributions are obtained. The mean values of the updated parameters s_u / σ'_v and E_i / σ'_v are then used to predict the maximum settlement at various target depths prior to Stage-4 excavation (starting from the depth of 8.6 m). These maximum settlement predictions are labeled with symbol "×" in Figure 6.6(a). After Stage 4 is completed, the maximum settlement at the depth of 11.8 m is observed to be 34mm and this new observation is used to further update s_u / σ'_v and E_i / σ'_v. The above process is repeated stage by stage till the end.

The maximum settlement predictions at the final excavation depth (19.7 m in this case), which are generally of primary concern, made prior to the start of Stages 3-, 4-, 5-, 6-, and 7- excavations are shown in Figure 6.7. Note that the depths at which the maximum settlement predictions were made prior to the start of Stages 3, 4, 5, 6, and 7 are 4.9m, 8.6m, 11.8m, 15.2m, and 17.3m, respectively. Prior to Stage 7 (when the excavation reached the depth of 17.3 m), the mean of the maximum settlement prediction for the final excavation depth of 19.7 m is 79 mm, which compares very well with the observed maximum settlement of 78 mm at the final excavation depth. For comparison, it

is noted that the maximum settlement prediction for the final excavation depth of 19.7 m is 114 mm prior to Stage 3 when the excavation reached the depth of 4.9 m. The accuracy of the predictions made with the updated soil parameters increases in the Bayesian updating process, as shown in Figure 6.7. In fact, for this TNEC excavation, the maximum settlement predictions for the final excavation depth prior to Stage 5 (starting at 11.8 m) and Stage 6 (starting at 15.2 m) are already very close to the observed maximum settlement of 78 mm. Figure 6.7 also shows the one-standard-deviation bounds of the predicted maximum settlement at the final excavation depth of 19.7 m in this TNEC case. The variation of the predictions is discussed later.

Next, the soil parameters are updated using the observed wall deflections only. Using the same procedure, the soil parameters are updated with the observed maximum wall deflections, and then the predictions for the subsequent stages are obtained accordingly, as shown in Figure 6.6(b). The updated wall deflection predictions for the final excavation depth (19.7 m in this TNEC case) made prior to Stages 3, 4, 5, 6, and 7 (with the corresponding starting depths of 4.9m, 8.6m, 11.8m, 15.2m, and 17.3m, respectively) are shown in Figure 6.8. The predicted maximum wall deflection for the final excavation depth of 19.7 m made prior to Stage 7 excavation is 116 mm, and the one-standard-deviation bounds are 102 mm to 130 mm. The observation at the final excavation depth is 106 mm, which falls within the predicted one-standard-deviation bounds. Meanwhile, the predicted mean (116 mm) at the final excavation depth is significantly improved over the mean prediction (143 mm) prior to Stage 3.

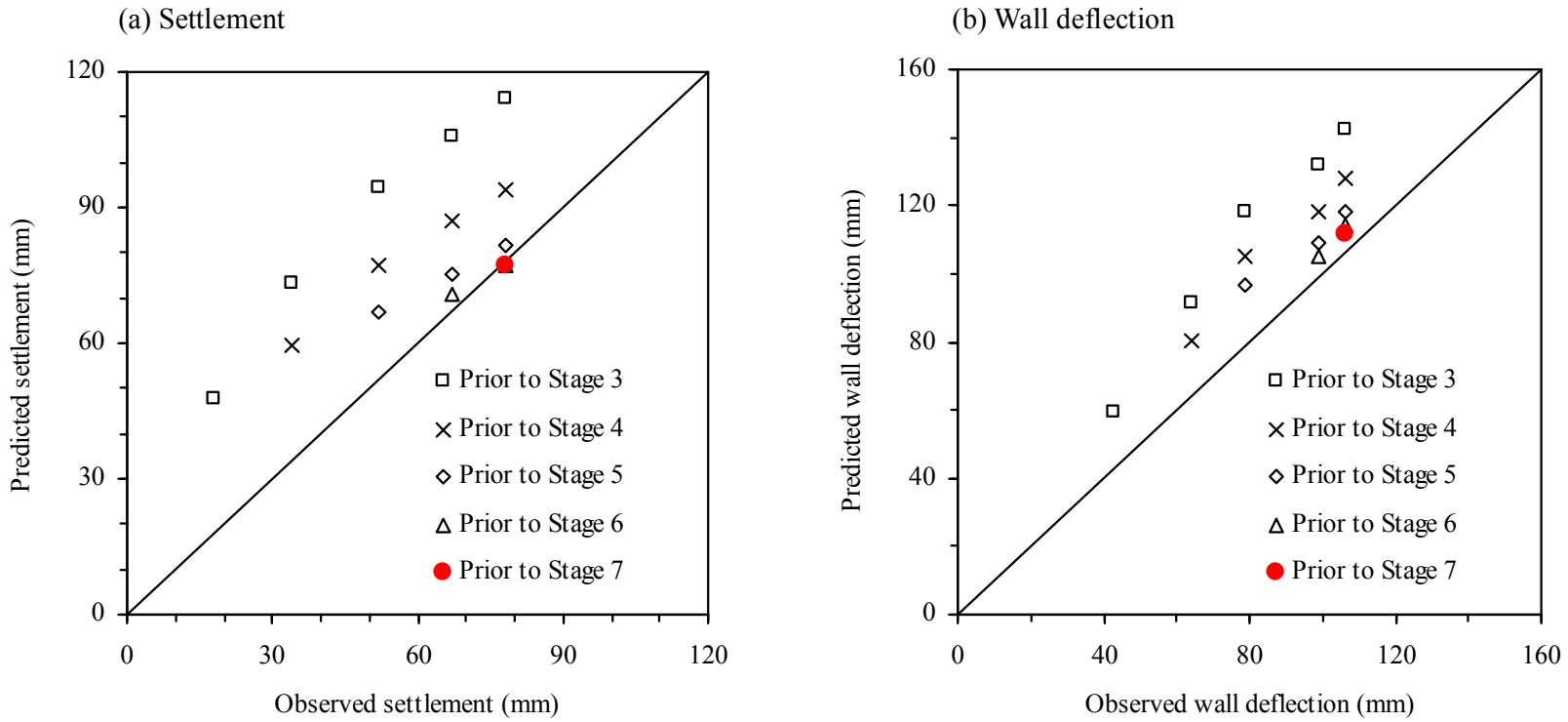

Figure 6.6: Maximum settlement and wall deflection predictions prior to excavation stages 3, 4, 5, 6, 7 (using Prior distribution 1).

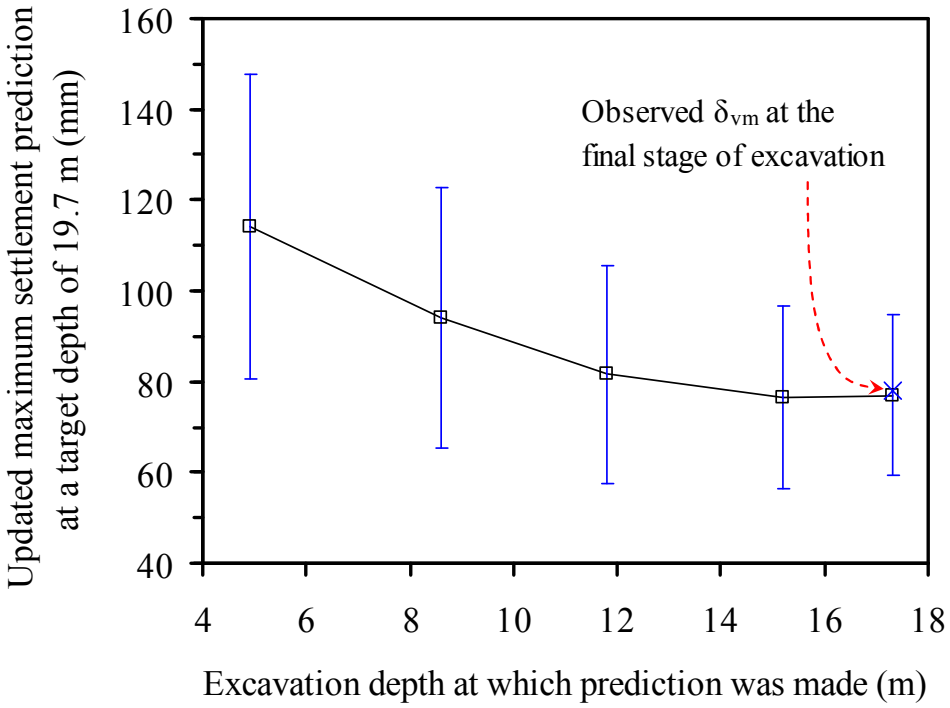

Figure 6.7: Updated mean value and one standard deviation bounds of the settlement predictions at target depth of 19.7 m prior to Stages 3, 4, 5, 6, and 7 of excavations (using Prior distribution 1 and the maximum settlement observations).

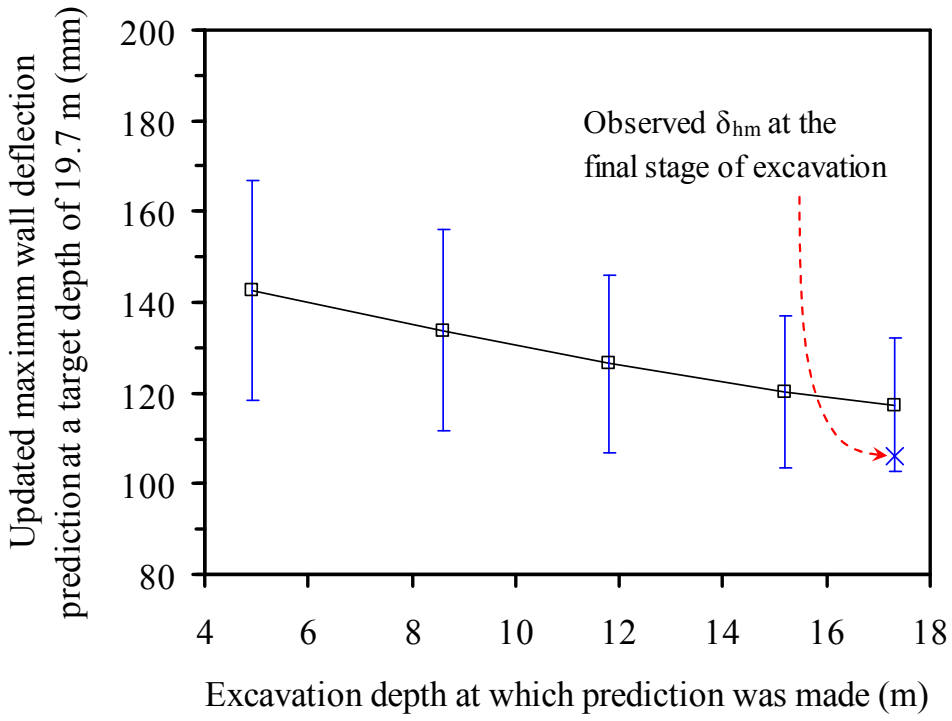

Figure 6.8: Updated mean value and one standard deviation bounds of wall deflection predictions at target depth of 19.7 m prior to Stages 3, 4, 5, 6, and 7 of excavations (using Prior distribution 1 and the maximum wall deflection observations).

The Bayesian framework is shown to be effective and efficient when the soil parameters are updated with only one type of response observation (either maximum settlement or maximum wall deflection) in a braced excavation. Updating with two types of response observations is presented in the next section.

Updating soil parameters using two types of response observations

In this section, updating of soil parameters using observations of both maximum settlements (δ_{vm}) and maximum wall deflections (δ_{hm}) is demonstrated with TNEC case.

As in the previous section, *Prior distribution 1* (listed in Table 6.1) is assumed for the two key soil parameters, s_u / σ'_v and E_i / σ'_v. The procedure for MCMC sampling of the posterior distribution of θ using the Metropolis-Hastings algorithm is basically the same as described previously for updating using one type of response observation except that Eq. (6.6) is used in lieu of Eq. (6.3). Note that in the analysis presented herein, the correlation coefficient between the two model bias factors (c_h and c_v), which is defined in the covariance matrix [Eq. (6.5)], is assumed to be ρ = 0. The effect of this correlation is examined later in a separate section.

Figure 6.9(a) shows the updated maximum settlement predictions using the posterior distribution of θ that is updated based on two types of observations (both maximum settlement and maximum wall deflection). For comparison, the updated maximum settlement prediction using the posterior distribution of θ that is updated based on one type of observation (either maximum settlement or wall deflection) is also included in Figure 6.9(a). Similarly, Figure 6.9(b) shows the updated maximum wall deflection predictions based on the three updating schemes. In Figure 6.9, all predictions are for the final excavation depth of 19.7 m in this TNEC case, and these predictions are made prior to Stages 3, 4, 5, 6, and 7 (with the corresponding starting depths of 4.9 m, 8.6 m, 11.8 m, 15.2 m, and 17.3 m, respectively). The following observations are made from Figure 6.9: (1) all three updating schemes (based on observations of maximum wall deflection only, maximum settlement only, and both maximum wall deflection and maximum settlement) are effective, (2) wall deflection is the easiest to measure in the field but the updating based on the wall deflection is the least effective among the three

schemes (note: the effectiveness here is based on the rate of changes and how close the prediction at the final stage is to the field measurement), and (3) updating with both types of observations is the most effective among the three schemes.

The results presented in Figure 6.9 are the mean values of the updated predictions of the wall and ground responses. It should be of interest to examine the variation of the updated predictions. As an example, Figure 6.10 shows the distribution of the final predictions (i.e., prior to the final stage of excavation) of the maximum settlement and maximum wall deflection with each of the three updating schemes. The observed responses at the end of excavation are also shown in Figure 6.10. Two observations can be made out of Figure 6.10. First, among the three updating schemes, the one using two types of response observations (maximum wall deflection and maximum settlement observations) yielded the smallest variation. Thus, the updated results are more robust using both types of response observations. This finding is not possible by examining only the mean values of the responses (as in Figure 6.9). Second, the claim of "excellent agreement" between the prediction and the observation in the traditional back analysis or after-the-fact prediction of the responses of an excavation case history, often reported in the literature, may not be all that meaningful if the variation in the input parameters and/or the variation in the computed responses are not full characterized.

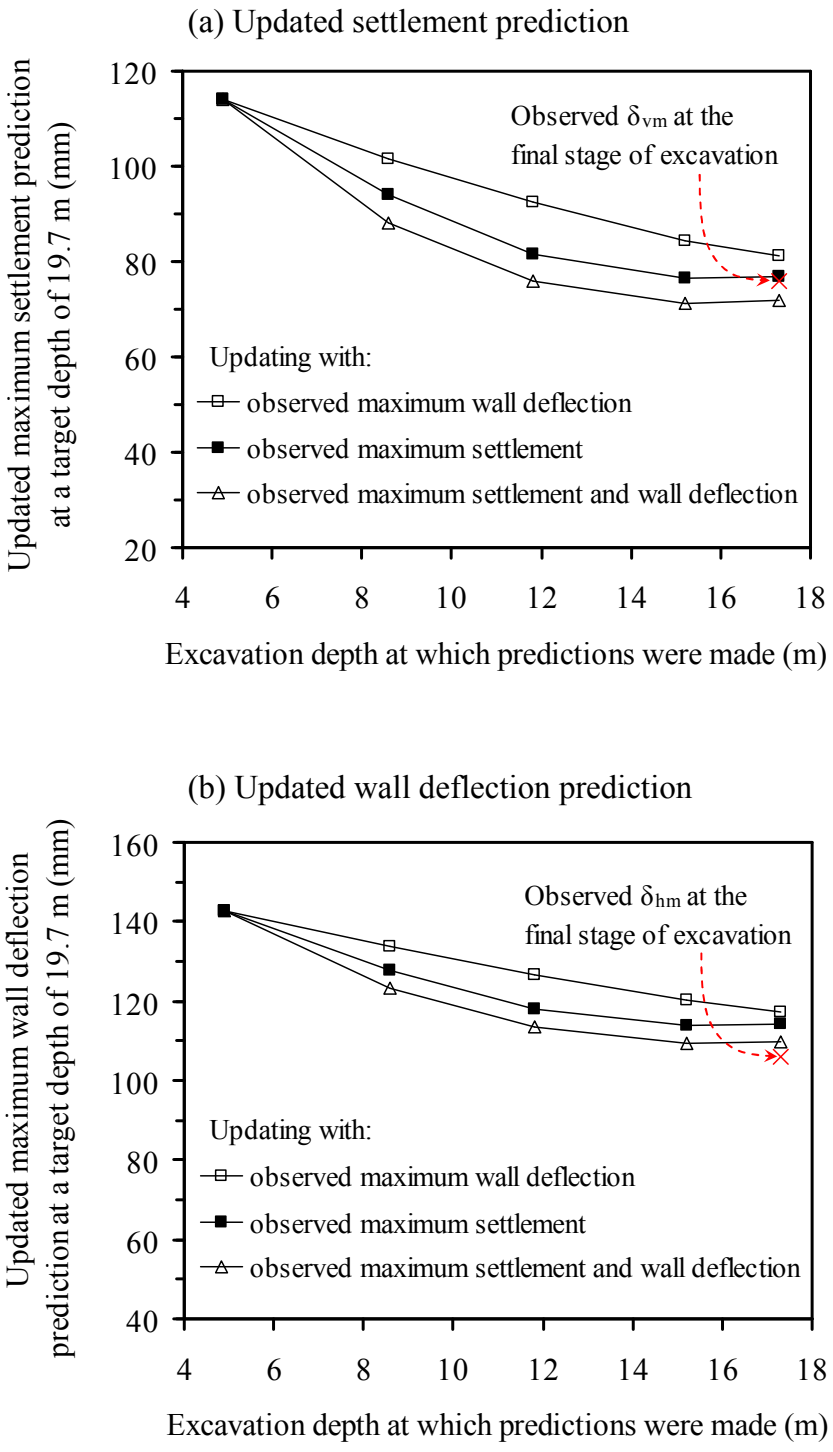

Figure 6.9: Comparisons of updated predictions with three updating schemes (using Prior distribution 1).

(a) Settlement prediction prior to final stage

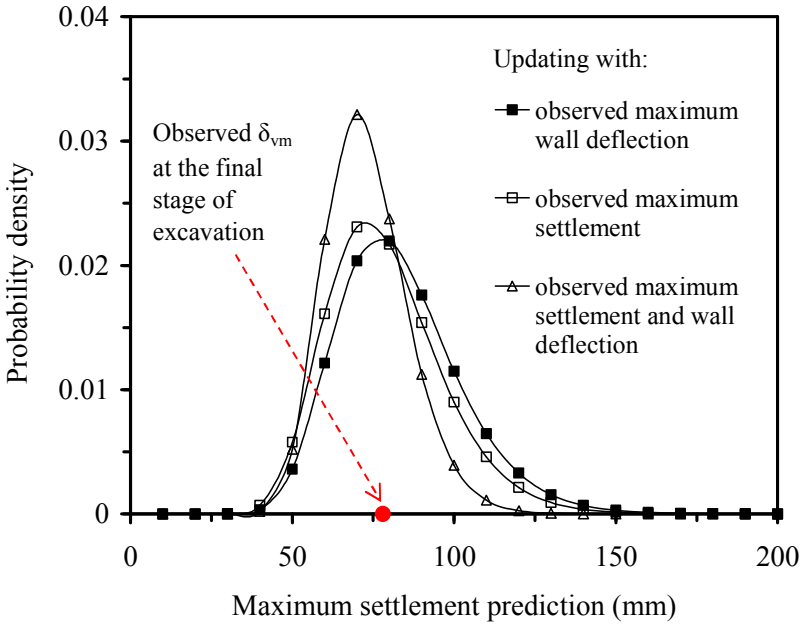

(b) Wall deflection prediction prior to final stage

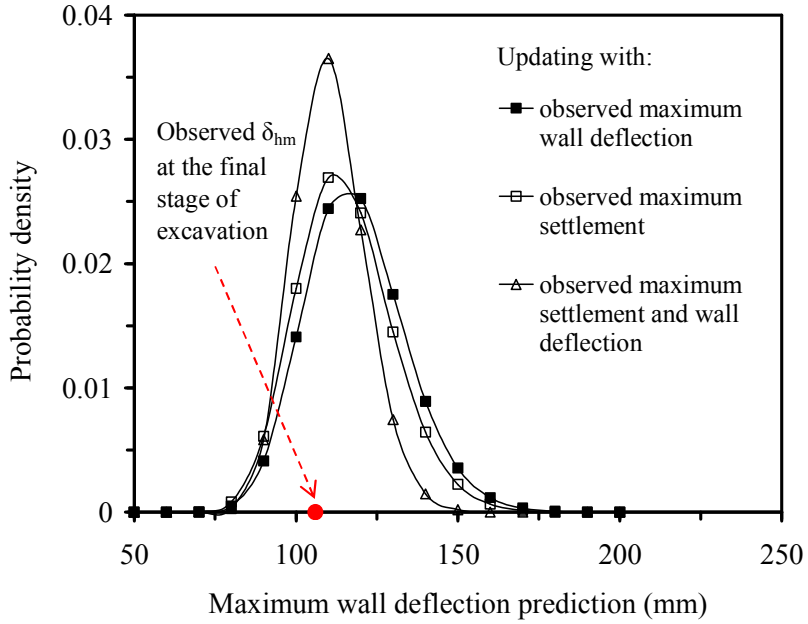

Figure 6.10: Distributions of predictions prior to final stage of excavation (using Prior distribution 1).

Effect of prior distribution on the outcome of Bayesian updating

In this section, the effect of the assumed prior distribution of soil parameters on the outcome of the Bayesian updating is examined. The focus is to determine whether the same final outcome can be obtained after various stages of Bayesian updating regardless of what the initial assumption regarding the prior distribution is. To this end, three other prior distributions are assumed (Table 6.1), in addition to *Prior distribution 1* that has been used in all previous analyses. These four prior distributions represent a wide range of parameter values such that the final response in TNEC excavation will be underestimated in some cases, and overestimated in others. Initially, the *COV*s of those prior distributions are set to be 0.16 (Hsiao et al. 2008). The influence of various assumed *COV* values will be examined next.

The same Bayesian updating procedure is performed with the assumption of *Prior distributions 2*, *3*, and *4*, and the updated mean values and *COV*s of s_u / σ'_v and E_i / σ'_v are shown in Figures 6.11 and 6.12, respectively. As evidenced in Figure 6.11, the updated mean values tend to converge to the "true" value as the excavation progresses. Figure 6.12 shows that with more observations from multiple stages, the *COV*s of the updated parameters tend to decrease; in other words, the updating with more information reduces the uncertainty of soil parameters.

The effect of the assumed *COV*s of soil parameters are further examined within the Bayesian framework. For demonstration purpose, the mean values of *Prior distribution 2* (Table 6.1) are adopted and a series of prior *COV*s for s_u / σ'_v and E_i / σ'_v are selected: 0.10, 0.16, and 0.30. Then the same updating procedure is performed with

the above selected *COV*s and the updated soil parameters are obtained. It is found that the updated mean values of s_u / σ'_v and E_i / σ'_v are almost the same regardless of what levels of prior *COV*s are used. Figure 6.13 shows the *COV*s of the updated soil parameters prior to Stages 3, 4, 5, 6, and 7 of excavations (at the corresponding starting depths of 4.9 m, 8.6 m, 11.8 m, 15.2 m, and 17.3 m, respectively). As shown in Figure 6.13, regardless of the level of the assumed *COV* in the prior distribution, the *COV*s of the updated soil parameters decreased from earlier stages to latter stages (i.e., with increasing number of observations and updating from multiple stages). Figure 6.14 further compares the variation of soil parameters before and after updating, using the case of prior *COV* = 0.3 from Figure 6.13 as an example. The COVs for both s_u / σ'_v and E_i / σ'_v after multi-stages updating with field response observations are reduced to less than 0.10. Thus, the uncertainty of soil parameters is shown to reduce significantly with the application of the Bayesian updating framework.

The above results show that while the prior knowledge is important, the Bayesian updating with observations through stages of excavation can reduce the influence of this prior knowledge, and converged results can be obtained even if the prior knowledge is imperfect. The results demonstrate that the proposed Bayesian updating framework is effective regardless of the assumption of the prior distribution.

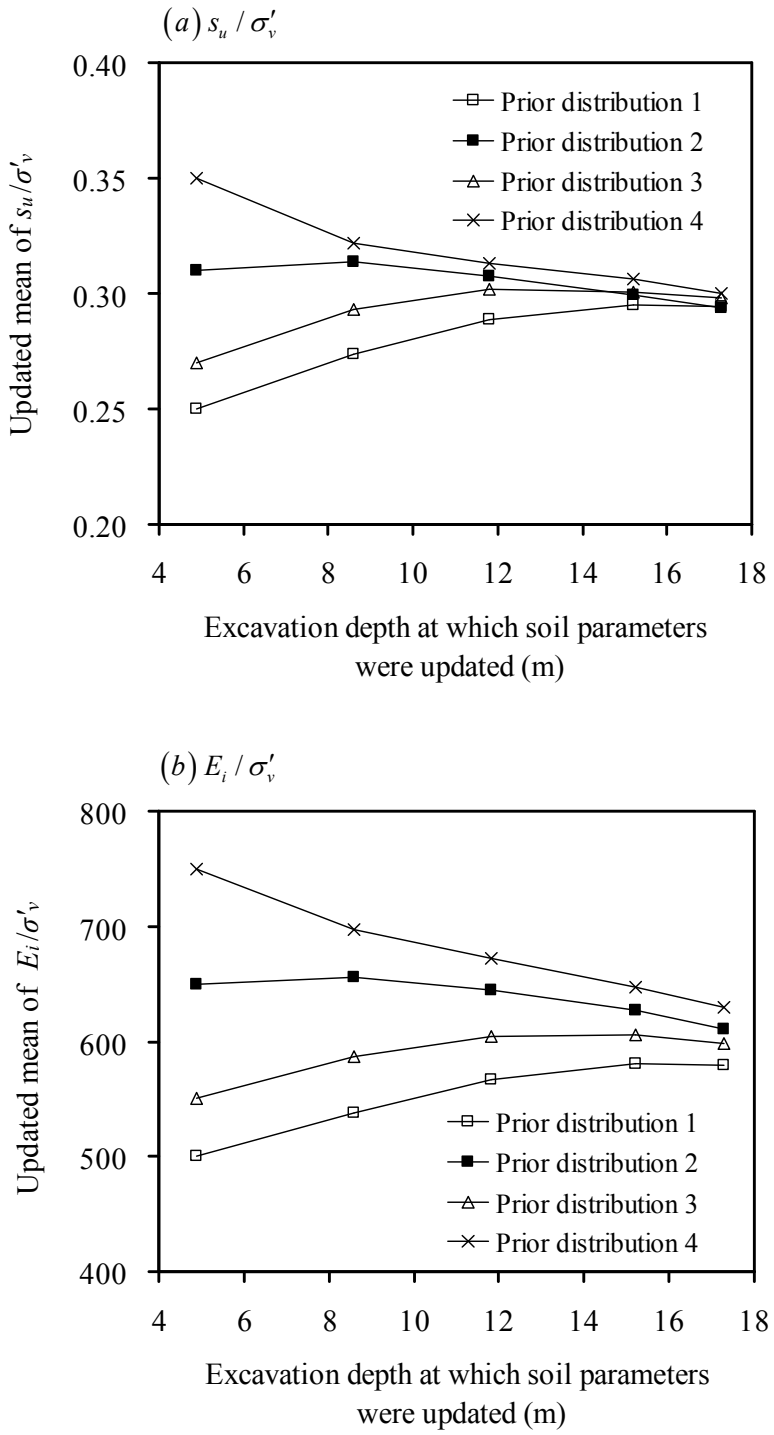

Figure 6.11: Updated mean of soil parameters prior to Stages 3, 4, 5, 6, and 7 of excavations using various prior distributions.

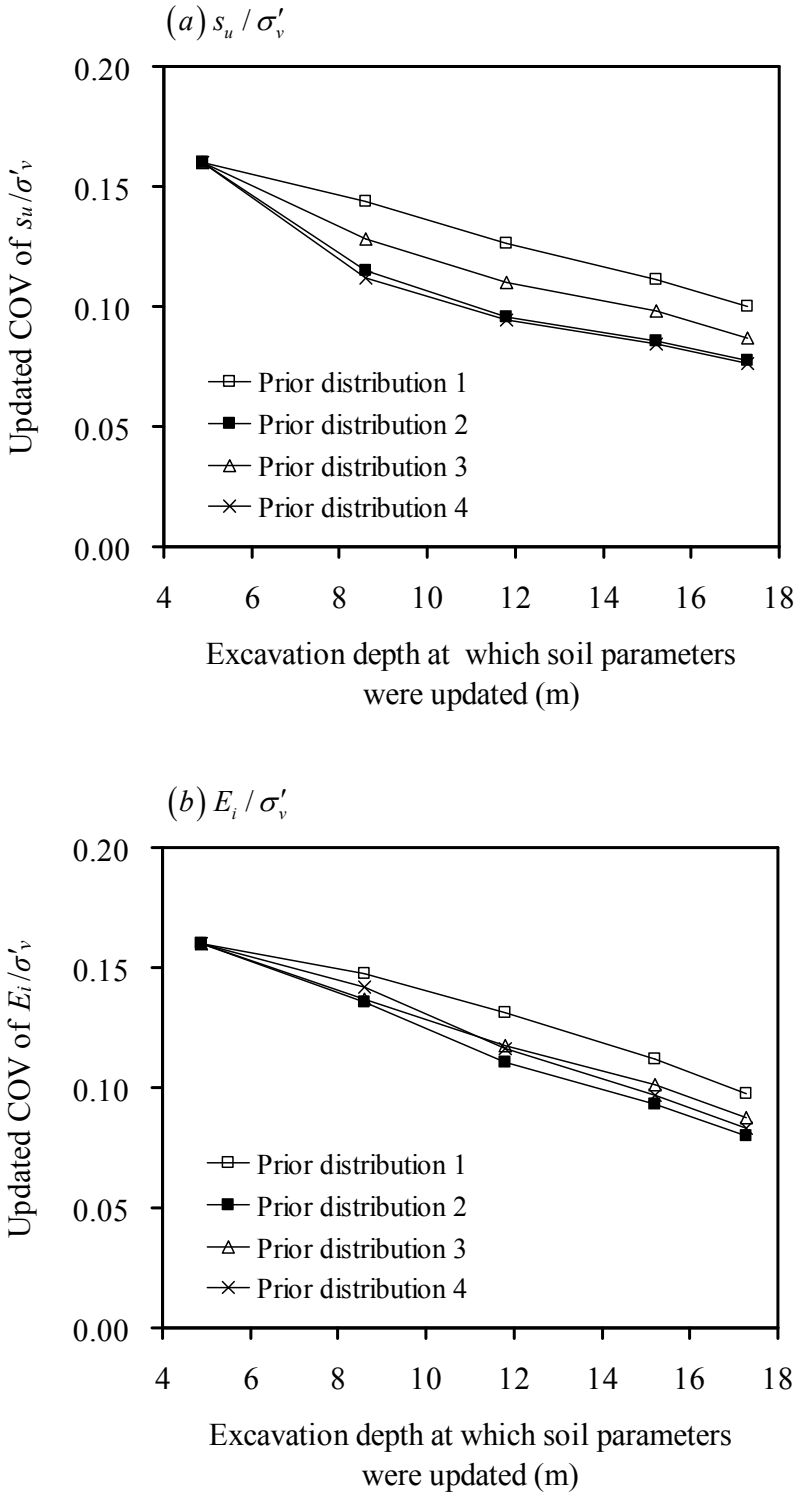

Figure 6.12: Updated *COV* of soil parameters prior to Stages 3, 4, 5, 6, and 7 of excavations using various prior distributions.

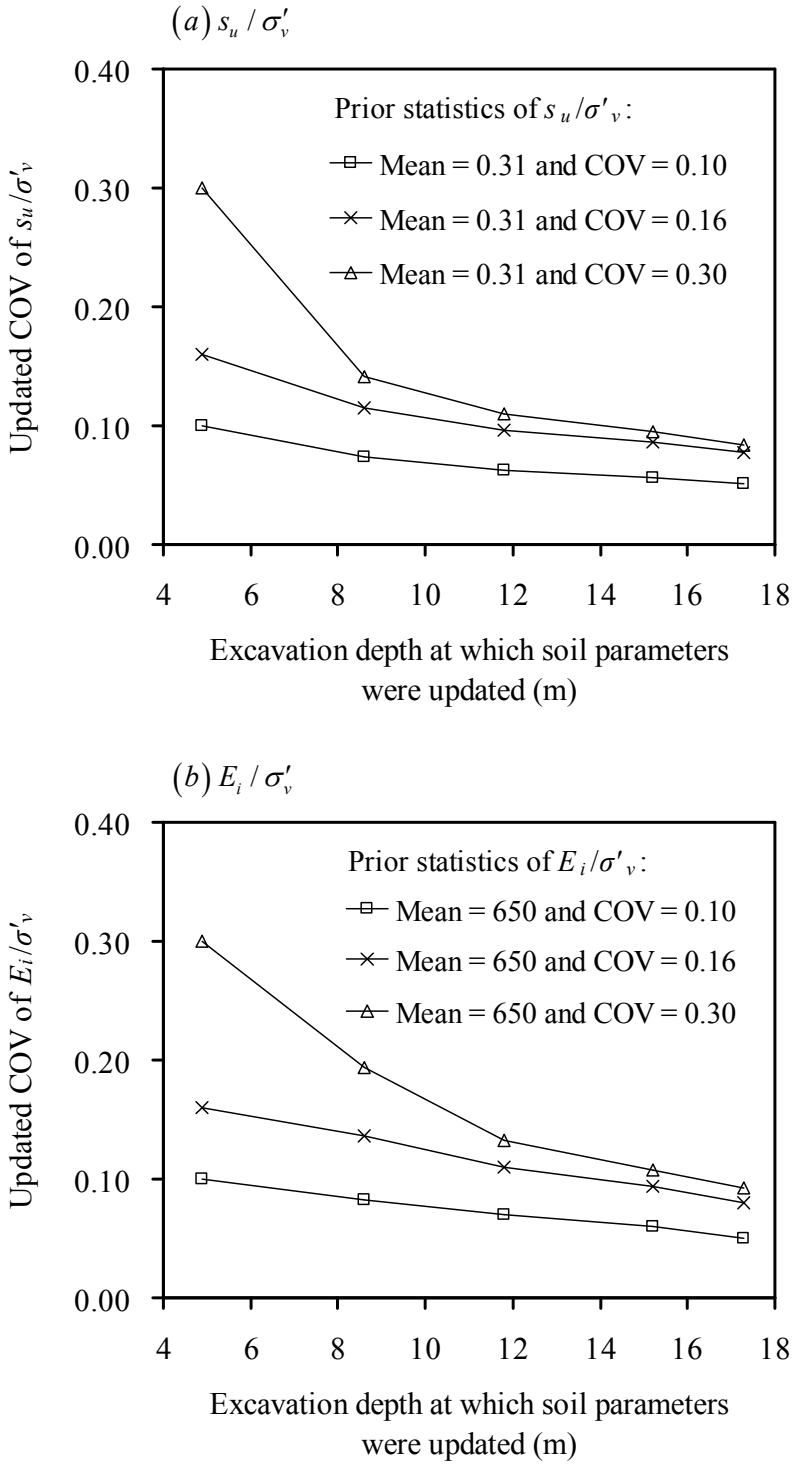

Figure 6.13: Updated COV of soil parameters prior to Stages 3, 4, 5, 6, and 7 of excavations using mean value of Prior distribution 2 and various *COV*s.

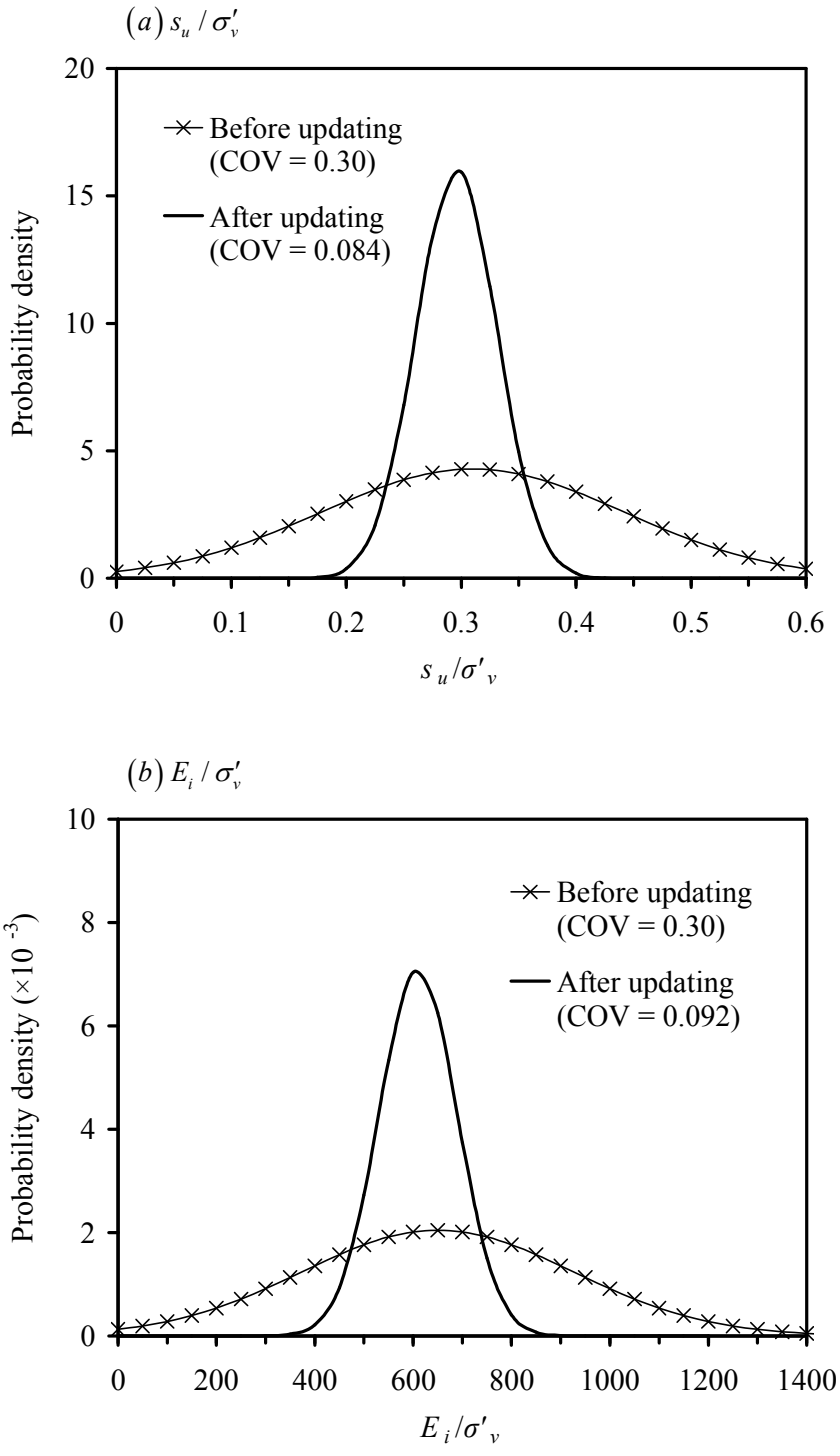

Figure 6.14: Updated distribution of soil parameters prior to final stage of excavation using mean value of Prior distribution 2 and *COV* = 0.30.

Effect of the correlation between bias factors of the two response models

When both observations of maximum wall deflection and maximum settlement are employed within the proposed Bayesian updating framework, the effect of the correlation between bias factors c_h and c_v [Eq. (6.5)] on the updating outcome needs to be assessed. Previous studies indicate that the maximum settlement generally increase with maximum wall deflection (e.g., Clough and O'Rourke 1990; Hsieh and Ou 1998; Kung et al. 2007a,b,c). Therefore, the effect of the coefficient of correlation ρ is examined by repeating the previous analysis with positive correlation assumptions of $\rho = 0.5$ and 0.8, respectively. Figure 6.15 shows the updated predictions of the maximum settlement (part *a*) and maximum wall deflection (part *b*) made prior to Stages 3, 4, 5, 6, and 7 of TNEC excavations (at the corresponding starting depths of 4.9m, 8.6m, 11.8m, 15.2m, and 17.3m, respectively) with three correlation scenarios. A couple of observations are perhaps worth mentioning: (1) the effect of this correlation on the outcome of Bayesian updating appears to be quite limited; and (2) the assumption of no correlation ($\rho = 0$) appears to yield no inferior outcome in the Bayesian updating. This finding is of course based on analysis of a single excavation case, and further study to confirm the finding is warranted. Nonetheless, the results of the analysis of the effect of the correlation between bias factors, along with those results on the effects of the prior distributions of soil parameters and the levels of coefficient of variation, clearly demonstrate the effectiveness and high flexibility of the proposed Bayesian updating framework.

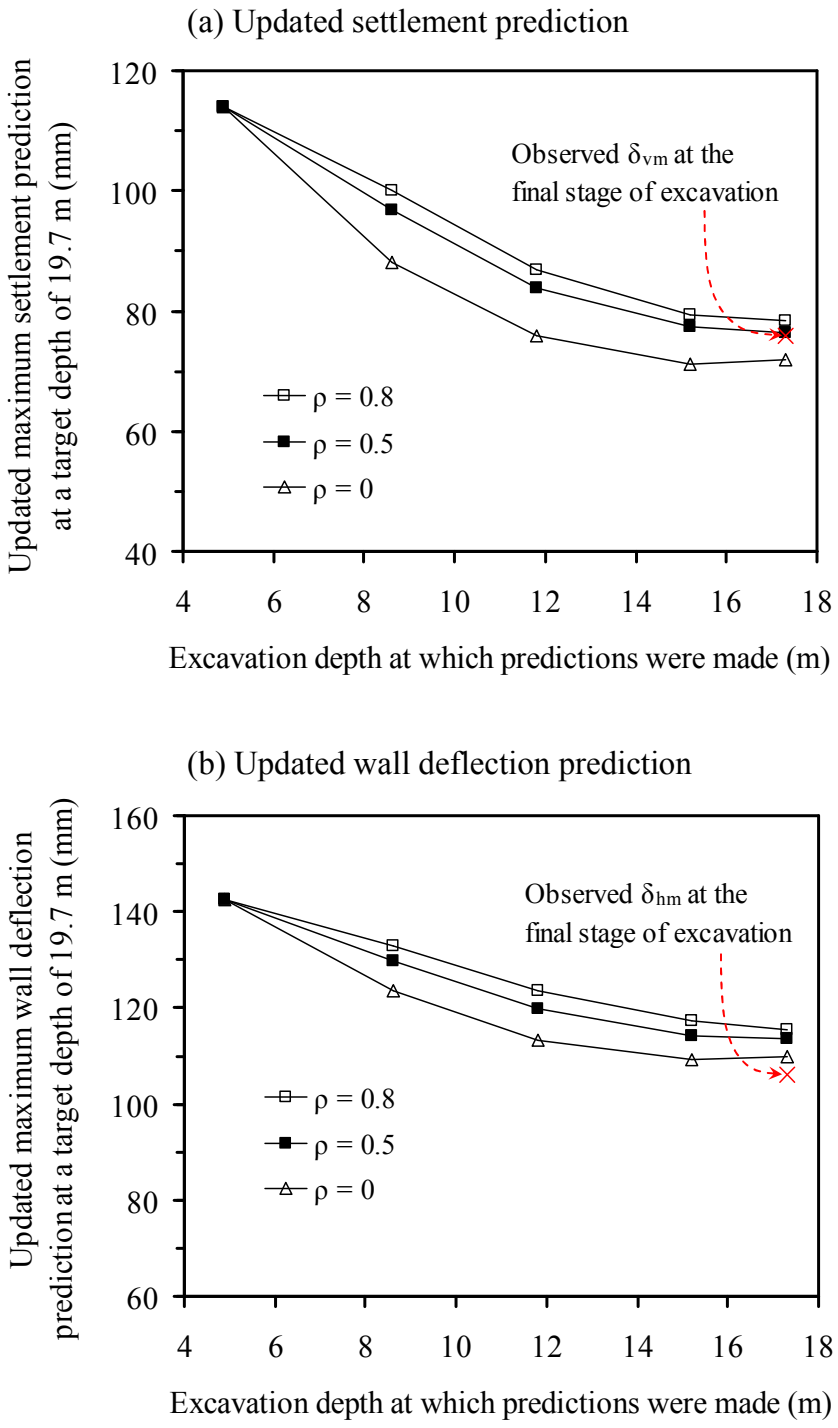

Figure 6.15: Influence of correlation coefficient ρ between model biases on predictions updated with observed maximum settlement and wall deflection (using Prior distribution 1).

Summary

The proposed Bayesian framework for updating soil parameters in a braced excavation is presented in this chapter. This framework uses KJHH model as an example for predicting maximum wall deflection and maximum settlement prior to a given excavation stage, and Bayes' theorem to update key soil parameters so that model predictions prior to next stage of excavation match well with field observations afterwards. Unlike the traditional back analysis, in which fixed parameter values are back-calculated based on observations, the proposed framework allows for consideration of the variation in these parameters and yields their posterior distributions. Thus, not only the "mean" prediction is improved but also the variation of the prediction is reduced. The proposed framework uses the Metropolis-Hastings algorithm-based Markov chain Monte Carlo (MCMC) method to construct the posterior distributions of soil parameters. The effectiveness and flexibility of the proposed framework is examined through a case study of TNEC excavation.

CHAPTER VII

CONCLUSIONS AND RECOMMENDATIONS

Conclusions

The following conclusions are drawn from the study on the effect of one-dimensional spatial variability on the basal-heave stability analysis in Chapter II:

(1) Study of the gamma sensitivity index for all input parameters shows that the normalized undrained shear strength s_u / σ'_v is the most influential factor in the basal-heave stability in a *given* braced excavation in clay, with the unit weight of clay being a distant second. This confirms the common understanding reflected in the existing stability theories on basal-heave stability.

(2) The results of RFM of s_u / σ'_v using the *Cholesky decomposition* method are deemed reasonable. The parametric study with the conventional RFM shows that the model with a smaller scale of fluctuation would yield a greater variance reduction in soil parameters (such as s_u / σ'_v), which in turn would yield a smaller variation in the output responses (for example, *FS* against basal-heave). The computed probability of basal-heave failure can be too high if the spatial variability is not considered in the reliability analysis. Thus, the basal-heave stability design will be too conservative if the effect of spatial variability is ignored.

(3) The algorithm (Figure 2.9) developed in this chapter for deriving the reduction factor, based on a prescribed equivalency of the first two moments obtained by

the RFM approach and the variance reduction-based simplified approach, for a given standard deviation and scale of fluctuation of a spatially random variable s_u / σ'_v is found to be effective. For other geotechnical problems that involve more complicated and nonlinear limit states, further study is needed to investigate general applicability of this algorithm.

(4) For the analysis of basal-heave stability, the proposed simplified approach with variance reduction technique is shown to be able to produce almost identical results with those obtained using the MCS-based RFM approach, provided that an appropriate characteristic length (and thus the reduction factor) can be determined. For the basal-heave stability problem, the appropriate characteristic length for the exponential reduction function is determined to be the distance from the final strut to the bottom of the diaphragm wall, which is the vertical scale of the random field in this case.

(5) For the braced excavation case examined, when the safety factor (*FS*) against basal-heave is less than 1.2 using the slip circle method, the variation in the scale of fluctuation has virtually no influence on the computed failure probability. For *FS* > 1.2, the computed failure probability increases with the increasing variability of the scale of fluctuation but the effect of the variability of the scale of fluctuation is far less significant than that of the magnitude of the scale of fluctuation itself.

(6) The proposed simplified approach for basal-heave analysis, which adopts the variance reduction technique, enables the traditional reliability methods such as

FORM to account for the spatial variability of soil parameters in an efficient way. This approach can easily be implemented in a spreadsheet for probabilistic analysis of basal-heave stability. Reliability or probability-based design can be realized by meeting a target probability of failure against basal-heave.

The following conclusions are drawn from the study on the effect of two-dimensional spatial variability on the basal-heave stability analysis in Chapter III:

(1) Traditional reliability analysis that considers variation of input soil parameters, but not spatial variability in a random field, can significantly overestimate the probability of basal-heave failure for a given deterministic design with a certain factor of safety (e.g., Figures 3.3 and 3.4). Negligence of the model bias of the slip circle method also leads to an overestimation of failure probability (Figure 3.8), albeit at a much lesser degree. The results help explain the unreasonably high probability of failure that is often reported in a traditional reliability analysis of a basal-heave design that achieves a satisfactory safety factor (for example, $FS > 1.2$). Thus, spatial variability must be properly accounted for in the reliability analysis.

(2) When proper characteristic lengths are selected, the reduction factor (Γ) computed using Eq. (3.8) agrees extremely well with that which was back-calculated from the "equivalency" analysis using the MCS-based RFM solution (Figure 3.5). This study found that for basal-heave analysis in a 2-D random field using the slip circle method (Figure 3.1), the vertical characteristic length L_v can be taken as the

vertical distance between the depth of the final strut and the bottom of the diaphragm wall (length $\overline{od}$ in Figure 3.1) and the horizontal characteristic length L_h can be taken as the horizontal scale of the slip circle (length $\overline{ec}$ in Figure 3.1). With these characteristic lengths, the reduction factor (Γ) can be accurately computed using the equivalent variance technique.

(3) A procedure for conducting reliability analysis of basal-heave in a braced excavation in a 2-D random field is presented. This reliability-based analysis procedure that considers spatial variability in the 2-D random field is based on an *equivalent* simplified approach. The equivalency in the computed probability of basal-heave failure is established through equivalent variance technique. The results presented in this study show the probability of basal-heave in a given braced excavation in clay with spatial variability can be determined through traditional reliability analysis of basal-heave using the equivalent simplified approach, in lieu of the Monte Carlo simulation (MCS) analysis. The developed procedure is implemented in a spreadsheet, which is shown to be an effective and efficient tool for performing reliability analysis that takes into account 2-D spatial variability of soils.

(4) The spreadsheet that implements the developed simplified approach facilitates reliability-based design of braced excavation against basal-heave, as the probability of basal-heave failure can be easily calculated even when spatial variability must be considered. Reliability-based design can be realized by satisfying a target reliability index or the acceptable probability of failure against

basal-heave. The developed reliability-based procedure (and spreadsheet), on the other hand, can accurately evaluate the probability of basal-heave failure because soil spatial variability is properly counted for through variance reduction. The developed reliability-based procedure is easy to use, especially with a spreadsheet tool which requires far less computational effort than the MCS-based RFM approach. Thus, this simplified approach can be a practical tool for reliability-based design against basal-heave failure.

The following conclusions are drawn from the study on the effect of one-dimensional spatial variability on the probabilistic serviceability assessment in Chapter IV:

(1) The fuzzy finite element approach (FFEA) is shown to be effective in the analysis of wall and ground responses in a braced excavation through a study of a well-documented excavation case history. The approach uses fuzzy sets to model uncertain soil parameters and allows for consideration of soil variability through variance reduction. The propagation of fuzzy input through finite element solution is carried out by means of the vertex method, which is shown to be an effective and efficient computational technique. The fuzzy output (the wall and ground responses expressed as fuzzy numbers) can readily be used to compute the probability of exceeding the specified limiting response in a braced excavation.

(2) Plaxis^{TM} with the modified pseudo plasticity (MPP) soil model is found to be satisfactory for predicting wall and ground responses in a braced excavation. The

Plaxis^{TM} solutions in this study are found to be as accurate as those obtained using the AFENA code with the same MPP soil model by Kung et al. (2007a). Both Plaxis^{TM} and AFENA predictions agree closely with field observations in a well-documented case history.

(3) The validity of the variance reduction technique in FEM analysis of braced excavation in clays is ascertained by the results of the checkerboard study. Although the checkerboard analysis in this study is not as rigorous as the random FEM method, it does demonstrate the effect of spatial correlation of soil properties on the responses in a braced excavation. The results (i.e., the demonstrated applicability of the variance reduction technique in braced excavations) provide a basis for incorporating soil variability into the fuzzy set model of the uncertain soil parameters, which in turn, allows for a simple FFEA analysis.

(4) Neglecting spatial variability of input soil parameters can lead to an overestimation of variation of wall and ground responses in a braced excavation. The effect of the scale of fluctuation on the "probability of exceedance" (exceeding the specified limiting response) is also observed in this study. Neglecting spatial variability in the FFEA analysis can lead to either overestimation or underestimation of the probability of exceedance, depending on the specified limiting response. Thus, it is important to assess spatial variability during site investigation and to incorporate this variability into the FFEA analysis of braced excavation.

The following conclusions are drawn from the study on the effect of small sample size of soil parameters on the probabilistic serviceability assessment in Chapter V:

(1) A simple procedure for assessing the probability of serviceability failure in a braced excavation, where the failure is defined as the state that the response of an excavation system, in terms of the maximum wall deflection or ground settlement, exceeds the specified limiting value, is presented and demonstrated with a case study.

(2) Because of the uncertainties in the analysis model and the input parameters, the question of whether the response of an excavation system will exceed the specified limiting value cannot be answered with certainty. Thus, it is useful to evaluate the probability of failure (or in this study, probability of exceedance) taking into account of these uncertainties *explicitly*. The probability of exceedance allows for a more informed decision to be made regarding the risk of serviceability failure in a braced excavation. However, use of reliability analysis for the probability of exceedance necessitates an evaluation of the means and standard deviations of critical soil parameters. In geotechnical practice, these means and standard deviations are often estimated from limited data, which leads to uncertainty in the derived sample statistics. Thus, there is a need to characterize the uncertainty in the sample statistics derived from a small sample, and to determine the effect of such uncertainty.

(3) Through the case study presented, this study demonstrates that the bootstrap

method is an effective tool for characterizing the uncertainty (or variation) in the sample statistics derived from a small sample, and that additional information (such as the confidence interval of the probability of serviceability failure, as opposed to a single, fixed probability) can be "gained" through bootstrapping analysis. The gained information enables the engineer to more rationally assess the probability serviceability failure (and the associated risk) in a braced excavation. The case study shows the potential of the bootstrap method in coping with the problem of having to evaluate failure probability with uncertain sample statistics.

The following conclusions are drawn from the study on Bayesian updating of soil parameters in braced excavation in Chapter VI:

(1) The proposed Bayesian framework is shown effective for updating key soil parameters in the staged excavation based on either maximum settlement or maximum wall deflection observation or both types of observations. Updating with both types of observations (i.e., maximum wall deflection and maximum settlement) is the most effective overall, and the updated predictions of the maximum wall and ground responses have the least variation. In the event that only the wall deflection is measured during the excavation, the updating of soil parameters and response predictions in the subsequent stages of excavation with the proposed framework still yields almost equally satisfactory results.

(2) Bayesian updating is shown effective in reducing the uncertainty (in terms of

coefficient of variation) of the updated soil parameters and model predictions through multi-stage of observations and updating. In the case study of the staged excavation, the mean values of the response predictions are getting increasingly closer to the field observations as the excavation proceeds. However, both the updated soil parameters and the updated response predictions still have to be expressed with a probability distribution to capture and reflect the uncertainty that cannot be removed completely in the updating process.

(3) The uncertain nature of the updated soil parameters and response predictions, even after multi-stage Bayesian updating, has an important implication. The claim of "excellent agreement" between the prediction and the observation in the traditional back analysis of an excavation case history, often reported in the literature, may not be all that meaningful if the variation in the input parameters and/or in the computed responses are not full characterized and reported.

(4) The final outcome of the Bayesian updating is not much affected by the assumed prior distributions and the levels of the coefficient of variation of the soil parameters. Thus, while the prior knowledge is important, the Bayesian updating with observations through stages of excavation can reduce the influence of this prior knowledge, and converged results can be obtained even if the prior knowledge is imperfect.

(5) Effect of the correlation between the maximum wall deflection and the maximum settlement, through the model factors, on the outcome of Bayesian updating appears to be quite limited. The assumption of no correlation appears to yield no

inferior outcome in the Bayesian updating in the case study of TNEC excavation. Although further study to confirm this finding is warranted, it is postulated that the proposed framework through multi-stages of observations and updating is able to compensate for the deficiency, if any, of this assumption.

(6) Markov chain Monte Carlo (MCMC) simulation implemented with Metropolis-Hastings algorithm is shown effective in this study. The construction of an effective Markov chain is, however, problem-specific and should be examined case by case through a proper parametric analysis. The MCMC parameter settings are likely to be valid for similar excavation problems.

Recommendations

To further expand the work presented in this dissertation, a number of research topics can be undertaken, which include the following:

(1) The proposed simplified approach for basal-heave stability analysis considering spatial variability of soil parameter is based on slip circle method, which is an empirical model. It is also advisable to perform the basal-heave stability analysis using finite element analysis through strength reduction method. The feasibility of using finite element method for basal-heave stability analysis in conjunction with the proposed simplified approach should be investigated.

(2) The probabilistic study on basal-heave stability and serviceability failure in this dissertation is limited to the 2-D empirical/finite element model. It should be of interest to consider the effect of 3-D spatial variability of soil parameters on the

reliability analysis, especially if 3-D modeling of the stability and deformation problems in braced excavations is desired.

(3) Within the Bayesian framework proposed for updating soil parameters in this dissertation, the uncertainty of the observed wall and ground responses may be considered. This can be realized by considering the uncertainty of observations in the covariance matrix of model bias (or model error) within the current Bayesian framework in this dissertation.

(4) The proposed Bayesian framework for updating key soil parameters in this dissertation does not simultaneously update the model bias of the semi-empirical model KJHH in the updating process. Considering that the KJHH model is a data-driven model, the model bias should also be calibrated in the Bayesian updating process. Thus, it should be of interest to improve the proposed Bayesian framework in this regards.

REFERENCES

Akbas, S.O., and Kulhawy, F.H. (2009). "Reliability-based design approach for differential settlement of footings on cohesionless soils." *Journal of Geotechnical and Geoenvironmental Engineering*, 135(12), 1779-1788.

Ang, A.H.-S., and Tang, W.H. (1984). Probability concepts in engineering planning and design. Vol. 2, Design, risk and reliability, Wiley, New York.

Ang, A.H.-S, and Tang, W.H. (2007). Probability concepts in engineering: Emphasis on applications to civil and environmental engineering. 2nd ed. New York: John Wiley and Sons.

Babu, G.L.S., and Dasaka, S.M. (2008). "The effect of spatial correlation of cone tip resistance on the bearing capacity of shallow foundations." *Geotechnical and Geological Engineering*, 26(1), 37-46.

Baecher, G.B., and Christian, J.T. (2003). Reliability and Statistics in Geotechnical Engineering. John Wiley and Sons, London and New York.

Baroth, J., and Malécot, Y. (2010). "Probabilistic analysis of the inverse analysis of an excavation problem." *Computers and Geotechnics*, 37(3), 391-398.

Beck, J.L., and Au, S.K. (2002). "Bayesian updating of structural models and reliability using Markov chain Monte Carlo Simulation." *Journal of Engineering Mechanics*, 128(4), 380-391.

Bjerrum, L., and Eide, O. (1956). "Stability of strutted excavations in clay." *Géotechnique*, 6(1), 32-47.

Brinkgreve, R.B.J., and Vermeer, P.A. (2002). PLAXIS: Finite Element Code for Soil and Rock Analyses, Version 8, Balkema.

Calvello, M., and Finno, R.J. (2004). "Selecting parameters to optimize in model calibration by inverse analysis." *Computers and Geotechnics*, 31(5), 411-425.

Chang, M.F. (2000). "Basal stability analysis of braced cuts in clay." *Journal of Geotechnical and Geoenvironmental Engineering*, 126(3), 276-279.

Chen, J.W., and Juang, C.H. (1996). "Determining drained friction angle of sands from CPT." *Journal of Geotechnical Engineering*, 122(5), 374-381.

Chen, D.S., Liao, C.L., Fan, C.B., Chung, L.J., and Pan, V.C. (2007). "Remedial methods for the deep excavation of KMRT O1 Station after the sand piping incidence." *In: Proceedings of the Cross-Straight Geotechnical Engineering Conference*, Tianjin, China, 13-22.

Cherubini, C. (2000). "Reliability evaluation of shallow foundation bearing capacity on c', φ' soils." *Canadian Geotechnical Journal*, 37(1), 264-269.

Christian J.T., and Baecher G.B. (1999). "Point estimate method as numerical quadrature." *Journal of Geotechnical and Geoenvironmental Engineering*, 125(9), 779-786.

Chua, C.G., and Goh, A.T.C. (2005). "Estimating wall deflections in deep excavations using Bayesian neural networks." *Tunnelling and Underground Space Technology*, 20(4), 400-409.

Clough, G.W., and O'Rourke, T.D. (1990). "Construction induced movements of in situ walls." *In: Proceedings of Design and Performance of Earth Retaining Structure*, Geotechnical Special Publication, No. 25, ASCE, New York, 439-470.

Dang, H.P. (2009). "Excavation behavior and adjacent building response analyses using user defined soil models in PLAXIS." MS. thesis, Dept. of Construction Engineering, National Taiwan University of Science and Technology, Taipei, Taiwan.

Der Kiureghian, A., and Ke, J.-B. (1985). "Finite element-based reliability analysis of framed structures." *In: Proceedings of the 4th International Conference on Structural Safety and Reliability*, Vol. 1, International Association for Structural Safety and Reliability, New York, 395-404.

DiMaggio, J.A. (2008). "Defining and applying quality in drilled deep foundations and earth retaining structures." *Keynote Address, ADSC Faculty Workshop 2008*, The International Association of Foundation Drilling, Dallas, Texas.

Dodagoudar, G.R., and Venkatachalam, G. (2000). "Reliability analysis of slopes using fuzzy sets theory." *Computers and Geotechnics*, 27(2), 101-115.

Dong, W.M., and Wong, F.S. (1987). "Fuzzy weighted averages and implementation of the extension principle." *Fuzzy Set and Systems*, 21(2), 183-199.

Draper, D. (2006). Bayesian hierarchical modeling, Springer, New York.

Duncan, J.M. (2000). "Factors of safety and reliability in geotechnical engineering." *Journal of Geotechnical Geoenvironmental Engineering*, 126(4), 307-316.

Duncan, J.M. (2001). "Closure to Factors of safety and reliability in geotechnical engineering." *Journal of Geotechnical Geoenvironmental Engineering*, 127(8), 717-721.

Efron, B. (1979). "Bootstrap methods: another look at Jackknife." *Annals of Statistics*, 7(1), 1-26.

Eide, O., Aas, G., and Josang, T. (1972). "Special applications of cast-in-place walls for tunnels in soft clay in Oslo." Pub. 91, Norwegian Geotechnical Institute, Oslo, Norway, 63-72.

Elton, D.J., Juang, C.H., and Lin, P.S. (2000). "Vertical capacity of piles using fuzzy sets." *Civil Engineering and Environmental systems*, 17(3), 237-262.

Fenton, G.A. (1997). "Probabilistic methods in geotechnical engineering." *In: Workshop presented at ASCE GeoLogan'97 conference*, Logan, Utah.

Fenton, G.A., and Griffiths, D.V. (2003). "Bearing capacity prediction of spatially random c - φ soils." *Canadian Geotechnical Journal*, 40(1), 54-65.

Fenton, G.A., Griffiths, D.V., and Williams, M.B. (2005). "Reliability of traditional retaining wall design." *Géotechnique*, 55(1), 55-62.

Fenton, G.A., and Griffiths, D.V. (2008). Risk Assessment in Geotechnical Engineering, John Wiley & Sons, New York.

Gamerman, D. (1997). Markov Chain Monte Carlo, Chapman & Hall, London.

Gelman, B.A., Carlin, B.P., Stem, H.S., and Rubin, D.B. (2004). Bayesian data analysis, Chapman & Hall, London.

Goh, A.T.C., Kulhawy, F.H., and Wong, K.S. (2008). "Reliability assessment of basal-heave stability for braced excavations in clay." *Journal of Geotechnical and Geoenvironmental Engineering*, 134(2), 145-153.

Griffiths, D.V., and Fenton, G.A. (2004). "Probabilistic slope stability analysis by finite elements." *Journal of Geotechnical and Geoenvironmental Engineering*, 130(5), 507-518.

Griffiths, D.V., Fenton, G.A., and Manoharan, N. (2006). "Undrained bearing capacity of two-strip footings on spatially random soil." *International Journal of Geomechanics*, 6(6), 421-427.

Griffiths, D.V., and Fenton, G.A. (2009). "Probabilistic settlement analysis by stochastic and random finite element methods." *Journal of Geotechnical and Geoenvironmental Engineering*, 135(11), 1629-1637.

Griffiths, D.V., Huang, J., and Fenton, G.A. (2009). "Influence of spatial variability on slope reliability using 2-D random fields." *Journal of Geotechnical and Geoenvironmental Engineering*, 135(10), 1367-1378.

Guo, S.X., and Lu, Z.Z. (2003). "Procedure for computing the possibility and fuzzy probability of failure of structures." *Applied Mathematics and Mechanics*, 24(3), 338-343.

Haldar, S., and Babu, G.L.S. (2008). "Effect of soil spatial variability on the response of laterally loaded pile in undrained clay." *Computers and Geotechnics*, 35(4), 537-547.

Harr, M. E. (1987). Probability-based design in civil engineering, Dover, Mineola, N.Y.

Hashash, Y.M.A., Jung, S., and Ghaboussi, J. (2004). "Numerical implementation of a neural network based material model in finite element analysis." *International Journal for Numerical Methods in Engineering*, 59(8), 989-1005.

Hashash, Y.M.A., Levasseur, S., Osouli, A., Finno, R., and Malecot, Y. (2010). "Comparison of two inverse analysis techniques for learning deep excavation response." *Computers and Geotechnics*, 37(3), 323-333.

Hastings, W.K. (1970). "Monte Carlo sampling methods using Markov chains and their applications." *Biometricka*, 57, 97-109.

Honjo, Y., Liu, W.T, and Soumitra, G. (1994). "Inverse analysis of an embankment on soft clay by extended Bayesian method." *International Journal for Numerical and Analytical Methods in Geomechanics*, 18,709-34.

Hsiao, C.L. (2007). "Wall and ground movements in a braced excavation in clays and serviceability reliability of adjacent buildings." Ph.D. dissertation, Dept. of Civil Engineering, Clemson University, Clemson, SC.

Hsiao, E.C.L., Schuster, M., Juang, C.H., and Kung, G.T.C. (2008). "Reliability analysis of excavation-induced ground settlement for building serviceability evaluation." *Journal of Geotechnical and Geoenvironmental Engineering*, 134(10), 1448-1458.

Hsieh, P.G., and Ou, C.Y. (1997). "Use of the modified hyperbolic model in excavation analysis under undrained condition." *Geotechnical Engineering Journal*, 28(2), 123-150.

Hsieh, P.G., Kung, T.C., Ou, C.Y., and Tang, Y.G. (2003). "Deep excavation analysis with consideration of small strain modulus and its degradation behavior of clay." *In: Proceedings of the 12th Asian Regional Conference on Soil Mechanics and Geotechnical Engineering*, Vol. 1, Fuisland Offset Printing, Singapore.

Hsieh, P.G., and Ou, C.Y. (1998). "Shape of ground surface settlement profiles caused by excavation." *Canadian Geotechnical Journal*, 35(6), 1004-1017.

Huang, J.S., Griffiths, D.V., and Fenton, G.A. (2010). "Probabilistic analysis of coupled soil consolidation." *Journal of Geotechnical and Geoenvironmental Engineering*, 136(3), 417-430.

Infopedia (2004). "Nicoll highway collapse." A website of the Singapore Government, http://infopedia.nlb.gov.sg/articles/SIP_430_2004-12-17.html.

Jaksa, M.B., Kaggwa, W.S., and Brooker, P.I. (1999). "Experimental evaluation of the scale of fluctuation of a stiff clay." *In: Proc. 8th Int. Conf. on the Application of Statistics and Probability*, R. E. Melchers and M. G. Stewart (eds.), Sydney, A. A. Balkema, Rotterdam, Vol. 1, 415-422.

JSA (1988). Guidelines of Design and Construction of Deep Excavation, Japanese Society of Architecture, Tokyo, Japan.

Juang, C.H., Wey, J.L., and Elton, D.J. (1991). "Model for capacity of single piles in sand using fuzzy sets." *Journal of Geotechnical Engineering*, 117(12), 1920-1931.

Juang, C.H., Huang, X.H., and Elton, D.J. (1992a). "Modeling and analysis of non-random uncertainties - A fuzzy set approach." *International Journal for Numerical and Analytical Methods in Geomechanics*, 16(5), 335-350.

Juang, C.H., Lee, D.H., and Sheu, C. (1992b). "Mapping slope failure potential using fuzzy sets." *Journal of Geotechnical Engineering*, 118(3), 475-494.

Juang, C.H., and Elton, D.J. (1996). "A practical approach to uncertainty modeling in geotechnical engineering." *In: Proceedings of Uncertainty in the Geologic Environment: from Theory to Practice*, Vol. 2, Geotechnical Special Publication No. 58, ASCE, New York.

Juang, C.H., Jhi, Y.Y., and Lee, D.H. (1998). "Stability analysis of existing slopes considering uncertainty." *Engineering Geology*, 49(2), 111-122.

Juang, C.H., Fang, S.Y., and Khor, E.H. (2006). "First-order reliability method for probabilistic liquefaction triggering analysis using CPT." *Journal of Geotechnical and Geoenvironmental Engineering*, 132(3), 337-350.

Juang, C.H., Fang, S.Y., Tang, W.H., Khor, E.H., Kung, G.T.C., and Zhang, J. (2009). "Evaluation model uncertainty of an SPT-based method for reliability analysis for probability of liquefaction." *Soils and Foundations*, 49(1), 135-152.

Kay, J.N. (1976). "Safety Factor Evaluation for Single Piles in Sand." *Journal of the Geotechnical Engineering*, 102(GT10), 1093-1108.

Klammler, H., McVay, M., Horhota, D., and Lai, P. (2010). "Influence of spatially variable side friction on single drilled shaft resistance and LRFD resistance factors." *Journal of Geotechnical and Geoenvironmental Engineering*, 136(8), 1114-1123.

Kung, T.C. (2003). "Surface settlement induced by excavation with consideration of small strain behavior of Taipei silty clay." Ph.D. dissertation, Dept. of Construction Engineering, National Taiwan Univ. of Science and Technology, Taipei, Taiwan.

Kung, G.T.C., Hsiao, C.L., and Juang, C.H. (2007a). "Evaluation of a simplified small-strain soil model for finite element analysis of excavation-induced movements." *Canadian Geotechnical Journal*, 44(6), 726-736.

Kung, T.C., Juang, C.H., Hsiao, C.L., and Hashash, Y. (2007b). "Simplified model for wall deflection and ground surface settlement caused by braced excavation in clays." *Journal of Geotechnical and Geoenvironmental Engineering*, 133(6), 731-747.

Kung, T.C., Hsiao, C.L., Schuster, M., and Juang, C.H. (2007c). "A neural network approach to estimating excavation-induced wall deflection in soft clays." *Computers and Geotechnics*, 34(5), 385-396.

Ladd, C.C., and Foott, R. (1974). "New design procedure for stability of soft clays." *Journal of Geotechnical Engineering Division*, 100(7), 763-786.

Ledesma, A., Gens, A., and Alonso, E.E. (1996). "Parameter and variance estimation in geotechnical back analysis using prior information." *International Journal for Numerical and Analytical Methods in Geomechanics*, 20,119-141.

Lee, I.K., White, W., and Ingles, O.G. (1983). Geotechnical Engineering, Copp Clark Pitman, Inc.

Low, B.K., and Tang, W.H. (1997). "Efficient reliability evaluation using spreadsheet." *Journal of Engineering Mechanics*, 123(7), 749-752.

MathWorks, Inc. (2010). Matlab user's manual, version 7, Natick, Mass.

Miranda, T., Gomes Correia, A., and Ribeiro e Sousa, L. (2009). "Bayesian methodology for updating geomechanical parameters and uncertainty quantification." *International Journal of Rock Mechanics and Mining Sciences*, 46(7), 1144-1153.

Most, T., and Knabe, T. (2010). "Reliability analysis of bearing failure problem considering uncertain stochastic parameters." *Computers and Geotechnics*, 37(3), 299-310.

Ou, C.Y., Liao, J.T., and Lin, H.D. (1998). "Performance of diaphragm wall constructed using top-down method." *Journal of Geotechnical and Geoenvironmental Engineering*, 124(9), 798-808.

Peschl, G.M., and Schweiger, H.F. (2003). "Reliability analysis in geotechnics with finite elements - comparison of probabilistic, stochastic and fuzzy set methods." *In: Proceedings of the 3rd international symposium on imprecise probabilities and their applications (ISIPTA'03)*, Carleton Scientific, Canada, 437-451.

Phoon, K.K., and Kulhawy, F.H. (1999a). "Characterization of geotechnical variability." *Canadian Geotechnical Journal*, 129(4), 612-624.

Phoon, K.K., and Kulhawy, F.H. (1999b). "Evaluation of geotechnical property variability." *Canadian Geotechnical Journal*, 129(4), 625-639.

Phoon, K.K., Kulhawy, F.H., and Grigoriu, M.D. (2003). "Multiple resistance factor design for shallow transmission line structure foundations." *Journal of Geotechnical and Geoenvironmental Engineering*, 129(9), 807-818.

PSCG (2000). Specification for Excavation in Shanghai Metro Construction, Professional Standards Compilation Group, Shanghai, China.

Rosenblueth, E. (1975). "Point estimates for probability moments." *In: Proceedings of the National Academy of Science*, 72(10), 3812-3814.

Saboya, F., Alves, M.G., and Pinto, W.D. (2006). "Assessment of failure susceptibility of soil slopes using fuzzy logic." *Engineering Geology*, 86(4), 211-224.

Schweiger, H.F., and Peschl, G.M. (2005). "Reliability analysis in geotechnics with the random set finite method." *Computers and Geotechnics*, 32(6), 422-435.

Srivastava, A., Babu, G.L.S., and Haldar, S. (2010). "Influence of spatial variability of permeability property on steady state seepage flow and slope stability analysis." *Engineering Geology*, 110(3-4), 93-101.

Suchomel, R., and Mašín, D. (2010). "Comparison of different probabilistic methods for predicting stability of a slope in spatially variable c-φ soil." *Computers and Geotechnics*, 37(1-2), 132-140.

Suchomel, R., and Mašín, D. (2011). "Probabilistic analyses of a strip footing on horizontally stratified sandy deposit using advanced constitutive model." *Computers and Geotechnics*, 38(3):363-374.

Tang, Y.G., and Kung, G.T.C. (2009). "Application of nonlinear optimization technique to back analysis of deep excavation." *Computers and Geotechnics*, 36(1-2), 276-290.

Terzaghi, K. (1943). Theoretical Soil Mechanics, Wiley, New York.

TGS (2001). Design Specifications for the Foundation of Buildings, Taiwan Geotechnical Society, Taipei, Taiwan.

United States Army Corps of Engineers. (1997). "Engineering and design: Introduction to probability and reliability methods for use in geotechnical engineering." *Engineering Circular No. 1110-2-547*, Dept. of the Army, Washington, D.C.

Valliappan, S., and Pham, T.D. (1995). "Elasto-plastic finite element analysis with fuzzy parameters." *International Journal for Numerical Methods in Engineering*, 38(4), 531-548.

Vanmarcke, E.H. (1977). "Probabilistic modeling of soil profiles." *Journal of the geotechnical engineering division*, 103(11), 1227-1246.

Vanmarcke, E.H. (1983). Random Fields - Analysis and Synthesis, Cambridge, MIT-Press, MA.

Wang, Y., Au, S.K., and Cao, Z. (2010). "Bayesian approach for probabilistic characterization of sand friction angles." *Engineering Geology*, 114(3-4), 354-363.

Wang, Y., Au, S.K., and Kulhawy, F.H. (2011a). "Expanded reliability-based design approach for drilled shafts." *Journal of Geotechnical and Geoenvironmental Engineering*, 137(2), 140-149.

Wang, Y., Cao, Z., and Au, S.K. (2011b). "Practical reliability analysis of slope stability by advanced Monte Carlo simulations in spreadsheet." *Canadian Geotechnical Journal*, 48(1), 162-172.

Whittle, A.J., Hashash, Y.M.A., and Whitman, R.V. (1993). "Analysis of deep excavations in Boston." *Journal of Geotechnical Engineering*, 119(1), 69-90.

Whittle, A.J., and Hashash, Y.M.A. (1994). "Soil modeling and prediction of deep excavation behavior." *In: Proceedings of the International Symposium on Pre-failure Deformation Characteristics of Geomaterials*, Vol. 1, A.A. Balkema, Rotterdam, The Netherlands.

Wu, S.H., Ou, C.Y., Ching, J., and Juang, C.H. (2010a). "Reliability-based design for basal heave in an excavation considering spatial variability." *In: GeoFlorida 2010: Advances in Analysis, Modeling & Design*, Geotechnical Special Publication No. 199, ASCE, West Palm Beach, Florida.

Wu, Y.T., Shiao, M., and Millwater, H.R. (2010b). "A Bayesian-updating computational method for probabilistic damage tolerance analysis." *In: Proceedings of the 51st AIAA/ASME/ASCE/AHS Structures*, Structural Dynamics and Materials Conference, Orlando, Florida.

Wu, S.H., Ou, C.Y., and Ching, J. (2011). "Reliability based design of base heave stability in wide excavations." *In: Georisk2011, Risk Assessment and Management*, Geotechnical Special Publication No. 224, ASCE, Atlanta, Georgia.

Xu, J., and Zheng, Y.R. (2001). "Random back analysis of field geotechnical parameter by response surface method." *Rock and Soil Mechanics*, 22(2), 167-170.

Zadeh, L.A. (1965). "Fuzzy sets." *Information and Control*, 8(3), 338-353.

Zhang, J., Tang, W.H., and Zhang, L.M. (2009). "Efficient probabilistic back-analysis of slope stability model parameters." *Journal of Geotechnical and Geoenvironmental Engineering*, 136(1), 99-109.

Zhang, L.L., Zhang, J., Zhang, L.M., and Tang, W.H. (2010). "Back analysis of slope failure with Markov chain Monte Carlo simulation." *Computers and Geotechnics*, 37(7-8), 905-912.